Sudan University of Science and Technology

College of Graduate Studies

Investigation of some Properties of Building Materials Available in Sudan and Used for Gamma - Rays Shielding

دراسة خصائص بعض مواد البناء المتاحة في السودان والمستخدمة في تدريع أشعة جاما

A Thesis Submitted in Fulfillment of Requirements for

The Degree of PhD in Physics

By:

Mohamed Daffallah Mohamednour Ali

Supervisor:

Professor: Mohamed Eltayed Mohamed Eisa

Co-supervisor:

Professor: Ahmed El Hassan El Faki

July 2019

الآيـــــــــــة

قال تعالى: (وَاخْفِضْ لَهُمَا جَنَاحَ الذُّلِّ مِنَ الرَّحْمَةِ وَقُل رَّبِّ ارْحَمْهُمَا كَمَا رَبَّيَانِي صَغِيرًا)

صدق الله العظيم

سورة الإسراء الآية (24)

Dedication

I dedicate this thesis to:

My parents and my dear brothers and sisters,

And every person who helped me to finish this work.

Acknowledgments

My acknowledgements especially go, but not limited, to those listed here. I would like to express my everlasting thanks and appreciations to Prof. Mohamed El tayeb Mohamed Eisa my main supervisor for giving me the independence and freedom in the work I did, while at the same time guiding and protecting me from the pitfalls and perils that can strike a PhD student. My sincere gratitude and thank to my co-supervisor Prof. Ahmed El Hassan El faki for his motivation, support and guidance during my PhD. A special thanks to Atomic Energy Commission, Radiation Safety Institute, University of Khartoum, Construction and Roads Research Institute, Yarmouk Industrial Complex and to anyone, who help and support all through the work. I also thank to Dr. Salma Gasmelseed to support me and for standing by me during the research period. Finally, I owe adverse thanks to my family, parents for their patience and support through the years I spent doing my PhD.

Abstract

As ionizing radiation is associated with a variety of different fields such as hospitals, industry, energy generation nowadays, it becomes part of our life. When radiation is produced in high doses, it can be hazardous for human and thus need to be shielded out in a theme known as radiation protection. The radiation protection becomes important subject in physics and there are several researches going on in this area. The main ways of radiation protection are time, distance and shielding. In radiation shielding the choosing of materials is important and thus recent works has been focused on selection of materials. For this purpose, in this study the gamma ray shielding properties of some building materials (lead, iron, concrete, cement and clay) used in Sudan has been investigated, in terms of photon attenuation coefficients and the half value layer (HVL) at different gamma ray energies, have been experimentally determined by using Cs-137 and Co-60 source and compared with the calculated values. The measurements were performed for radiation intensity without shielding and with specific thickness of selected samples (building materials), using ion chamber placed at 2 meters from the gamma ray source. The obtained results showed that the linear attenuation coefficient (μ) has a linear relationship with the corresponding densities of the samples studied and inversely with photon energy, and the half value layer (HVL) was proportional directly with photon energy. As results of this evaluation, the selected samples could be used as a shielding for gamma radiation. The usage of lead combined with the selected materials mentioned above resulted in an improvement of the efficiency of building materials as gamma ray shielding.

المستخلص

نسبة لإرتباط الإشعاع المؤين بمجالات متنوعه مثل المستشفيات والصناعه وتوليد الطاقه في الوقت الحاضر، فقد أصبح جزءاً لايتجزأ من حياتنا. عندما يتم إنتاج الإشعاع بجرعات عاليه قد يصبح خطراً علي الانسان، وبالتالي لابد من الوقايه منه بالتدريع، وهذا ما يعرف إصطلاحا بالحماية الإشعاعية. الحماية من الإشعاع قد أصبحت موضوعاً مهماً في الفيزياء، لذلك نجد أن هنالك عدة بحوث جارية في هذا المجال. إن الطرق الرئيسيه للحماية من الإشعاع هي الزمن، المسافه والتدريع، ويعد إختيار المواد للتدريع منه أمراً في غاية الأهميه، وبالتالي فقد ركزت الابحاث والدراسات الحاليه علي إختيار المواد ولهذا الغرض تم في هذه الدراسه التحقق من خصائص بعض مواد البناء (الرصاص – الحديد – الخرصانه - الاسمنت - الطين) المتاحة في السودان والمستخدمة في تدريع أشعة جاما من حيث معاملات توهين الفوتون وسمك النصف (HVL) في مختلف طاقات أشعة جاما، التي تم تحديدها تجريبياً باستخدام المصادر المشعه Cs-137 و Co-60 ومقارنتها بالقيم المحسوبة. لقد تم إجراء قياس شدة الإشعاع دون التدريع ثم بسماكة محددة للعينات المختارة (مواد البناء)، بإستخدام غرفة التأين التي تم وضعها علي بعد مترين من مصدر أشعة جاما. أظهرت النتائج التي تم الحصول عليها أن معامل التوهين الخطي **(μ)** له علاقه خطيه بكثافة العينات التي تمت دراستها وعلي علاقة عكسيه مع طاقة الفوتون، وكانت سماكة النصف (HVL) متناسبة طردياً مع طاقة الفوتون. نتيجة لهذا التقييم يمكن إستخدام العينات المختارة للتدريع من أشعة جاما، وكذلك إستخدام الرصاص مدمجاً مع المواد المختاره المذكورة أعلاه، أظهرت تحسناً في كفاءة مواد البناء كتدريع لأشعه جاما.

TABLE OF CONTENTS

LIST OF TABLES

LIST OF FIGURES

Chapter One

1.1 Introduction

The study of interaction of nuclear radiations with matter is the important research area for the development of materials which can be used in high radiation environment. Nuclear radiation protective shield play many functions most important to reduce radiation exposure to people in the where a bouts of radiation, they are working on the attenuation of radiation and reducing the intensity. So the theme of the protective shields of radiation has become an important part in our daily lives, especially after the great scientific progress which began to concentrate on the subject of the use of radioactive materials and other sources of radiation in medical and agricultural fields as well as other scientific fields such as building of nuclear reactors, used in researches and in the field of power generation (Kaundal, 2016)(AL-Dhuhaibat, 2015). Shielding is generally preferred due to its efficiency in intrinsically safe working conditions, whereas reliance on distance and time of exposure involves continuous administrative control over workers. The type and amount of shielding required depend on the type of radiation, the activity of radiation source and the dose rate that is acceptable for outside the shielding materials; however, there are other factors for choice of shielding material such as their cost and weight. An effective shield will cause a large energy loss in a small penetration distance without emission of more hazardous radiation. Furthermore, the good shielding material should have high absorption coefficient for radiation. Study of absorption of gamma and neutron radiations in shielding materials has been an important subject in the field of radiation physics (Mehmet Erdem, 2010). The interaction of ionizing radiation with the human body, arising either from external sources outside the body or from internal contamination of

the body by radioactive substances leads to biological effects which may later show up as clinical symptoms (Alan Martin, 1980). The nature and severity of these symptoms and the time at which they appear depend on the amount of radiation absorbed and the rate at which it is received. Radiation injuries can be divided into two classes: somatic effects in which the damage appears in the irradiated person himself, and hereditary effects which arise only in the offspring of the irradiated person as result of radiation damage to germ cells in the reproductive organs-the gonads (Alan Martin, 1980). Directly ionizing radiation interacts very strongly with shielding media and is therefore easily stopped. By contrast, indirectly ionizing radiation, may be quite penetrating and the shielding required may be quite massive and expensive. For these reasons, nowadays much attention has been paid to the shielding of neutrons and photons, then direct ionizing radiation most frequently encountered. Along with understanding characteristics and potential benefits of different types of radiation came awareness of their potential harm. Thus from the need for protection was radiation shielding design and analysis born. Radiation shielding serves a number of functions. Foremost among these is reducing the radiation exposure to persons in the vicinity of radiation sources. Shielding used for this purpose is named biological shielding. Shields are also used in some reactors to reduce the intensity of ɤ-rays incident on the reactor vessel, which protects the vessel from excessive heating due to ɤ-ray absorption and reduces radiation damage due to neutrons. These shields are named thermal shields. Sometimes shields are used to protect delicate electronic apparatus that otherwise would not function properly in a radiation shield. Such apparatus shields are used, for example, in some types of military equipment (Turner, 2007). Because the gamma ray has no mass and no charge; it is difficult to stop and has a very high penetrating power. There are three methods of

attenuating gamma rays. The first method is referred to as the Photoelectric effect is where a gamma interacts with an electron orbiting an atom. The entire energy of the gamma is transferred to the electron, and the electron is ejected from its orbit and this occurs with gamma ray having energy above 1 MeV (Fundamentals, 1993). However annihilation of the gamma results, any gamma energy in excess of the binding energy of the electron is carried off by the electron in the form of kinetic energy. The second method of attenuation of gammas is Compton scattering, a gamma interacts with an orbital electron, but only part of the gamma energy is transferred to the electron, the electron is ejected from its orbit and the gamma is scattered off at a lower energy, this reaction becomes important for gamma energies of about 0.1 MeV and higher. A third method of attenuation is pair-production, a gamma interacts with the electric field of a nucleus and is converted into an electron-positron pair and gamma must have energy greater than 1.02 MeV for this to occur (Fundamentals, 1993). The protection of people against exposure to ionizing radiation or radioactive substances and the safety of radiation sources need various procedures and devices for keeping people's doses and risks as low as can reasonably be achieved and below prescribed dose constraints, as well as the means for preventing accidents and for mitigating the consequences of accidents should they occur (Nations, 1996). Intensity of gamma rays can be controlled by three parameters: time, distance and shielding. The most effective method for attenuation of radiation is shielding. Shielding design parameters depend on facilities and on shielding material price (Majid Jalalia, 2008) .The attenuation of gamma ray depend on interaction of gamma-rays with the materials, the probability of interaction per unit of length of a given absorber characterizes its linear attenuation coefficient which depends on the material physical state, nature and density, as well as gamma ray initial

energy (Tarim, 2016)(Medhat, 2009). Shielding can be in various shapes and thicknesses depending on the radiation type and energy; γ rays require large amounts of lead or concrete. Shielding is especially important in places where radiation is used, therefore the vicinity of radioactive area is covered with lead or concrete bricks in order to protect the working environment from the harmful effects of radiation (Hamby, 2014). However, this type of shielding has high costs and is very cumbersome. The gamma emission from radioactive materials constitute the immediate radiological hazard to public health, shielding properties of housing as the protective action response refer to the advantages of building materials as the shielding materials, therefore it is very important to understand the differences between each materials type in order to develop building shielding factors applicable to specific generalized residential housing designs that depend on absorption parameters (Hamby, 2014).

1.2 Statement of the Problem

This dissertation is addressing the main problem of meeting radiological protection from gamma radiation to the surrounding environment, like wise achieving structural integrity and durability of shielding materials with advantages of availability and low cost.

1.3 Objectives

The purpose of radiation shielding is to prevent hazard of radiation and to keep the probability of harmful effects at an acceptable level by limiting the exposed dose to below certain threshold values. The aim of this study is to determine some energy absorption parameters of different building materials samples (clay, cement, concrete, iron and lead) and estimate the shielding effectiveness of them. The intention of this contribution is to

add something in the available information regarding the suitability with low cost and available building materials in Sudan.

1.4 Significance of the Study

The importance of this research is to provide the building materials that best suit the shielding of gamma rays, given the additional need for reduction and practical considerations, there is a need for multifunctional materials which could perform structural or other roles while providing good radiation shielding capability. The proposed materials generally evaluated as environmental _ friendly, cheap and available with reasonable radiation absorption coefficient and good attenuation.

1.5 Scope of the Work

The modified building materials (clay, cement, concrete iron and lead) are the most common shielding material for ionizing radiation. It is extensively used in facilities such as nuclear reactors, spent nuclear fuel repositories, particle accelerators, radiotherapy rooms, x-ray clinic and among others. As a shielding material, these building materials is very attractive because its attenuation properties which can be easily tailored by controlling its chemical composition. Moreover, this materials have relative inexpensive fabrication cost and can be cast in many complex forms exhibiting good mechanical, structural and physicochemical properties. All these characteristics make these materials suitable for the aforementioned shielding applications. There has been extensive work about the optimization of the key properties of these materials for shielding applications in both nuclear and medical industries. An important area of research has looked at the improvement of radiation shielding properties through the use of admixtures. Experimental techniques were used to characterize the properties of these materials,

measure the density of the samples and determine their attenuation properties. The results of this work are focused on the number and type of materials investigated; only selected available materials will be tested. Further measurements are required to study other shielding materials.

1.6 Thesis Structure

This thesis is organized as follows:-

Chapter One briefly presents introduction of radiation protection, shielding.

Chapter Two shows the previous studies. And discuss the radiation type sources, Interaction of Radiation with Matter and radiation hazards. In addition to radiation detection and protection.

Chapter Three illustrates the experimental part, method of samples collection, experimental setup and procedure.

Chapter Four shows the obtained results.

Chapter Five shows the discussion of results, conclusion and recommendations.

Chapter Two
Physical Background

2.1 Previous Studies

The study of building materials as a shield for gamma energy source was done with the aim of finding out the level of shielding and the thickness (Ayodeji, 2016). So numerous studies have been made in the building materials, especially by using nanotechnology in cement-based materials, so that clay materials enhance the shielding effect and decrease the penetration of the radiation. Hence, it can be taken as an alternative solution in shielding problems (Suat Akbulut, 2015). Heavy metals, such as lead, is mainly used for source heads, but it is very expensive for protective barriers, such as walls and flooring, in which instances concrete and the iron-ore concrete are mostly used. In most cases lead can be used when additional protection is required, for example in doors (Thoraeus, 1965). Lead is the most used material in nuclear technology as shielding material and collimator, in addition to the good properties of lead like easy to get and having high attenuation coefficients (A.B.Tugru, 2014). Shielding material produced by a metallurgical solid waste containing lead has been analyzed so as to make a shielding material against gamma radiation (Kh. REZAEE EBRAHIM SARAEE, 2015). Iron is used for higher and lower energies, it has been chosen due to its structural, temperature, and economic considerations (Hefne JAMEEL, 2010). The calculations of mass attenuation coefficient, half-value layer was studied in order to estimate gamma shielding effectiveness of the alloys contain iron mainly (Vishwanath P. Singh, 2014). Concrete is used widely as radiation shielding material because of its low price and good shielding performance, consisting of cement, water, and aggregate by the

mixing of water and cement, so used as material for reactor shielding due to its cheapness and satisfactory mechanical properties (Ouda, 2015). Concretes with added materials in the aggregate can give advantages to γ-ray shielding when compared to ordinary concrete (El-Sayed A. Waly, 2015).Furthermore, shielding of gamma radiation by several types of houses in European continent has been investigated; in these houses limestone mostly used as the external building material, supported by a wall of concrete or bricks, while internal partition walls are mainly of bricks (Mohammad I. Awadallah, 2007). The composition of concrete that contains a mixture of many heavy elements play an important role in improving concrete shielding properties because it has a good shielding properties for the attenuation of photons and neutrons (I. Akkurta & Günoglua, 2012). Buildings are constructed mostly from concretes and bricks. In the construction, two main points have to be considered, resistance against earthquake expressed as strength of the building and resistance against radiation expressed to attenuate γ -ray (Medhat, 2009). An ordinary Portland cement and lead of grain size 110 mm were used as starting materials for shielding (F.I. El-Hosin, 2000). The linear and mass attenuation coefficients of different types of soil such as sand, building materials and heavy beach mineral samples from the Chittagong and Cox's Bazar area of Bangladesh were measured using a high-resolution HPGe detector and the g-ray energies ranges 276.1, 302.8, 356.0, 383.8, 661.6 and 1173.2 and 1332.5 KeV emitted from point sources of Ba^{133}, Cs^{137} and Co^{60}, respectively (M.N. Alam, 2001). The clays can be used as additives as the shielding of radioactive materials (Suat Akbulut, 2015). Clay is a useful material and can be used in different purposes in different filed, besides using it in industry or medical field, it is important to use clay in wall design and plastering, so plastering wall by clay could be an important method to dispose radioactive waste. In addition, the

radiation shielding properties of the clay can be improved by adding boron into clay (I. Akkurt, 2011). The bricks are made from mixtures of sand, clay, cement, fly ash, gypsum, red mud and lime. Shielding effectiveness of five soil samples and two fly ash samples have been studied using some energy absorption parameters (Kulwinder SinghMann, 2013).

2.2 Radiation (ionizing and non ionizing)

Radiation is a fact of life, all around us all the time we live in naturally radioactive world, so radiation was used to describe electromagnetic waves. Today, radiation refers to the whole electromagnetic spectrum as well as to the atomic and subatomic particles that have been discovered. Radiation is classified into two main categories, non-ionizing and ionizing, depending on its ability to ionize matter (Tsoulfanidis, 1995). Ionizing radiation consists of subatomic particles or electromagnetic waves that are energetic enough to separate electrons from atoms or molecules, i.e. ionizing them. Non-ionizing radiation cannot ionize matter because its energy is lower than the ionization potential[i] of matter. Ionizing radiation (wavelength: λ=0.01→10nm), can ionize matter either directly or indirectly because its energy exceeds the ionization potential of matter. That is; directly ionizing radiation (charged particles) such as electrons, protons, alpha particles and heavy ions. While indirectly ionizing radiation (neutral particles) such as photons (X-rays, gamma rays) and neutrons (Tsoulfanidis, 1995) (Cardarelli, 2011). Directly ionizing radiation deposits energy in the medium through direct Coulomb interactions between the directly ionizing charged particle and orbital electrons of atoms medium. Indirect ionizing radiation (photons or neutrons) deposits energy in the medium through two-step processes: In the first step a charged particle is released in the medium (photons release

electrons or positrons, neutrons release protons or heavier ions). In the second step, the released charged particles deposit energy to the medium through direct Coulomb interactions with orbital electron of the atoms in the medium (Podgorsak, 2005) (Knoll, 2000).

2.3 Gamma Radiation

A photon is a packet, a quantum, of energy, in the form of electromagnetic radiation and as such travels at the speed of light. The energy of a photon **E** is equal to $\boldsymbol{h}.\boldsymbol{v}$**,** where $\boldsymbol{h}$ is Planck's constant (6.626 x 10^{-34} j.s) and $\boldsymbol{v}$ is the frequency of the electromagnetic wave. The interest here is in photons that have a sufficient energy to penetrate matter includes x-rays and gamma rays, while gamma-rays consist of photons emerging from nuclear decay. Gamma-ray sources are typically radioisotopes, such as Co-60 and Cs-137 in the energy range of commonly used x-ray and gamma-ray photon sources, 0.01 to 10 MeV. When the photon is traveling in a medium; it slows down due to interaction with the medium and acquires an effective mass. In vacuum, however, it is considered to be mass less. Photons are involved in all types of electromagnetic interactions. The energy carried by a photon can be absorbed in a number of ways by other particles with which it interacts. Also, like other particles, a photon can scatter off from other particles and even experience gravitational pull. In terms of radiation exposure and biological damage we are generally concerned with high energy photons, such as γ-rays. Having high energies, these photons can penetrate deeper and cause more damage than the low energy photons such as visible light. The basic properties of gamma photons have no rest mass and, no electrical charge (HUSSEIN, 2004) (Ahmed, 2007).

2.4 Radiation Sources

The sources of radiation are classified into:

2.4.1 Natural Sources

There are three types of natural sources of radiation: cosmic, terrestrial, and internal. Exposure from most of these sources is very minimal and therefore does not cause any measurable damage to our bodies.

2.4.1.1 Cosmic Radiation Sources

The outer space is filled with radiation that comes from a variety of sources such as Sun and stars. These bodies produce immense amounts of radiation, some of which reach earth but fortunately the earth's atmosphere acts as a shield to the worst of these radiations, such as ultraviolet rays from the Sun are blocked by the ozone layer. Some of unblocked radiation reach the surface of earth has impact on the health of human population like skin burns and cancer in people who remain exposed to sun light for extended periods of time (Ahmed, 2007) (Bodansky, 2004). The situation is even worse in places where the ozone layer has depleted due to some reason. There is also a background radiation of low energy photons, this radiation is thought to be the remnant of the so called big bang that created this universe, it is known as cosmic microwave background radiation since the photon spectrum peaks in the microwave region of the electromagnetic spectrum (Ahmed, 2007). Although these photons reach the earth's surface but due to their low energies, they are not deemed harmful. Apart from photons, there are other particles as well that are constantly being produced in the outer space. Most of them, however, never reach the earth either due to magnetic deflection or the earth's upper protective atmosphere. Some of the particles, like muons, electrons, and neutrinos, are produced when other cosmic particles interact with atoms in the upper atmosphere.

Shower of these particles reach earth's surface time but due to their low energies and low interaction probabilities, they do not pose any significant health hazard. Muons and neutrinos directly produced by luminous objects in space also manage to reach earth due to their low interaction capabilities but are not considered hazardous to health due to their extremely low interaction cross sections. At higher elevations, the amount of atmospheric shielding decreases and thus the dose increases. The total average annual dose to the general population from cosmic radiation is about 27 mrem (California, 2000).

2.4.1.2 Terrestrial Radiation Sources

Everything in and on the Earth contains primordial radionuclide's. This type of radiation is present in small quantities all around us and is more or less inescapable. Our surroundings, the water we drink, the air we breathe in, and the food we consume, all are contaminated with minute quantities of radiation emitting isotopes (Ahmed, 2007). Although these isotopes, in general, are extremely hazardous, they are not supposed to cause any appreciable harm to our bodies except when they are present in higher than normal concentrations. The main source of terrestrial radiation is the element uranium and its decay products such as thorium, radium, and radon. Although the overall natural concentration of these radioactive materials is within the tolerable range of humans, some parts of the world have been identified where higher levels of uranium and thorium in surface soil have increased the radiation to dangerous levels (Ahmed, 2007) (Bodansky, 2004) (R. L. Grasty, 2004). Unfortunately man has also contributed to this dilemma by carrying out nuclear explosions and by dumping nuclear waste. The total average annual dose to the general population from terrestrial radiation is 28 mrem (California, 2000).

2.4.1.3 Internal Radiation Sources

Our bodies contain some traces of radioactive elements that expose our tissues to continuous low level radiation. This internal radiation primarily comes from Potassium-40 and Carbon-40 isotopes (Ahmed, 2007) (R. L. Grasty, 2004). However the absorbed dose and the damage to tissues due to this radiation are minimal. Combined exposure from internal sources of natural background radiation account for a radiation dose of about 39 mrem per year (California, 2000).

2.4.2 Man-Made Sources

The artificial sources add to the radiation dose from natural sources for both individuals and the global population. Scientists started working on developing sources that can be used to produce radiation in controlled laboratory environments, the five major sources of human-made radiation exposures are:

2.4.2.1 Medical Radiation Sources

The use of radiation in medicine to diagnose and treat certain diseases plays such an important role that it is now by far the main artificial source of exposure in the world; a typical radiation dose from a chest x-ray is about 10 mrem, the total average annual dose to the general population from medical x-rays is about 39 mrem (California, 2000) (Bodansky, 2004). In addition to x-rays, radioactive sources are used in medicine for diagnosis and therapy. The total average annual dose to the general population from these sources is 14 mrem (California, 2000).

2.4.2.2 Atmospheric Testing of Nuclear Weapons

Another human-made source of radiation includes residual fallout from atmospheric nuclear weapons testing in the 1950’s and early 1960’s. Atmospheric testing is now banned by most nations; the average annual dose from residual fallout is less than one mrem (California, 2000) (R. L. Grasty, 2004).

2.4.2.3 Consumer Products

These types of radiation include TVs, older luminous dial watches, and some smoke detectors, airport luggage inspection systems and building materials. The estimated annual average whole body dose equivalent to the U.S. population from consumer products is approximately 10 mrem, the major portion of this exposure (approximately 70%) is due to radioactivity in building materials (California, 2000) (Bodansky, 2004).

2.4.2.4 Nuclear Facilities

By 1988, 90 nuclear power plants had been licensed in the U.S. In addition, over 300 other reactors, classed as non-power reactors, are being operated. Current estimates of the yearly average dose equivalent in the U.S. from environmental releases are less than one mrem (California, 2000) (Bodansky, 2004).

2.4.2.5 Radioactive Sources of Gamma Rays

Gamma rays are high-energy electromagnetic radiation emitted in the deexcitation of the atomic nucleus; there are a large number of radioactive elements that emit γ-rays. These radiations are often accompanied by α- and β-particles. Besides naturally occurring sources it is possible to produce these isotopes in laboratory as well, this is normally done by bombarding a source material by neutrons, the nuclei as a result, go into unstable states and try to get rid of these extra neutrons, in this process they also release energy in the form of γ-rays (Ahmed, 2007). The two most commonly used radioactive sources of γ-rays are iridium-192 and cobalt-60. The easiest way to produce cobalt-60 is by bombarding cobalt-59 with slow neutrons as represented by the following reaction:-

$$^{59}_{27}Co + n \rightarrow {}^{60}_{27}C0 + \gamma \quad (7.492)\ MeV \qquad (2.1)$$

However the neutrons produced in this way have higher kinetic energies than needed for them to be optimally captured by cobalt-59. Therefore

some kind of moderator, such as water, is used to slow down these neutrons before they reach the cobalt atoms. The resultant cobalt-60 isotope is radioactive and gives off 2 energetic γ-rays: 1.173 MeV and 1.332MeV and half life of 5.271 years; and Cesium(Cs-137) which has energy 661.657 KeV and half life of 30.07 years (Ahmed, 2007).

2.5 Interaction of Radiation with Matter

The interaction of radiation with matter is useful for many applications to ensure adequate protection from the point view of public health and safety. The nature of interactions in matter depends on the incoming type of radiation and energy e.g. heavy particles lose energy in medium at a faster rate than light particles:-

2.5.1 Alpha Particles

Alpha particle which contains two neutrons and two protons, and has a mass of four units, which makes it a heavy particle, has a positive charge of two times that of the electron; hence the alpha particle is highly interactive. The effect of its large mass and double charge makes an alpha particle highly interactive in the vicinity of Interaction of Directly Ionizing Particles in which it is produced; hence it never penetrates far into any material (Marilyn E. Noz, 2007). A thin sheet of paper is usually sufficient to stop all but the most energetic alpha particles. When alpha particles travel through a material, they lose energy by collision with atomic electrons and cause ionization to occur. Alpha particles are the least penetrating of all forms of radiation. Alpha particles will travel only a few cm in air, and will penetrate soft tissue only to a distance of micrometers (Stabin, 2007). As is true of any heavy-charged particle, alpha particles all travel nearly, but not precisely, the same distance in a given medium before coming to rest. This variation in travel distance toward path end is known as straggling and is due to the probabilistic

nature of the collisions between alpha particles (and other heavy charged particles) and atomic electrons. To assess the range of alpha particles, it should be noted that 5 MeV alpha particles are all stopped by 35 mm of air at 15 °C and standard pressure and have a range determined by the distance at which one half of the original number are detected (Marilyn E. Noz, 2007).

2.5.2 Beta Particles

Beta radiation is in between alpha and gamma in terms of its penetrating power, so beta (electrons) are very light particles, and many have a negative or positive charge. Because of its light mass and single charge, an electron is not as interactive as an alpha particle and, therefore, has a much longer range in matter. Also, electrons tend to travel through matter in tortuous paths rather than in straight lines. In addition to losing energy by collision with atomic electrons, another mechanism by which electrons can lose energy is a braking action known as bremsstrahlung (Marilyn E. Noz, 2007). Whenever a charged particle undergoes a change in direction or magnitude of its motion, it emits energy in the form of a photon. This change is proportional to the nuclear charge Z, which causes it, divided by the mass of the particle experiencing the change. An electron, because of its small mass can, in the presence of a nucleus, experience a large variation in its motion. Since the amount of change of motion is inversely related to the particle's mass, bremsstrahlung does not become important for heavy-charged particles until energies of billions of electron volts (GeV) are reached (Marilyn E. Noz, 2007). The amount of energy lost by bremsstrahlung, relative to that lost by collision, is generally very small in materials that have a low atomic number such as air and tissue. For high energy electrons interacting with high atomic number materials, however the amount of energy lost can be considerable. In the case of electrons interacting with lead, the two mechanisms (direct collision and

bremsstrahlung) contribute equally to the electron's loss of energy, for that it becomes important in shielding considerations. The maximum range can be established, which depends on the maximum beta energy in the decay spectrum (Stabin, 2007).

2.5.3 Photon Interaction

There are three different energy loss mechanisms by which such high energy photon interact with the target atoms: Compton scattering, the photo electric effect and pair production.

2.5.3.1 In Compton Scattering the incoming photon bounces off an electron and continuous on in a new direction with reduced energy. This scattered photon may subsequently interact with another target electron (Protection, 2000). The photon is scattered at an angle that depends on the amount of energy transferred from the photon to the electron. The scattering angle can range from 0◦ to 180◦. Consequently, the atomic Compton attenuation coefficient depends linearly on the atomic number $\boldsymbol{Z}$ of the attenuator, whiles the electronic and mass Compton attenuation coefficients, are independent of $\boldsymbol{Z}$ (Podgorsak, 2005).

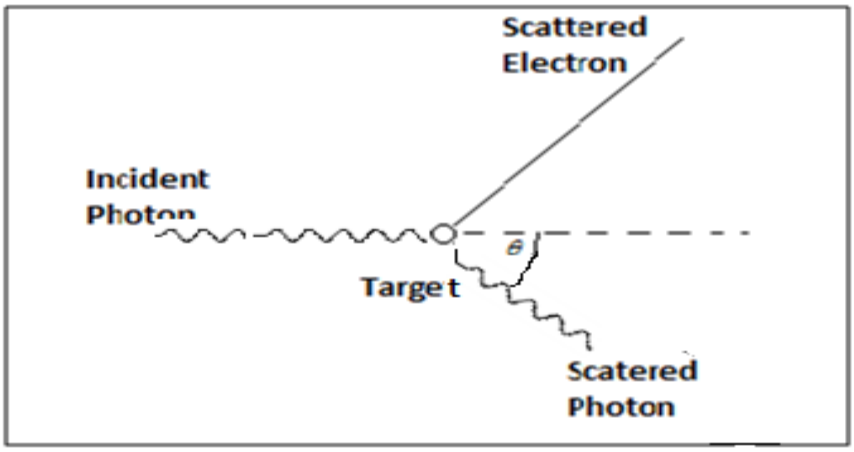

Figure 2.1: Schematic representation of Compton effect.

2.5.3.2 In Pair Production only occurs with very high photon energies greater than 1020 KeV (Powsner, 2006). The photon falling near the

nucleus of an atom, is subjected to strong field effects from the nucleus and may disappear as a photon and reappear as a positive and negative electron pair, it is easy to calculate that 0.511 MeV of energy is needed to produce the mass of an electron (9.11 x 10^{-31} kg), of course, the same amount for a positron. The atomic attenuation coefficient for pair production and the mass attenuation coefficient for pair production vary approximately as $\boldsymbol{Z^2}$ and $\boldsymbol{Z}$, respectively, where $\boldsymbol{Z}$ is the atomic number of the attenuator (Podgorsak, 2005).

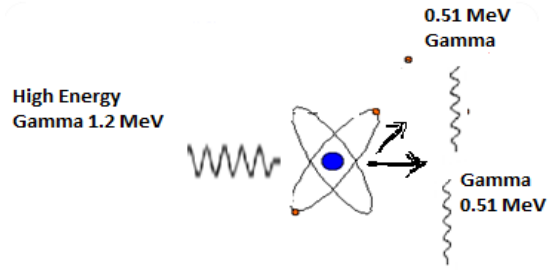

Figure 2.2: Schematic representation of pair production effect.

2.5.3.3 In Photo Electric Effect a photon undergoes an interaction with an absorber atom in which the photon completely disappears, and the ejected electron is called a photoelectron (Podgorsak, 2005)**.** This electron leaves the atom with energy equal to the energy of the incident gamma ray diminished by the binding energy of the electron (Powsner, 2006).

$$E_{photoelectron} = E_{photon} - E_{Binding} \quad (2.2)$$

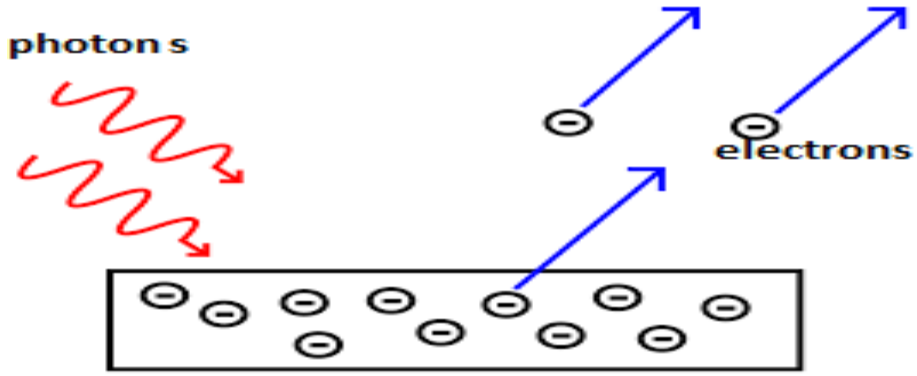

Figure 2.3: Schematic representation of photoelectric effect.

The atomic attenuation coefficient for the photoelectric effect at is proportional to $Z4/(h\upsilon)^3$, while the mass attenuation coefficient for the photoelectric effect is proportional to $(Z/h\upsilon)^3$, where Z is the atomic number of the attenuator and $h\upsilon$ is the photon energy (Podgorsak, 2005).

2.6 Biological Effects of Radiations

Radiation can cause damage to human cells by the ionization of atoms in the cells and the damage begins with the atoms which make up the cells in the tissues of the body.

2.6.1 Mechanism of Radiation Damage to Biological Systems

The conventional particularly, the DNA from ionization and excitation events, ultimately result in cell transformation or death. Cell transformation may be fatal, or may lead to expression of disease (typically cancer) at a later time. Ionizing **radiation** generates both direct and indirect **damage to biological** molecules, the damage to the DNA may be direct like the ionizing particle interacts with an atom in the

DNA, causing damage to occur) or indirect (radiation interacts with water near the DNA, with subsequent attack of the formed free radicals on the DNA molecules).

2.6.2 Biological Effect in Human

There are two broad categories of radiation effects in humans, stochastic and non-stochastic and there are three important characteristics that distinguish them.

2.6.2.1 Non Stochastic Effects

Health effects, the severity of which varies with the dose and for which a threshold is believed to exist, now officially called deterministic effects or acute effects, are effects that are generally observed soon after exposure to radiation. In nature, they will always be observed if the dose threshold is exceeded, and there is generally no doubt that they were caused by the radiation exposure. The major identifying characteristics of non-stochastic effects are (1) there is a threshold of dose below which the effects will not be observed, (2) above this threshold, the magnitude of the effect increases with dose and (3) the effect is clearly associated with the radiation exposure like erythema (reddening of the skin), epilation (loss of hair), depression of bone marrow cell division (observed in counts of formed elements in peripheral blood), NVD (nausea, vomiting, diarrhea), often observed in victims after an acute exposure to radiation Central nervous system damage, damage to the unborn child (physical deformities, microcephaly (small head size at birth) and mental retardation.

2.6.2.2 Stochastic Effects

Health effects that occur randomly and for which the probability of the effect occurring, they may or may not occur in any given exposed

individual. These effects generally manifest many years, even decades after the radiation exposure (and were once called “late effects”). Their major characteristics in direct contrast with those for non-stochastic effects are a threshold may not be observed, the probability of the effect increases with dose and the effect cannot be definitively associated with the radiation exposure like cancer induction and genetic effects (Stabin, 2007)(Herman Cember, 2009).

2.7 Radiation Protection

There are three basic methods that control the amount of radiation dose received from a source. Radiation exposure can be managed by a combination of these factors:

2.7.1 Time

The absorbed dose is directly proportional to time, only the minimal necessary amount of time should be spent in the vicinity of a radioactive source, so accumulated dose is directly dependent on the exposure time (Fred A. Mettler, 2002) (HUSSEIN, 2003).

2.7.2 Distance

Maintaining the greatest possible distance, without undermining the effectiveness of the work involved between the radiation source and the worker, the absorbed dose decreases rapidly with the square of the distance from the source (Antoni, 2017) (Shapiro, 2002).

2.7.3 Shielding

The purpose of radiation shielding is to limit radiation exposures to members of the public and employees to an acceptable level (National Council on Radiation Protection, 2006). Placing, between the radiation source and the worker, suitable protective shielding and, if necessary, using other shielding to protect people in the vicinity of the source or

adjoining areas (Antoni, 2017). As a common practice, all radiation sources are provided with an appropriate shielding; both during use and storage, different shielding materials are utilized for different types of radiation. Photons (x- or gamma-rays) are effectively shielded using electron-rich materials (heavy metals), such as lead, steel and concrete, since photons interact mainly with the atomic-electrons (HUSSEIN, 2004).

2.8 Passage of Photons through Matter

Behavior of photons in matter is very different from that of charged particles. Now that we have learned the basic processes that define the interactions of photon that may undergo while passing through matter, but their overall effect on a beam of photons and the material through which it passes can be characterized by some simple relations. Before we go on to define these relations, let us have a qualitative look at the passage of a photon beam through matter. A photon beam consists of a large number of photons moving in a straight line. The beam may or may not be monochromatic, such as, all the photons in the beam may or may not have the same energy. Of course the term same is somewhat loosely defined here since even a so called monochromatic photon beam has some variations in energy around its mean value. Depending on their energy, each photon in the beam may undergo one of the several interactions. It is hard, even impossible, to say with absolute certainty that a photon with a certain energy will definitely interact with an atom and in a defined way. The good thing is that the gross interaction mechanisms of a large number of photons can be quite accurately predicted with the help of statistical quantities such as cross section. In radiation measurements, a photon beam is relatively easier to handle as compared to a beam of massive particles. The reason is that the interaction of photons with

matter is localized or discrete. That is, a photon that has not interacted with any other particle does not loose energy and remains a part of the beam. This means that the energy of all non-interacting photons in a beam remains constant as the beam passes through the material. However the intensity of the beam decreases as it traverses the material due to loss of interacting photons (Ahmed, 2007). It has been found that at any point in a material, the decrease in intensity of a photon beam per unit length of the material depends on material and the photon energy as in the equation below (Turgay Korkut, 2011):-

$$\mathbf{I = I_0 e^{-\mu x}} \qquad \mathbf{(2.3)}$$

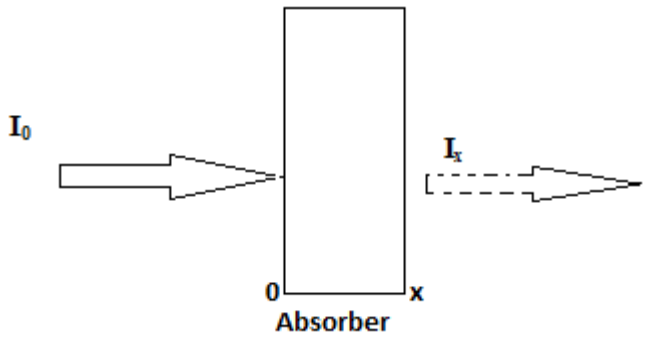

Figure 2.4: Schematic illustrating decreases of intensity of beam as it traverses a material e.g. shielding.

Where $\mathbf{I_0}$is the intensity of the photon beam just before it enters the material, **I** is its intensity at a depth $\boldsymbol{x}$ and $\boldsymbol{\mu}$ it is linear attenuation coefficient (Ahmed, 2007).

2.9 Basic Shielding Parameters

The shielding effectiveness of materials can be examined on the basis of different parameters which include:

2.9.1 Linear Attenuation Coefficient

The attenuation coefficient measures the probability of all possible interactions between gamma rays and atomic nuclei, it is important for solving various problems in radiation physics and in radiation dosimetry. The probability of a photon interacting in a particular way with a given material, per unit path length is usually called the linear attenuation coefficient $\boldsymbol{\mu}$, and it is of great importance in radiation shielding. Linear attenuation coefficients depend on the density $\boldsymbol{\rho}$ of the shielding material, the incident photon energy and the nature of the absorbing material. The following relation holds (M.N. Alam, 2001):

$$\boldsymbol{\mu} = \frac{\mathbf{1}}{\boldsymbol{x}} \mathbf{ln}\left(\frac{\mathbf{I_0}}{\mathbf{I}}\right) \qquad \textbf{(2.4)}$$

Where $\boldsymbol{\mu}$ is the linear attenuation coefficient in (cm^{-1}), and $\boldsymbol{x}$ is the thickness of sample in (cm). The theoretical values of linear attenuation coefficient of combined samples is calculated using the equation below,

$$\boldsymbol{\mu} = \sum \frac{\boldsymbol{\mu_i x_i}}{\mathbf{x_i}} \qquad \textbf{(2.5)}$$

Where $\boldsymbol{\mu_i}$ is the linear attenuation coefficient, and $\mathbf{x_i}$ is the thickness of combination samples.

(Abdo, 2002)(I.C.P. Salinas, 2006).

2.9.2 Mass Attenuation Coefficient

Mass attenuation coefficient $\boldsymbol{\mu_m}$ is an important parameter for study of interaction of radiation with matter that gives us the fraction of energy scattered or absorbed, it is a measure of probability of interaction that occurs between incident photons and matter in a given mass per unit area thickness of the material encountered. It is a basic quantity used in the calculation of photon penetration and energy deposition in biological studies, shielding and other dosimetric materials. The magnitude of $\boldsymbol{\mu_m}$ depends on the incident photon energy, the chemical structure and

bonding in the absorbing material and parameters such as thickness and density $\boldsymbol{\rho}$; the following relation holds:

$$\mu_m = \mu/\rho \ cm^2 g^{-1} \qquad (2.6)$$

(Nil Kucuk, 2013)(Y. Elmahroug, 2015)(Charanjeet Singh, 2004)

2.9.3 Half Value Layer

The thickness of any given material where 50% of the incident energy has been attenuated is known as the half value layer HVL (I. Akkurta & Günoglua, 2012), and it is useful parameter for understanding the interaction of gamma ray and depends on linear attenuation coefficient, and it is expressed in units of distance (cm). A half value of layer of shielding material, $X_{1/2}$ defined at $I = \frac{I_0}{2}$, is given as:

$$X_{1/2} = \frac{0.693}{\mu} \qquad (2.7)$$

(El-Sayed A. Waly, 2016)(Ravinder Singh, 2017).

2.10 Building Materials as Shielding

Ionizing radiations are shield best shielded by high density materials and heavy atoms such as lead. Unfortunately, although its benefits, lead is toxic and its mechanical properties are weak (H. M. Soylu, 2015). For high-density radiation shielding, iron is the most commonly used to shield gamma ray which has low-cost and high-density (K Srinivasan, 2017). Concrete is one of the most important materials used for radiation shielding in facilities containing radioactive sources and radiation generating equipment, the concrete shielding properties may vary depending on the composite of the concrete (M.H. Kharita, 2008). The most important binding agent for construction specially in industry is cement which is produced world-wide in large amounts. Also it is the most active component of concrete and usually has the greatest unit cost,

the selection and proper use of it is important in obtaining most economically the balance of properties desired for any particular concrete mixture (N. Chanthima, 2012). Clay is a naturally occurring material composed of fine grain minerals, which shows plasticity when moist and becomes hard when dried or fired. Clay has been used in the manufacturing of bricks since ancient times. The clay soils have better photon energy absorption characteristics than other soils (Harjinder Singh Mann, 2016).

2.11 Detection of Gamma Radiation

Detection of gamma radiation is critically depend on the interaction that transfers all or part of photon energy to an electron in the absorbing material, so the ultimate goal for the detection is to investigate potential differences in gamma ray properties depending on the reaction mechanism, therefore the key process of detecting gamma ray is by ionization which is give up part or all of its energy to an electron. The energized electrons then collide with other atoms and liberate electrons. The liberated charge is collected either directly, using gas ionization type (ion chambers, proportional counters and Geiger–Muller counters, or indirectly (as with scintillation detector), in order to record the presence of gamma ray and measure its energy. The instruments that are used to detect the ionizing radiation are based on ionization of the gas inside a chamber, and they are categorized as ion chamber, proportional counter and Geiger tubes (Gupta, 2013).

2.11.1 General Characteristics of Ionization Detectors

Several common criteria are used to evaluate the performance of any detector type; the criteria used for this purpose are as follows:

The sensitivity of the detector, reflect what types of radiation will the detector detects? For example, solid scintillation detectors are normally

not used to detect α-particles from radioactive decay because the α-particles cannot penetrate the detectors covering. **The energy resolution of the detector**, shows how will the Detector measure the energy of the radiation striking it, and if so, how precisely does it do this? If two γ-rays of energies 1.10 MeV and 1.15 MeV Strike the detector, can it distinguish between them?.**The time resolution of the detector**, or its pulse-resolving time, demonstrates how high a counting rate will be measured by the detector without error? How accurately and precisely can one measure the time of arrival of a particle at the detector. **The detector efficiency**: this illustrates that if 100 γ-rays strike a detector, exactly how many will be detected? (Cerrito, 2017).

2.11.2 Gas-Filled Detectors

Radiation passing through a gas can ionize the gas molecules, provided that the energy delivered by it is higher than the ionization potential of the gas. The charge pairs thus produced can be made to move in opposite directions by the application of an external electric field. The result is an electric pulse that can be measured by an associated measuring device. This process has been used to construct the so called gas filled detectors. A typical gas filled detector would consist of a gas enclosure and positive and negative electrodes. The electrodes are raised to a high potential difference that can range from less than 100 volts to a few thousand volts depending on the design and mode of operation of the detector. The creation and movement of charge pairs due to passage of radiation in the gas perturbs the externally applied electric field producing a pulse at the electrodes. The resulting charge, current, or voltage at one of the electrodes can then be measured, which together with proper calibration gives information about the energy of the particle beam and/or its intensity (Ahmed, 2007).

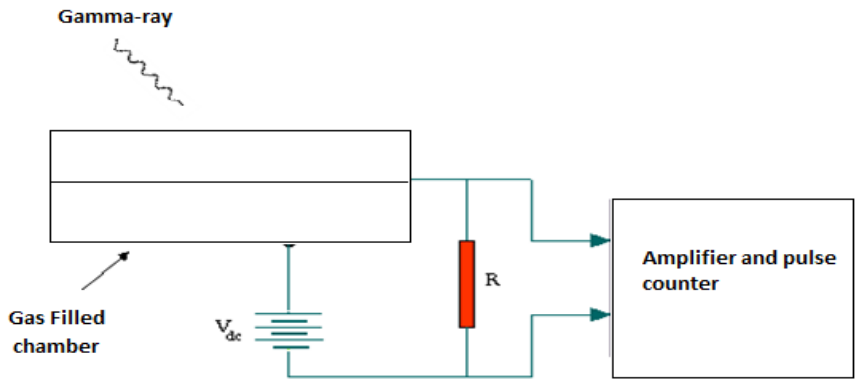

Figure 2.5: Schematic illustration of electronic circuit of a Gas-filled detector.

2.11.2.1 Operation of Gas Filled Detectors

Figure 2.6 illustrates different regions of operation of a gas filled detector. Based on the applied bias voltage, a detector can be operated in a number of modes, which differ from one another by the amount of charges produced and their movement inside the detector volume. Choice of a particular mode depends on the application and generally detectors are optimized to work in the range of the applied voltage that is typical of that particular mode only. These operation regions are discussed here briefly (Ahmed, 2007).

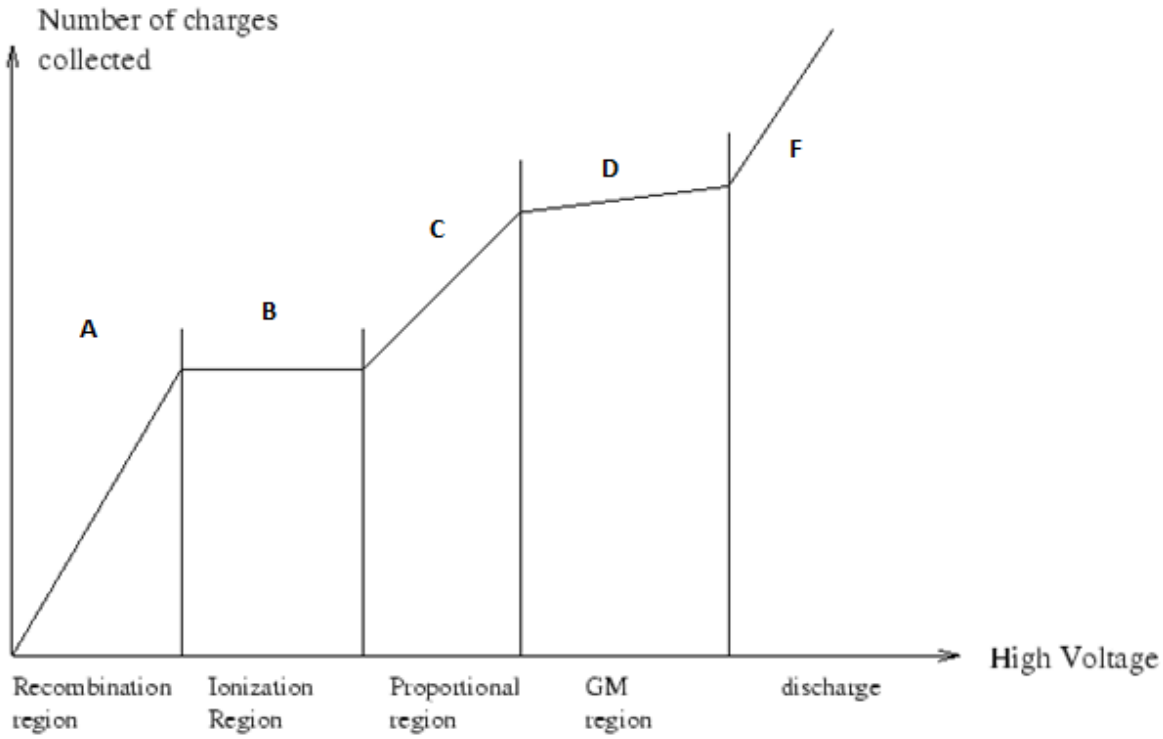

Figure 2.6: Relation between applied voltage and charge collected in a gas filled detector.

Region A: Here V_{dc} is relatively low so that recombination of positive ions and electrons occurs. As a result not all ion pairs are collected and the voltage pulse height is relatively low. It does increase as the dc voltage increases however as the amount of recombination reduces.

Region B: V_{dc} is sufficiently high in this region so that only a negligible amount of recombination occurs. This is the region where a type of detector called the Ionization Chamber operates.

Region C: $V_{dc}$is sufficiently high in this region so that electrons approaching the centre wire attain sufficient energy between collisions with the electrons of gas atoms to produce new ion pairs. Thus the number of electrons is increased so that the electric charge passing through the resistor, R, may be up to a thousand times greater than the charge produced initially by the radiation interaction. This is the region

where a type of detector called the Proportional Counter operates. **Region D:** $V_{dc}$is so high that even a minimally-ionizing particle will produce a very large voltage pulse. The initial ionization produced by the radiation triggers a complete gas breakdown as an avalanche of electrons heads towards and spreads along the centre wire. This region is called the Geiger-Müller Region, and is utilized in the G-M counter.

Region F: Here $V_{dc}$is high enough for the gas to completely breakdown and it cannot be used to detect radiation (Tsoulfanidis, 2015).

2.11.2.2 Types of Gas-filled Detectors

Gas-filled detectors take their name from the voltage region in which they operate.

2.11.2.2.1 Proportional Counters

Operate in region C; charge multiplication takes place, but the output signal is still proportional to the energy deposited in the counter. Measurement of particle energy is possible. Proportional counters may be used for the detection of any charged particle. Identification of the type of particle is possible with both ionization and proportional counters. An alpha particle and an electron having the same energy and entering either of the detectors, will give a different signal. The alpha particle signal will be bigger than the electron signal. The voltage applied to proportional counters ranges between 800 and 2000 V.

2.11.2.2.2 GM Counters

Operate in region D; GM counters are very useful because their operation is simple and they provide a very strong signal, so strong that a preamplifier is not necessary. They can be used with any kind of ionizing radiation (with different levels of efficiency). The disadvantage of GM counters is that their signal is independent of the particle type and its energy. Therefore, a GM counter provides information only about the number of particles. Another minor disadvantage is their relatively long

dead time (200–300 ms). The voltage applied to GM counters ranges from 500 to 2000 V (Tsoulfanidis, 2011).

2.11.2.2.3 Ionization Chambers

Operate in region B; no charge multiplication takes place, the output signal of an ionization chamber is proportional to the particle energy dissipated in the detector; therefore, measurement of particle energy is possible. Since the signal from an ionization chamber is not large, only strongly ionizing particles such as alphas, protons, fission fragments, and other heavy ions are detected by such detectors. The voltage applied is less than 1000 V (Tsoulfanidis, 2015).

2.11.2.2.3.1 Standard Ionization Chamber

Ionization chamber based dosimetry systems are in principle quite simple and consist of three main components: a suitable ionization chamber, electrometer and power supply. The circuitry of a simple ionization chamber based dosimetry system resembles a capacitor (ionization chamber) connected to a battery (power supply), with the electrometer measuring the ‘capacitor’ charging or discharging current.

In standard free air ionization chamber, the chamber measures the air kerma in air according to its definition by collecting all ions produced by the radiation beam that result from the direct transfer of energy from photons to primary electrons in a defined volume in air, the determination of air kerma required accurate knowledge about the use of the standard free air ionization chamber, and it is limited to photons below 0.3 MeV. Ionization chamber dosimetry, the ionization chamber is the most practical and most widely used type of dosimeter for accurate measurement. It may be used as an absolute or relative dosimetry. It is sensitive volume is usually filled with ambient air. And the dose or dose rate related measured quantities are the ionization charge Q or ionization current I, respectively produced by radiation in the chamber sensitive air

mass m_{air} (Attix, 1986). The sensitive air volume or mass in an ionization chamber is determined directly by measurement (the chamber becomes an absolute dosimeter under special circumstances) or indirectly through calibration of the chamber response in a known radiation field (the chamber is used as a relative dosimeter) (Burns, 2009).

Chapter Three

Materials and Methods

3.1 Materials

Several materials were investigated in this study include lead, iron, concrete, cement and clay, so as to evaluate the highest gamma radiation shielding effectiveness. This chapter briefly - gives description of each material, composition details, measured thicknesses and densities and pictures of each type used to build shielding system. The samples of lead and iron were collected from Yarmouk Industrial Complex, while the samples of concrete, cement and clay were collected from University of Khartoum, Construction and Roads Research Institute.

3.1.1 Lead:-

The density of lead is 11.34 (g/cm^3**)** and its chemical composition is as follows using Bruker Quantron Q4 Tasman device (Model: Q4/UVU, Serial No: M0295):

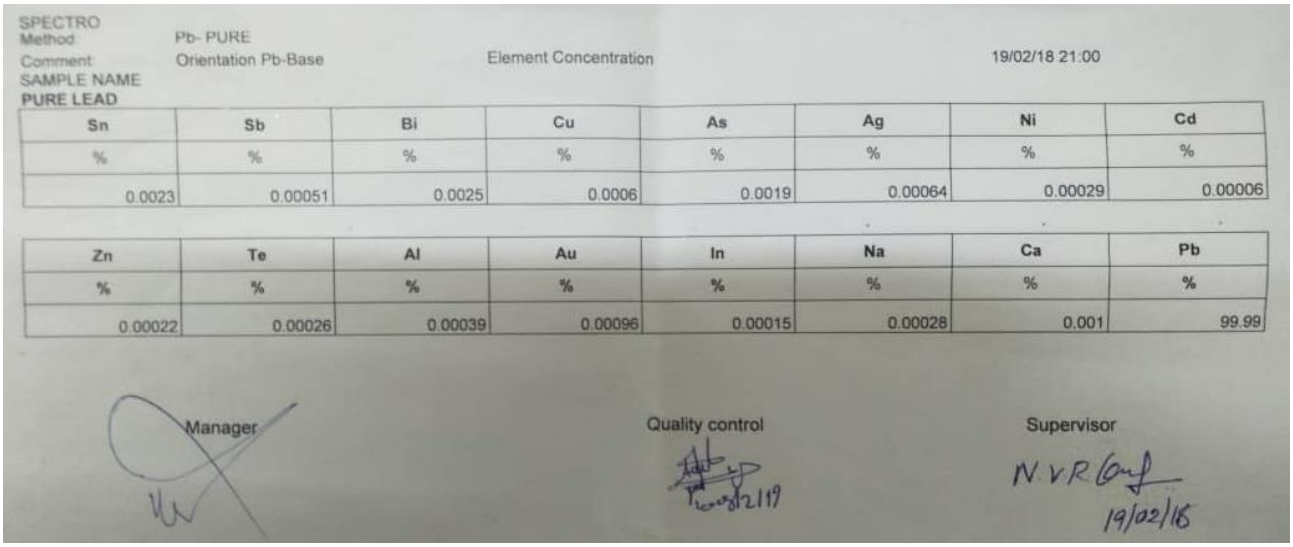

SPECTRO
Method Pb- PURE
Comment Orientation Pb-Base
Element Concentration
19/02/18 21:00
SAMPLE NAME
PURE LEAD

Sn	Sb	Bi	Cu	As	Ag	Ni	Cd
%	%	%	%	%	%	%	%
0.0023	0.00051	0.0025	0.0006	0.0019	0.00064	0.00029	0.00006

Zn	Te	Al	Au	In	Na	Ca	Pb
%	%	%	%	%	%	%	%
0.00022	0.00026	0.00039	0.00096	0.00015	0.00028	0.001	99.99

Figure 3.1: A picture of lead composition.

Figure 3.2: A picture of lead slabs.

3.1.2 Iron:-

The density of iron is 7.87 (g/cm^3**)** and its chemical composition as follows using metal analyzer device (Model: ESA PORT 07, Serial No: 12 082 ESP 07):

Date: 08/15/17 15:32:51
Sample:
Ref. Alloy:

Program: Fe_Orientation
Operator: Mr.Sami
Analysis Mode: Standardized concentration

	C %	Si %	Mn %	Cr %	Mo %	Ni %	Al %	Cu %	Ti %	V %
1	0.070	0.041	0.333	0.000	0.019	0.000	0.010	0.000	0.000	0.000
2	0.055	0.033	0.349	0.000	0.022	0.000	0.010	0.000	0.000	0.000
3	0.061	0.032	0.352	0.000	0.025	0.000	0.010	0.000	0.000	0.000
Avg.	0.062	0.035	0.345	0.000	0.022	0.000	0.010	0.000	0.000	0.000

	Nb %	Co %	W %	Pb %	Fe %
1	0.000	0.043	0.000	0.006	99.478
2	0.000	0.047	0.000	0.006	99.478
3	0.000	0.048	0.000	0.006	99.465
Avg.	0.000	0.046	0.000	0.006	99.474

Figure 3.3: A picture of iron composition.

Figure 3.4: A picture of iron slabs.

These samples of lead and iron were collected from Yarmouk Industrial Complex.

3.1.3 Concrete: concrete tests were carried out at University of Khartoum, Construction and Roads Research Institute, prior to the design of the concrete mix as follows:

1. **Aggregate:** the sieve analysis test for aggregate was performed and the results were graded and larger size than 20 mm; in accordance with BS 882,1992.

2. **Sand:** the sieve analysis test was performed and the results were coarse sand and gradient zone1; in according with BS 882, 1992. The silt ratio in sand was tested and the results were 2.5%, accordance with BS 882, 1992. The standard recommends that the silt should not exceed5%.

3. **Cement:** the initial uncertainty time, the time of final uncertainty and the water ratio needed to make a standard cement paste were performed, according to BS 12, 1996.Cement resistance was tested and the results were found to be as follows:

Table 3.1: Test of cement resistance.

Cement Test	Results	Specification
initial setting time	1 hour and 15 minutes	Min. 1 hour
final setting time	4 hours and 22 minutes	Max. 10 hours
Water percentage	29.5%	Max. 33%
Strength	At 2 days 21 N/mm^2	Min. 10 N/mm^2
	At 28 days 44.5 N/mm^2	Min. 42.5 N/mm^2

Concrete Mix Design:

The concrete mix was designed accordance with the British design method BS 882, 1992, and the design result was found to be as, cement 375 kg, gravel 1115 kg, sand 805 kg, and water 185 kg.

The mixture was designed to give strength of 25 n / mm2 and the concrete was then mixed and casted into (150 * 150 * 150 mm and 100 * 100 * 100 mm) cubes.

The casting method is as follows:

Fill the cube on three layers, and doubt each layer with iron bar dedicated to casting, the number of 35 blows per layer.

Figure 3.5: A picture of concrete cubes.

3.1.4 Cement mortar:

Cement and sand tested mix by 1: 4, 1 cement was mixed with 4 sand and 0.5 water and Cubes were casting in the same way for the concrete mix.

Figure 3.6: A picture of cement mortar cubes.

3.1.5 Clay:-

Proctor test was performed of clay sample to determine the optimum moisture content of the clay. The result was found to be 40% optimum moisture content, of clay weight.

Figure 3.7: A picture of clay cubes.

Concrete, cement and clay were made as cubes, the mass was measured with Digital balance (model, CTG12H+, serial number 3901049005) then the density was calculated and found to be 2.374 (g/cm^3), 2.139 (g/cm^3) and 1.335 (g/cm^3) respectively.

3.2 Methods

Gamma ray shielding material attenuated the radiation beam through the density, so materials with different densities can attenuate differently.

3.2.1 Experimental Setup

The intensity of radiation was the quantity (air Kerma) which is measured by standard ionization chamber: Spherical 1 liter chamber LS-01type 32002 with PTW electrometer and polarizing voltage 400 V(max), which calibrated at IAEA laboratories in 2012, wall material from POM (CH2O)n, electrode material graphite coated energy ranged from 45 KeV to 50 MeV.

Figure 3.8: Experimental setup of determination of gamma radiation intensity (air kerma) before placing and after shielding samples.

Measurements were performed at the irradiation room at the Secondary Standard dosimetry laboratory Khartoum at SAEC on model OB-85

gamma calibrator manufactured by buchler GmbH by using Cs-137, Co-60 radioactive sources. Experimental measurements were made using a secondary standard ionization chamber which has a volume of 1000 cm^3, The ionization chamber was placed with its reference point which was chosen to be the center of the sphere relative to the reference source 2m distances from source to reference point (SSD). The holder of shielding samples was placed closed to OB-85 gamma calibrator, then shielding materials were placed inside the holder one by one for the same material or mixed with other material, these procedures were followed for all shielding materials. Through these measurements the intensity of radiation was recorded, before and after shielding material in the holder. The linear attenuation coefficient, mass attenuation coefficient and half value layer were calculated using equations **(2.4), (2.6)** and **(2.7)** mentioned in chapter2**.** Calculated linear attenuation coefficient of combined samples were estimated by the equation **(2.5)** mentioned in chapter2 as well**.**

Through all these procedures the result for each shielding material sample was compared with each other using statistical analysis and scientific view.

Chapter Four

RESULTS

The results is carried out to obtain and evaluate the gamma ray shielding properties through attenuation of some building materials available in Sudan.

Table 4.1: The value of doses through different lead slabs thickness by using Cs-137 source. The measuring time, temperature and pressure were 60s, 24.6c^0 and 968.9hpa, respectively.

Material	Thickness (cm)	Frequency	Mean (Dose(µGy))	Std. Deviation
Lead	0.000	10	474.76	0.1075
	0.154	10	400.46	0.1350
	0.472	10	274.69	0.0316
	0.812	10	190.42	0.0422
	0.966	10	164.63	0.0675

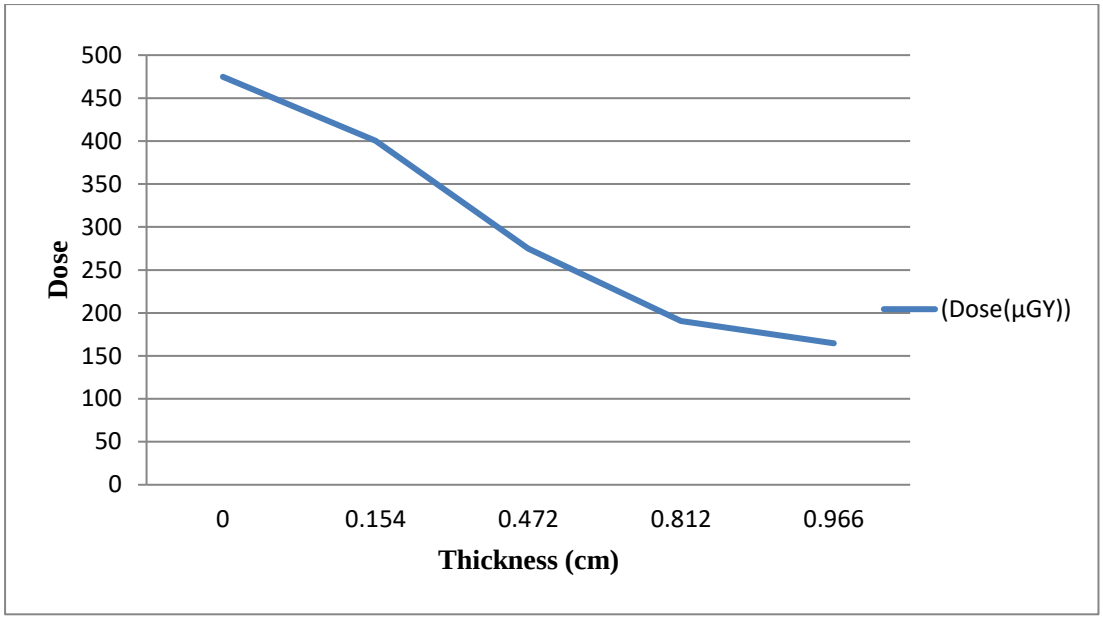

Figure 4.1: Attenuation of Cs-137 gamma rays as they pass through lead samples.

Table 4.2: The value of doses through different lead slab's thickness by using Co-60 source. The measuring time, temperature and pressure were 30s, 24.5c^0 and 968.9hpa, respectively.

Material	Thickness (cm)	Frequency	Mean (Dose(µGy))	Std. Deviation
Lead	0.000	10	1.906	0.007
	0.154	10	1.744	0.003
	0.472	10	1.428	0.003
	0.812	10	1.169	0.002
	0.966	10	1.079	0.002

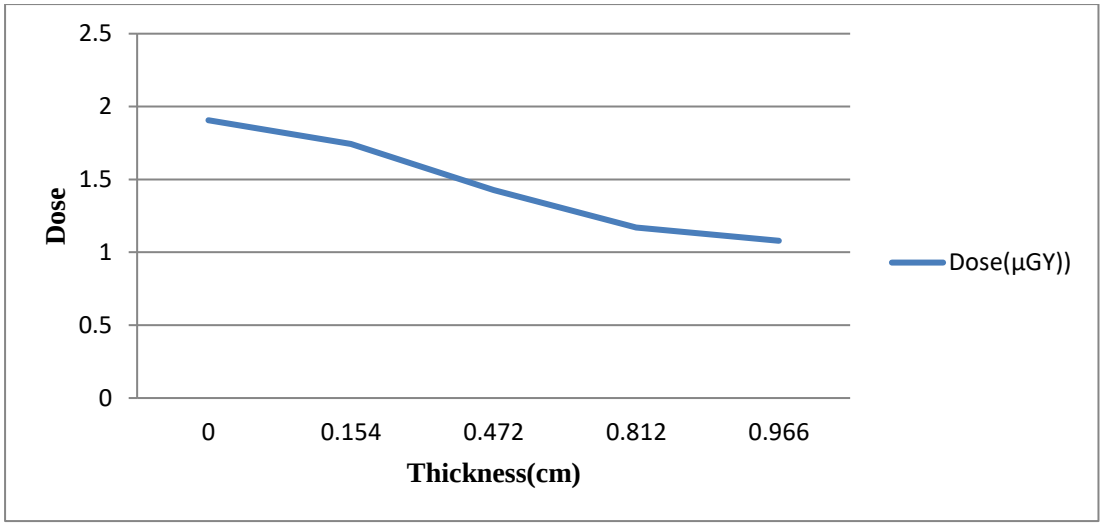

Figure 4.2: Attenuation of Co-60 gamma rays as they pass through lead samples.

Table 4.3: Attenuation coefficient and half value layer for lead slabs using Cs-137 gamma rays with initial dose 474.76 µGy.

Thickness(cm)	Dose (µGy)	Linear attenuation coefficient µ (cm^{-1})	Mass attenuation coefficient μ_m (cm^2/g)	Half value layer (cm)
0.154	400.46	1.105	0.097	0.627
0.472	274.69	1.159	0.102	0.597
0.812	190.42	1.125	0.099	0.615
0.966	164.63	1.096	0.096	0.632

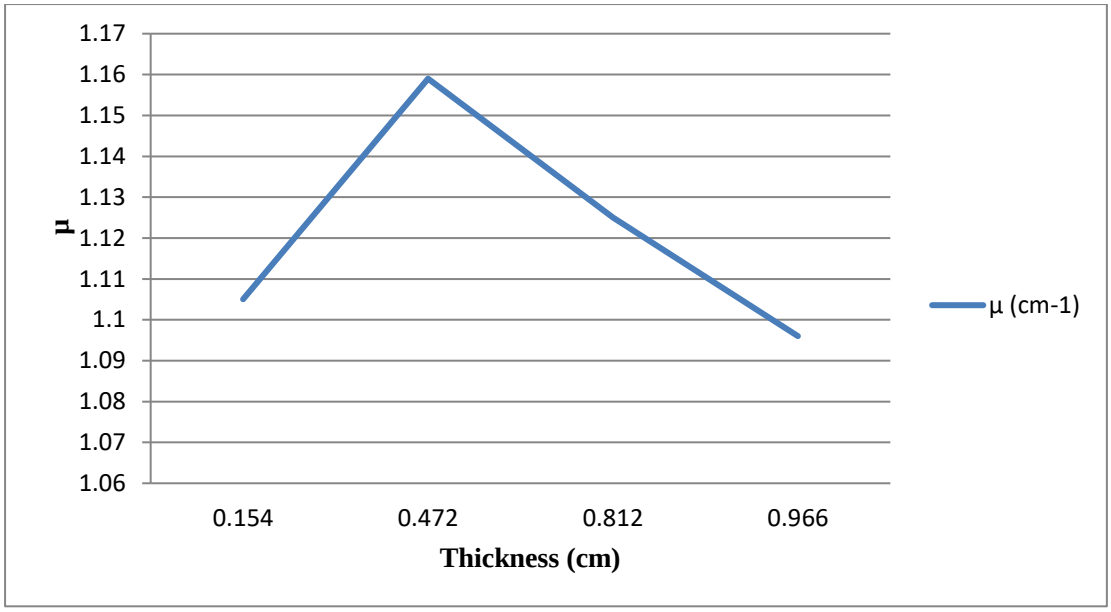

Figure 4.3: Linear attenuation coefficient of Cs-137 source through lead samples as a function of the thickness.

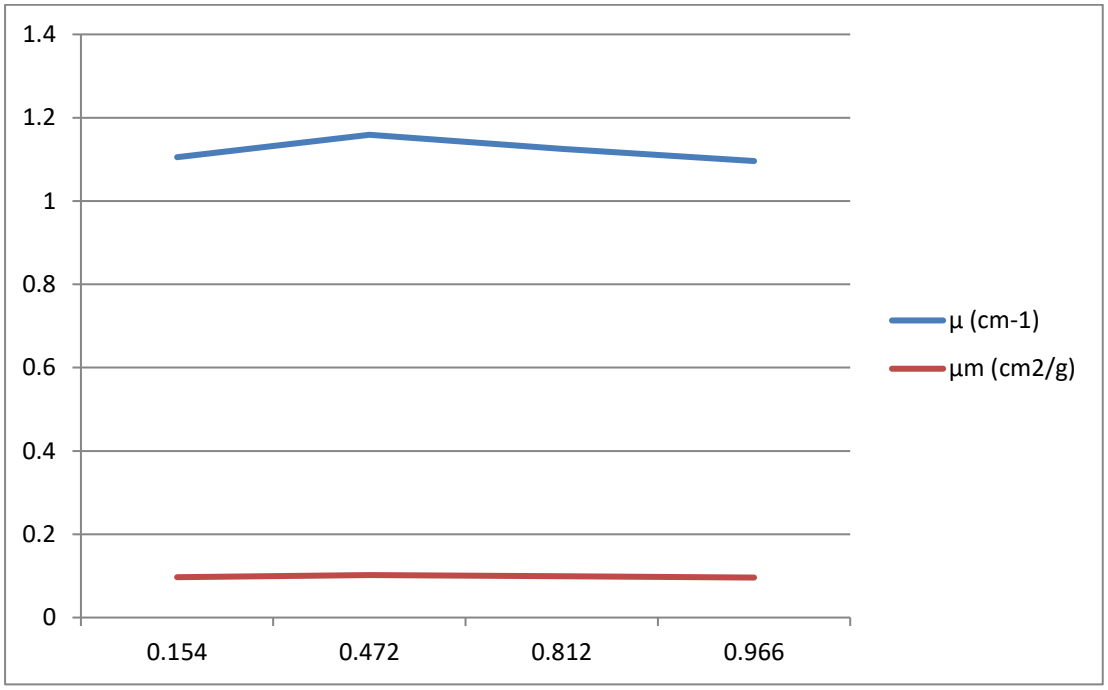

Figure 4.4: Comparison of linear and mass attenuation coefficient of Cs-137 gamma rays through lead samples thickness.

Table 4.4: Attenuation coefficient and half value layer for lead slabs using Co-60 gamma rays with initial dose1.906 µGy.

Thickness (cm)	Dose (µGy)	Linear attenuation coefficient µ (cm^{-1})	Mass attenuation coefficient μ_m (cm^2/g)	Half value layer (cm)
0.154	1.744	0.576	0.050	1.211
0.472	1.428	0.611	0.053	1.132
0.812	1.169	0.602	0.053	1.151
0.966	1.079	0.589	0.051	1.176

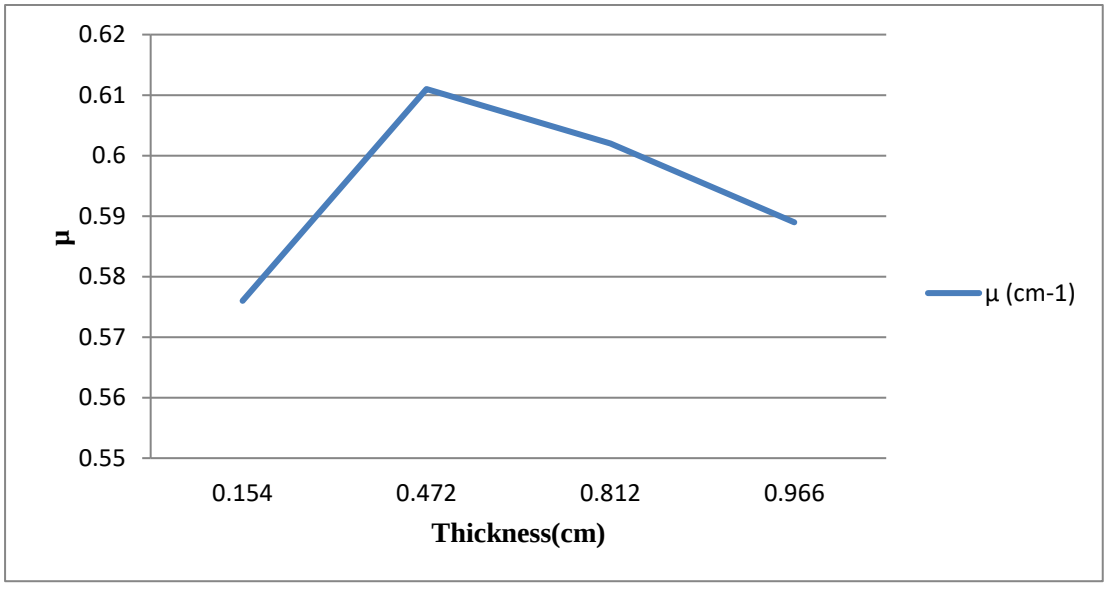

Figure 4.5: Linear attenuation coefficient of Co-60 source through lead samples as a function of the thickness.

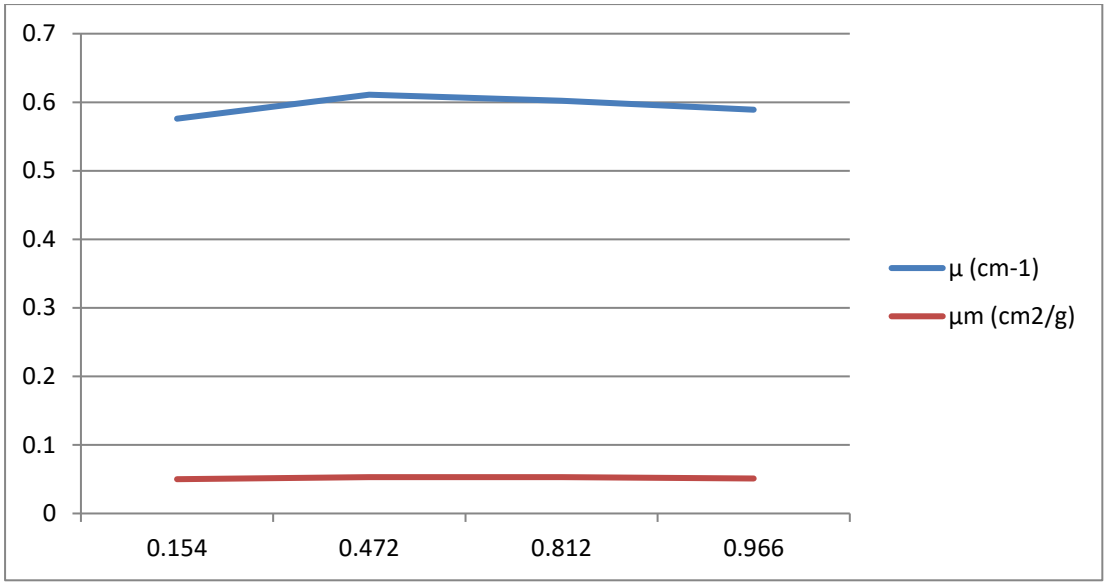

Figure 4.6: Comparison of linear and mass attenuation coefficient of Co-60 gamma rays through lead samples thickness.

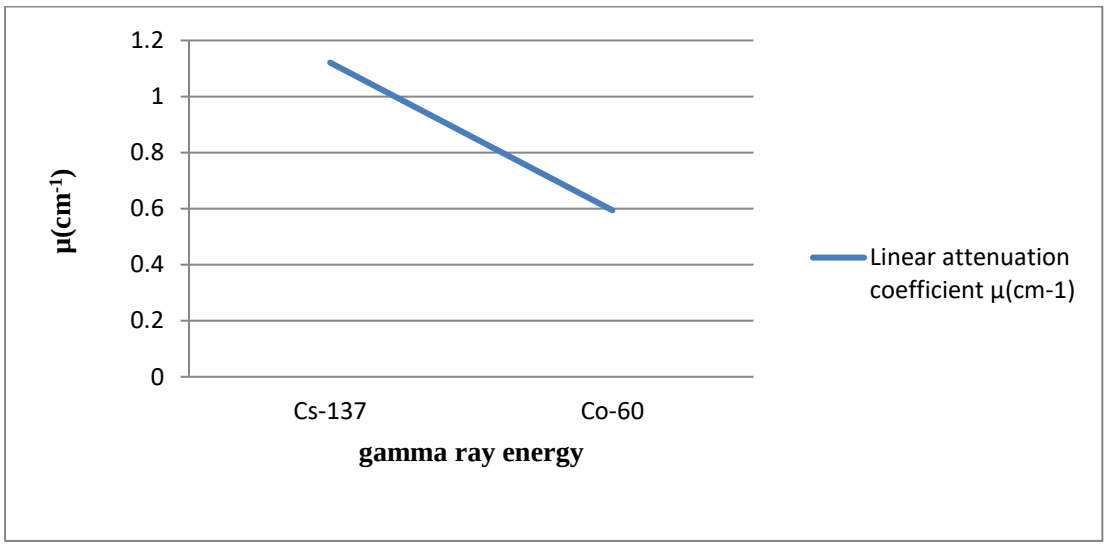

Figure 4.7: Linear attenuation coefficient of lead samples through different gamma rays energies.

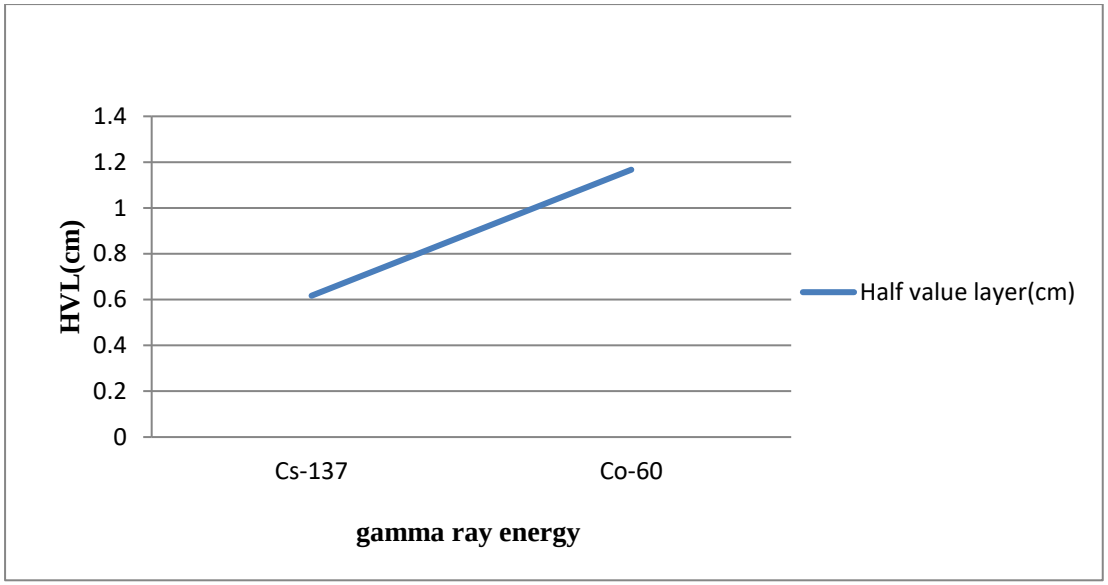

Figure 4.8: Half value layer of lead samples through different gamma rays energies.

Table 4.5: The value of doses through different iron slabs thickness by using Cs-137 source. The measuring time, temperature and pressure were 60s, 24.6$c^0$and 968.9hpa, respectively.

Material	Thickness (cm)	Frequency	Mean (Dose(µGy))	Std. Deviation
Iron	0.000	10	474.74	0.1174
	0.202	10	434.58	0.0789
	0.522	10	373.03	0.0823
	1.036	10	289.54	0.0516
	1.350	10	249.21	0.0568

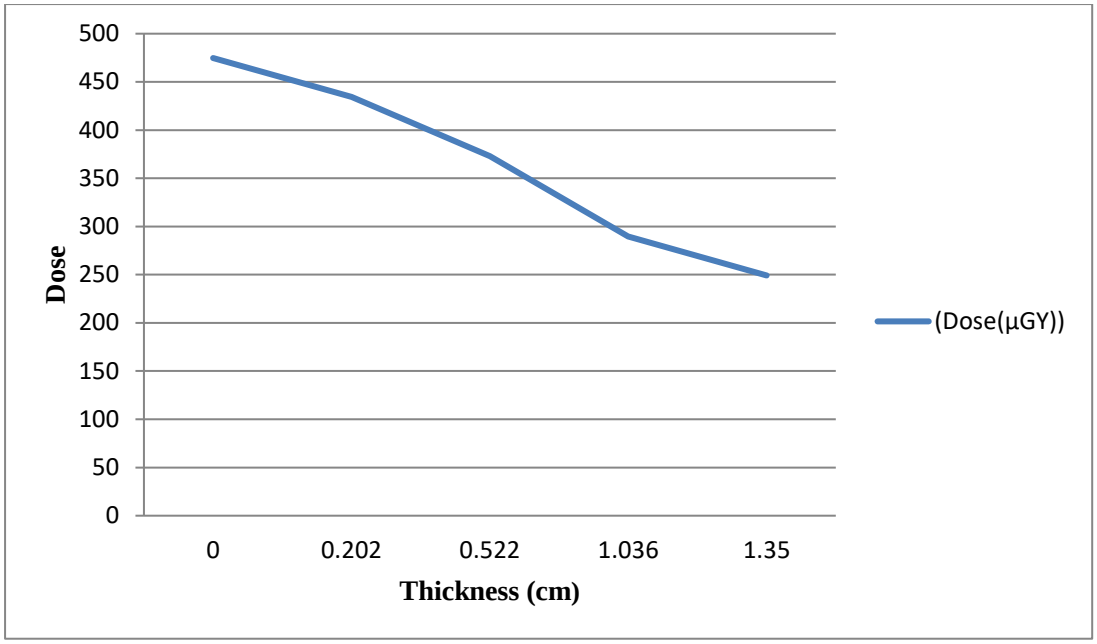

Figure 4.9: Attenuation of Cs-137 gamma rays as they pass through iron samples.

Table 4.6: The value of doses through different iron slabs thickness by using Co-60 source. The measuring time, temperature and pressure were 30s, 24.6c^0 and 968.9hpa, respectively.

Material	Thickness (cm)	Frequency	Mean (Dose(µGy))	Std. Deviation
Iron	0.000	10	1.906	0.007
	0.202	10	1.797	0.002
	0.522	10	1.602	0.003
	1.036	10	1.346	0.002
	1.350	10	1.202	0.003

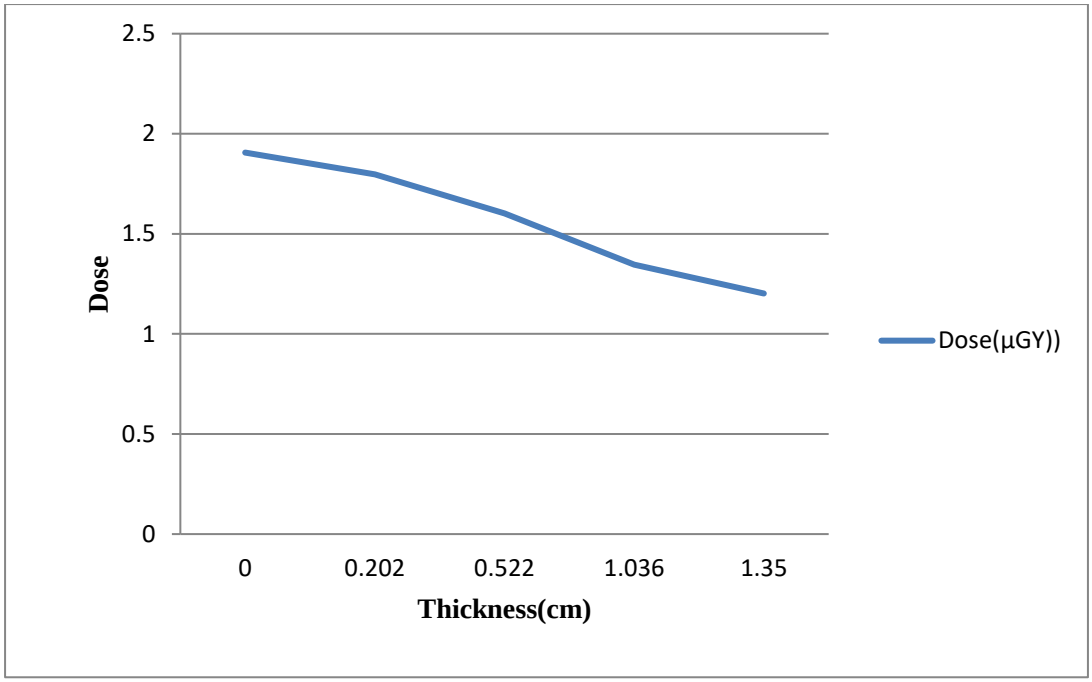

Figure 4.10: Attenuation of Co-60 gamma rays as they pass through iron samples.

Table 4.7: Attenuation coefficient and half value layer for iron slabs using Cs-137 gamma rays with initial dose 474.76 µGy.

Thickness(cm)	Dose (µGy)	Linear attenuation coefficient µ (cm^{-1})	Mass attenuation coefficient μ_m (cm^2/g)	Half value layer (cm)
0.202	434.58	0.437	0.055	1.583
0.522	373.03	0.462	0.058	1.500
1.036	289.54	0.477	0.060	1.451
1.350	249.21	0.477	0.060	1.451

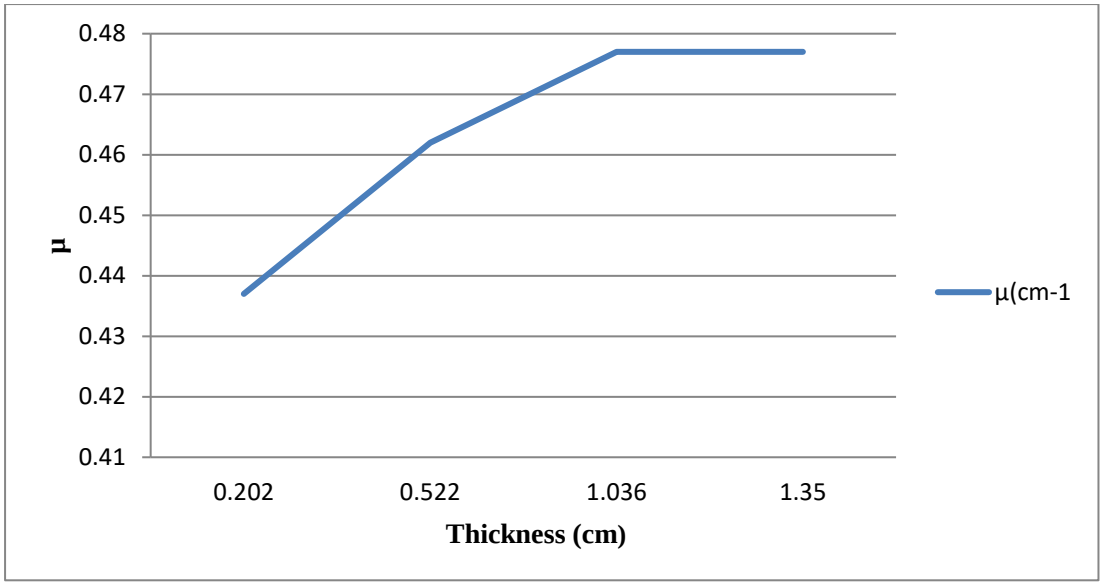

Figure 4.11: Linear attenuation coefficient of Cs-137 source through iron samples as a function of the thickness.

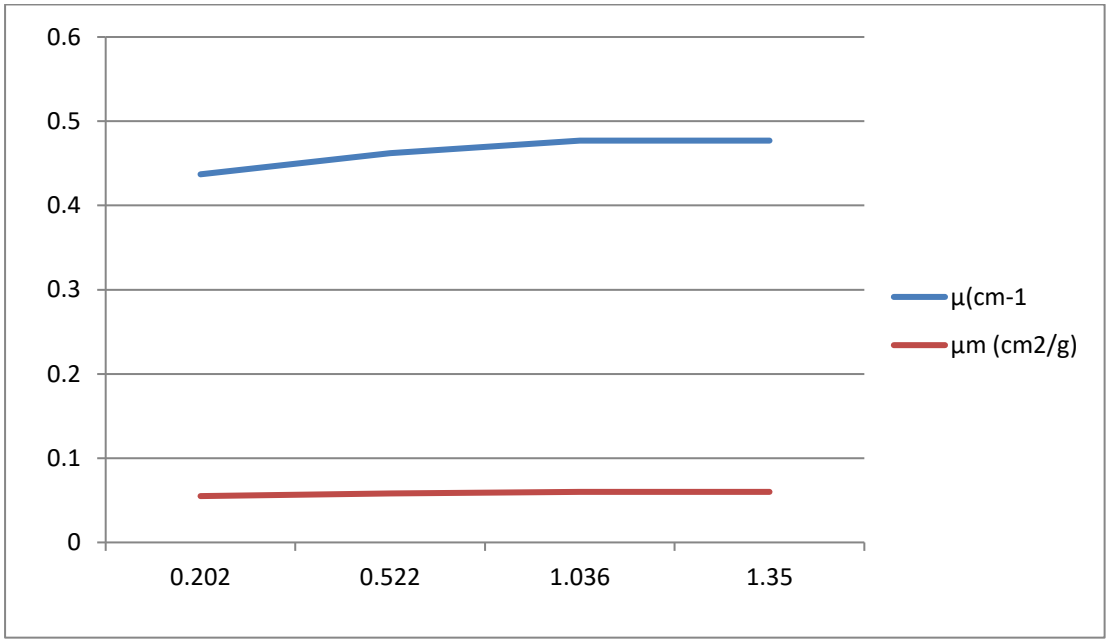

Figure 4.12: Comparison of linear and mass attenuation coefficient of Cs-137 gamma rays through iron samples thickness.

Table 4.8: Attenuation coefficient and half value layer for iron slabs using Co-60 gamma rays with initial dose1.906 µGy.

Thickness (cm)	Dose (µGy)	Linear attenuation coefficient µ (cm^{-1})	Mass attenuation coefficient μ_m (cm^2/g)	Half value layer (cm)
0.202	1.797	0.291	0.037	2.377
0.522	1.602	0.332	0.042	2.081
1.036	1.346	0.335	0.042	2.063
1.350	1.202	0.341	0.043	2.029

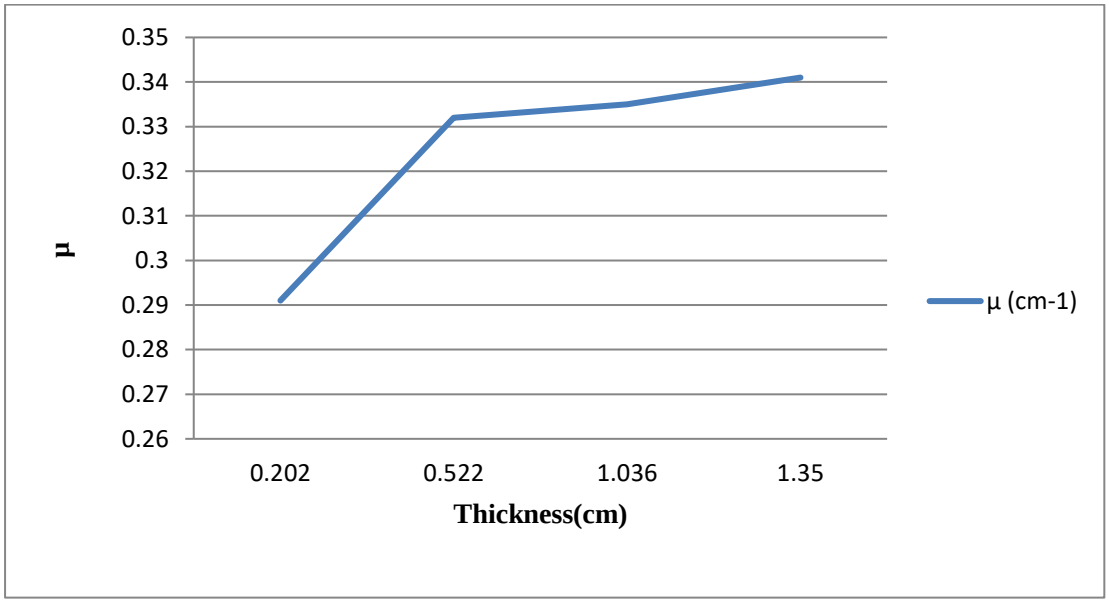

Figure 4.13: Linear attenuation coefficient of Co-60 source through iron samples as a function of the thickness.

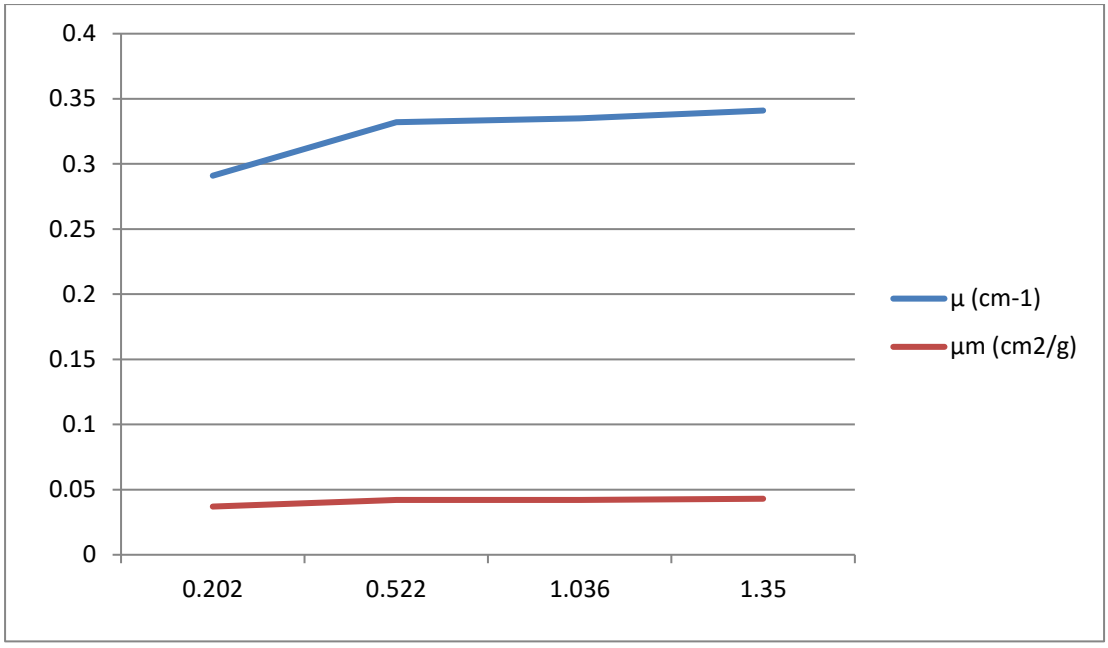

Figure 4.14: Comparison of linear and mass attenuation coefficient of Co-60 gamma rays through iron samples thickness.

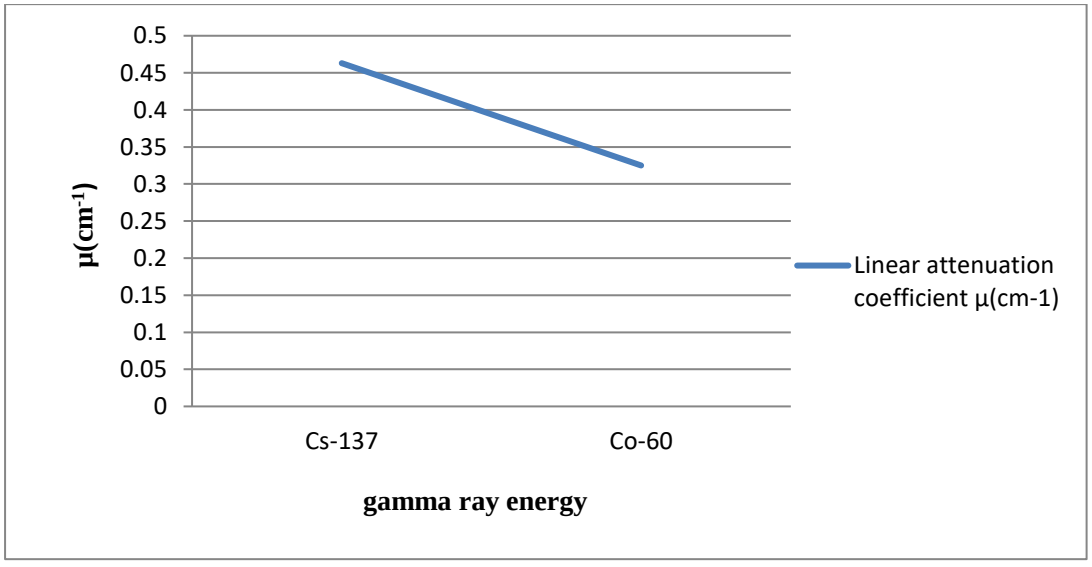

Figure 4.15: Linear attenuation coefficient of iron samples through different gamma rays energies.

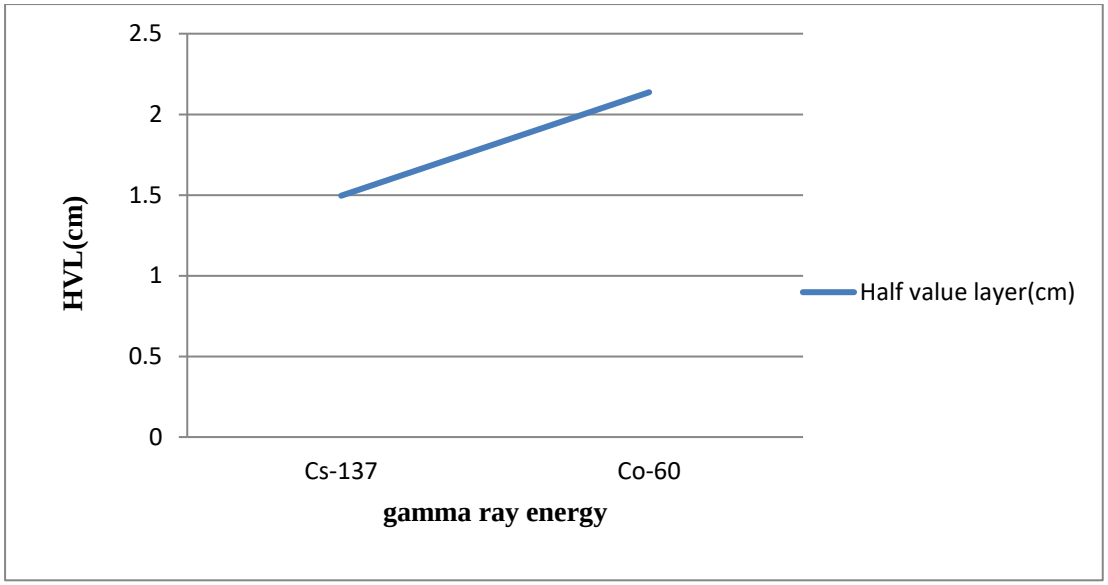

Figure 4.16: Half value layer of iron samples through different gamma rays energies.

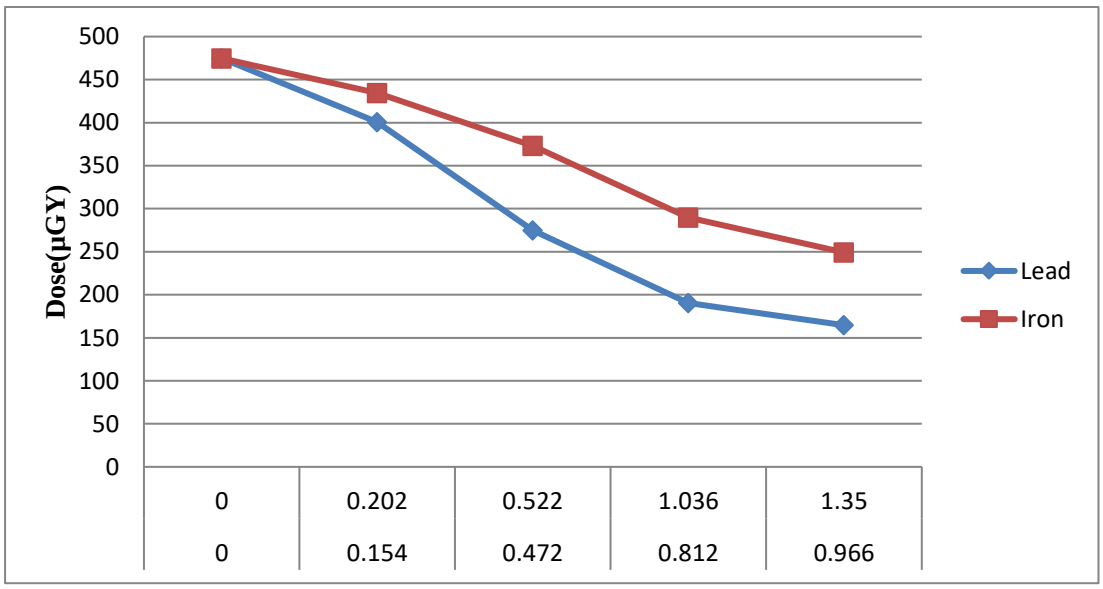

Figure 4.17: Attenuation of Cs-137 gamma rays as a function of thickness through different shield materials.

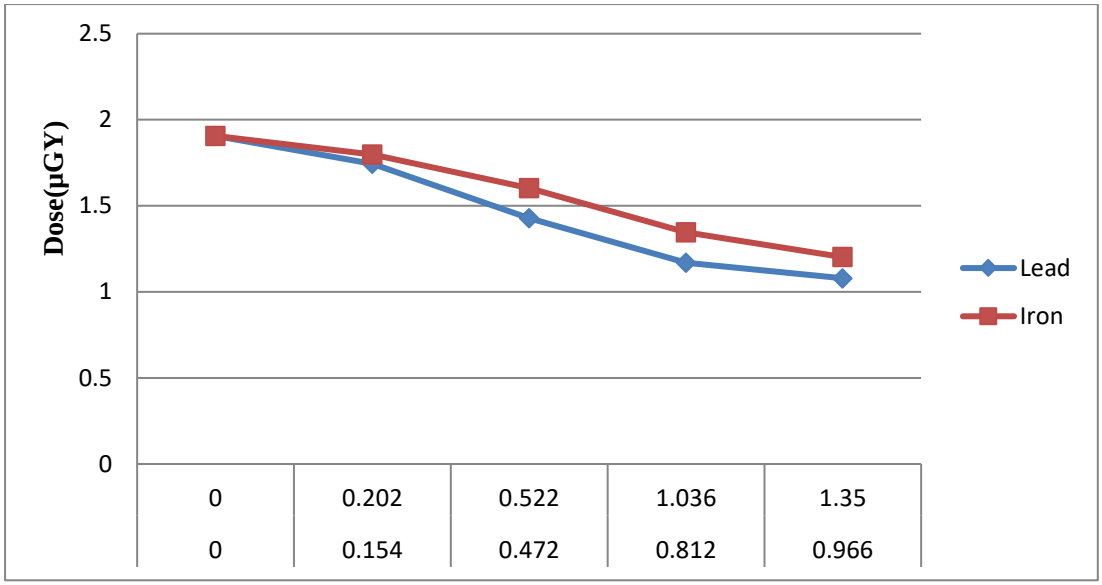

Figure 4.18: Attenuation of Co-60 gamma rays as a function of thickness through different shield materials.

Table 4.9: The value of doses through different concrete cubic's thickness by using Cs-137 source. The measuring time, temperature and pressure were 30s, 30 c^0 and 964.7hpa, respectively.

Material	Thickness (cm)	Frequency	Mean (Dose(µGy))	Std. Deviation
Concrete	0	10	225.65	0.0527
	10	10	43.37	0.0125
	20	10	9.45	0.0062
	25	10	4.93	0.0070
	35	10	2.27	0.0027

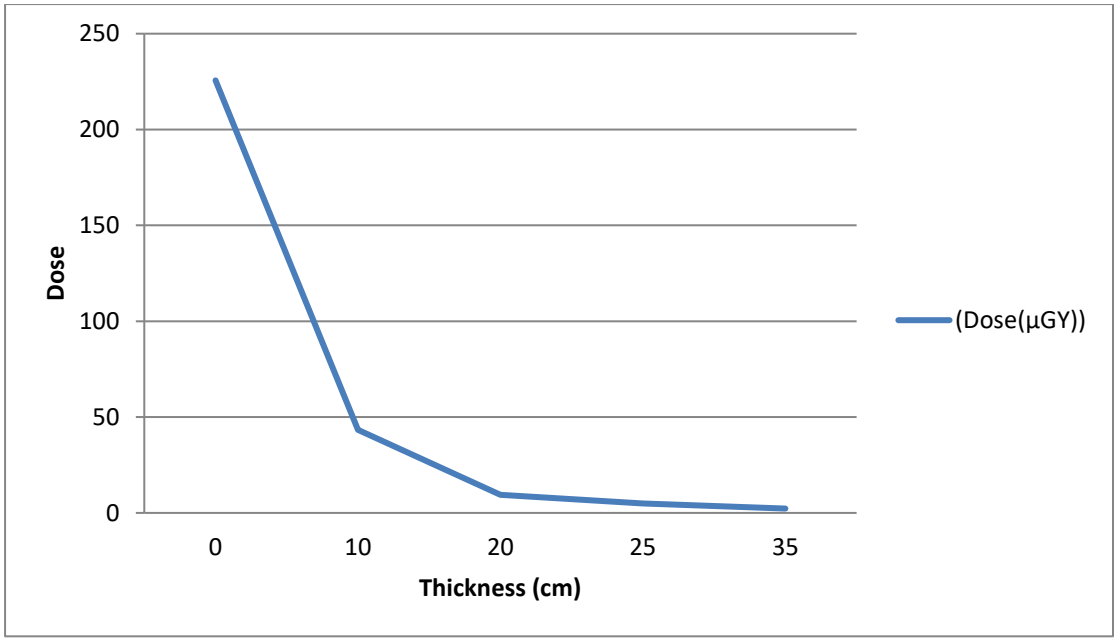

Figure 4.19: Attenuation of Cs-137 gamma rays as they pass through concrete samples.

Table 4.10: The value of doses through different concrete cubic's thickness by using Co-60 source. The measuring time, temperature and pressure were 30s, 34.5c^0 and 964.8hpa, respectively.

Material	Thickness (cm)	Frequency	Mean (Dose(µGy))	Std. Deviation
Concrete	0	10	1.906	0.007
	10	10	0.561	0.002
	20	10	0.178	0.002
	25	10	0.109	0.001
	35	10	0.053	0.001

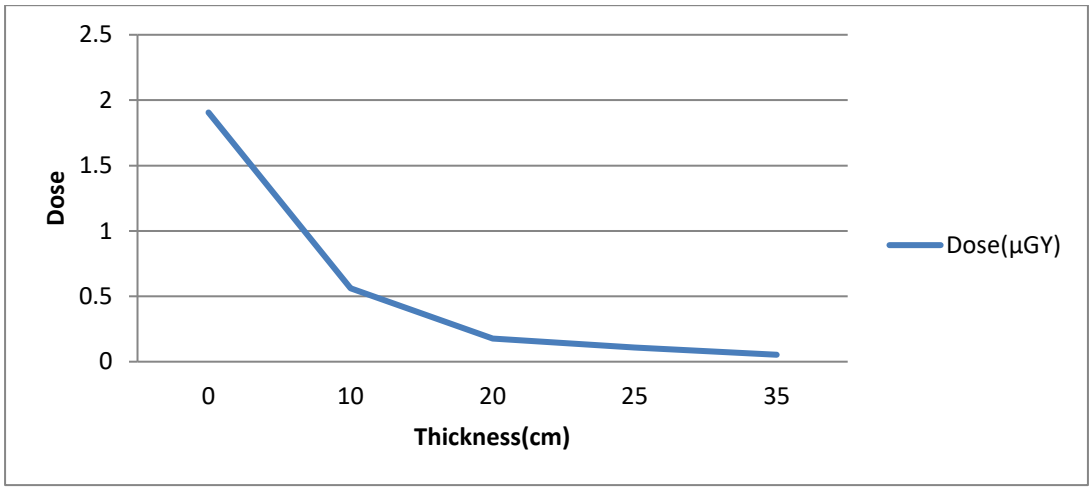

Figure 4.20: Attenuation of Co-60 gamma rays as they pass through concrete samples**.**

Table 4.11: Attenuation coefficient and half value layer for concrete cubic's using Cs-137 gamma rays with initial dose 225.65 µGy.

Thickness (cm)	**Dose (µGy)**	**Linear attenuation coefficient µ (cm^{-1})**	**Mass attenuation coefficient μ_m (cm^2/g)**	**Half value layer (cm)**
10	43.37	0.164	0.069	4.202
20	9.45	0.158	0.066	4.368
25	4.93	0.152	0.064	4.531
35	2.27	0.131	0.055	5.273

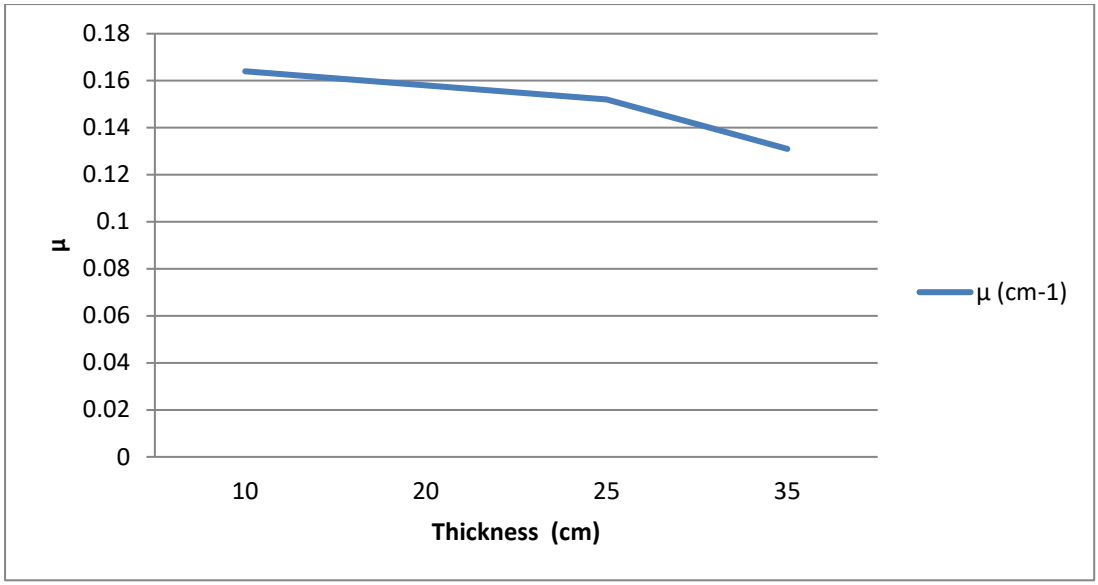

Figure 4.21: Linear attenuation coefficient of Cs-137 source through concrete samples as a function of the thickness.

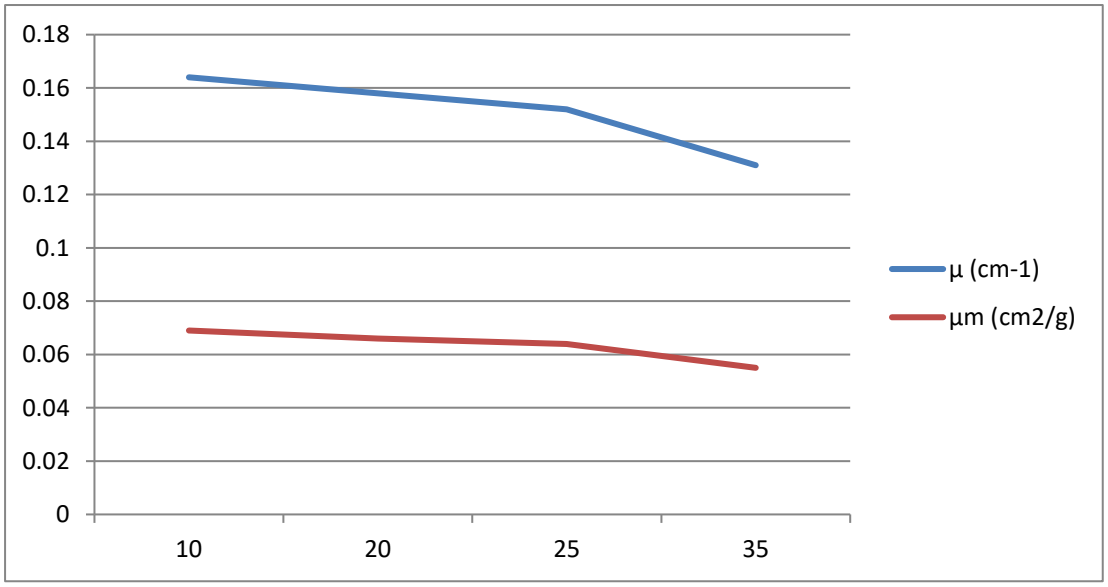

Figure 4.22: Comparison of linear and mass attenuation coefficient of Cs-137 gamma rays through concrete samples thickness.

Table 4.12: Attenuation coefficient and half value layer for concrete cubic's using Co-60 gamma rays with initial dose1.906 µGy.

Thickness (cm)	Dose (µGy)	Linear attenuation coefficient µ (cm^{-1})	Mass attenuation coefficient μ_m (cm^2/g)	Half value layer (cm)
10	0.561	0.122	0.051	5.666
20	0.178	0.118	0.049	5.845
25	0.109	0.114	0.042	6.054
35	0.053	0.102	0.043	6.770

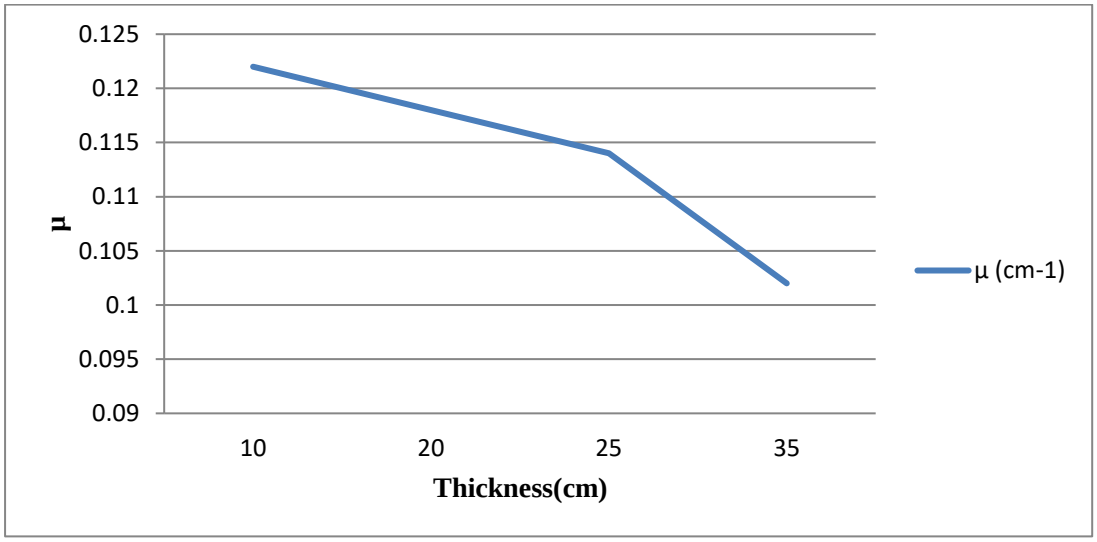

Figure 4.23: Linear attenuation coefficient of Co-60 source through concrete samples as a function of the thickness.

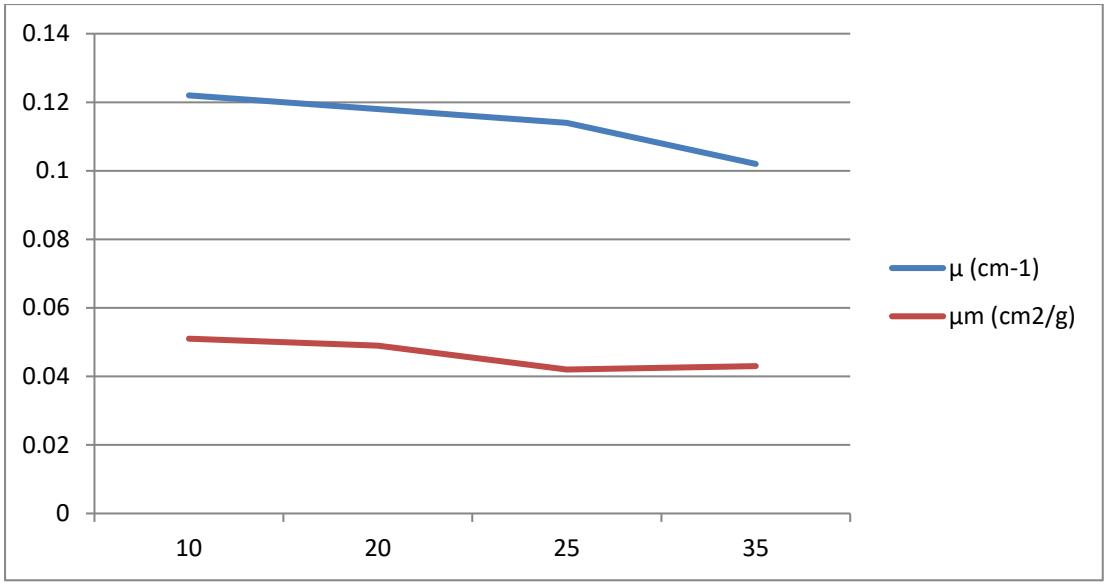

Figure 4.24: Comparison of linear and mass attenuation coefficient of Co-60 gamma rays through concrete samples thickness.

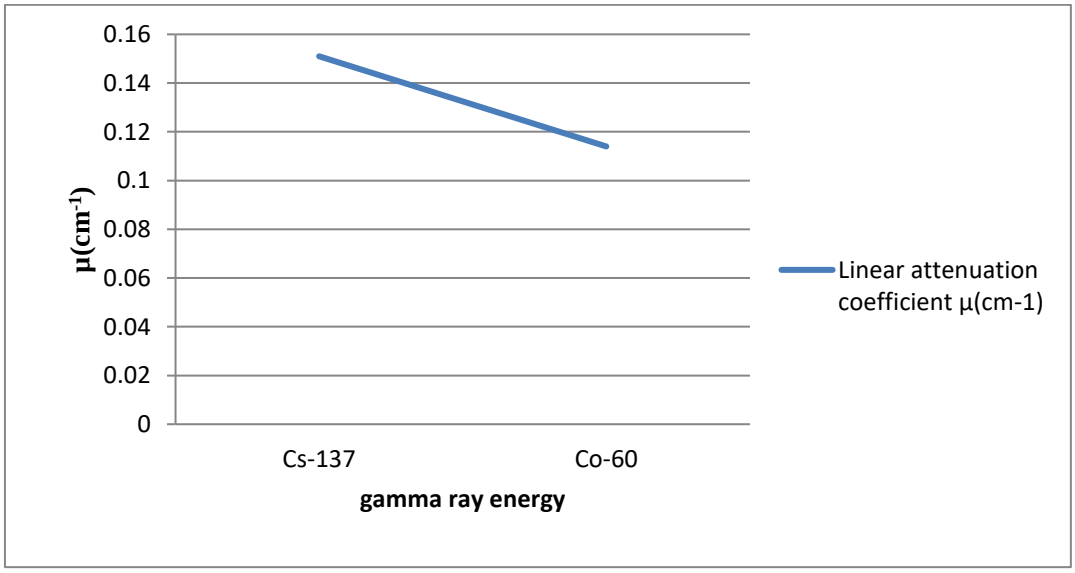

Figure 4.25: Linear attenuation coefficient of concrete samples through different gamma rays energies.

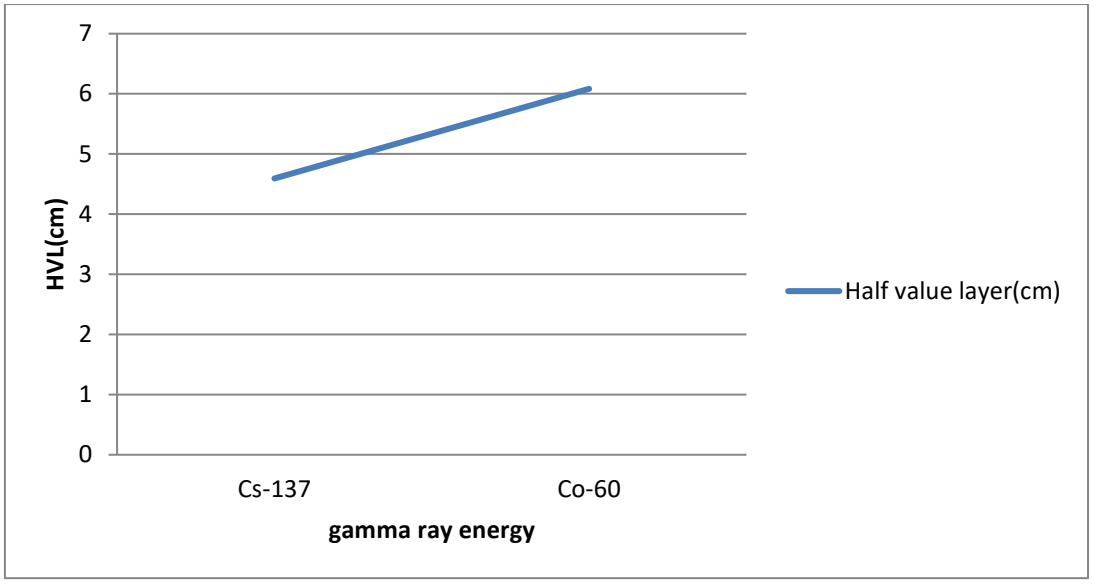

Figure 4.26: Half value layer of concrete samples through different gamma rays energies.

Table 4.13: The value of doses through different cement cubic's thickness by using Cs-137 source. The measuring time, temperature and pressure were 30s, 30 c^0 and 964.7hpa, respectively.

Material	Thickness (cm)	Frequency	Mean (Dose(µGy))	Std. Deviation
Cement	0	10	225.65	0.0527
	10	10	49.99	0.0210
	20	10	12.10	0.0085
	25	10	7.04	0.0103
	35	10	2.81	0.0035

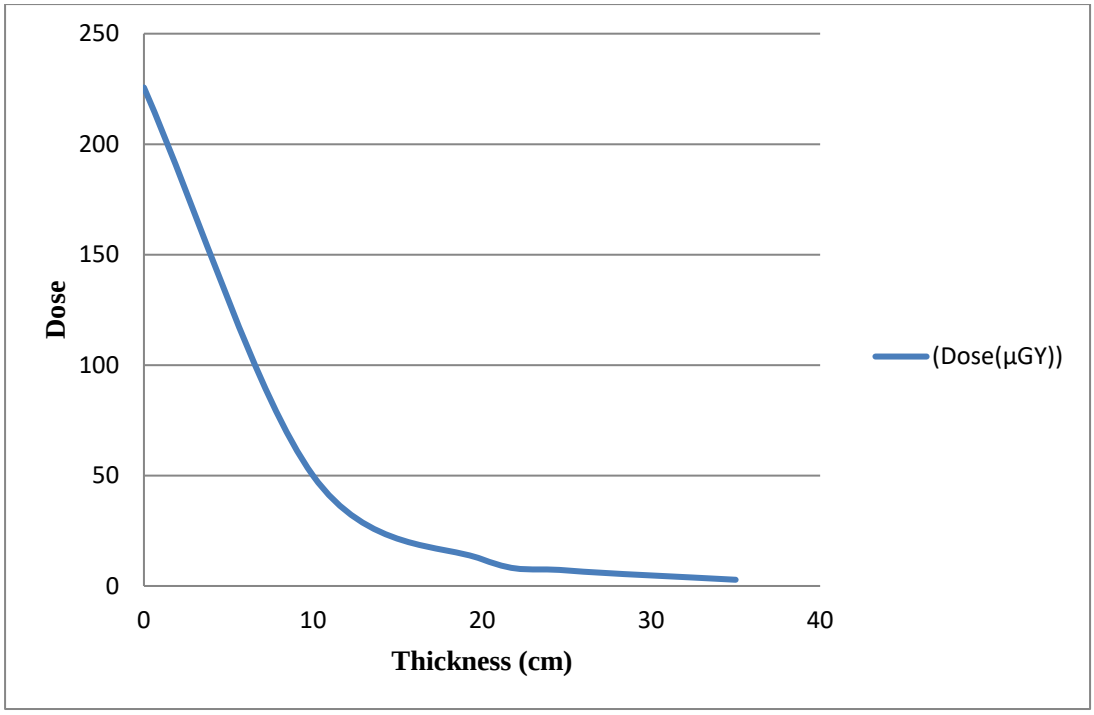

Figure 4.27: Attenuation of Cs-137 gamma rays as they pass through cement samples.

Table 4.14: The value of doses through different cement cubic's thickness by using Co-60 source. The measuring time, temperature and pressure were 30s, 34.5 c^0 and 964.8hpa, respectively.

Material	Thickness (cm)	Frequency	Mean (Dose(µGy))	Std. Deviation
Cement	0	10	1.906	0.007
	10	10	0.636	0.001
	20	10	0.218	0.001
	25	10	0.141	0.000
	35	10	0.072	0.001

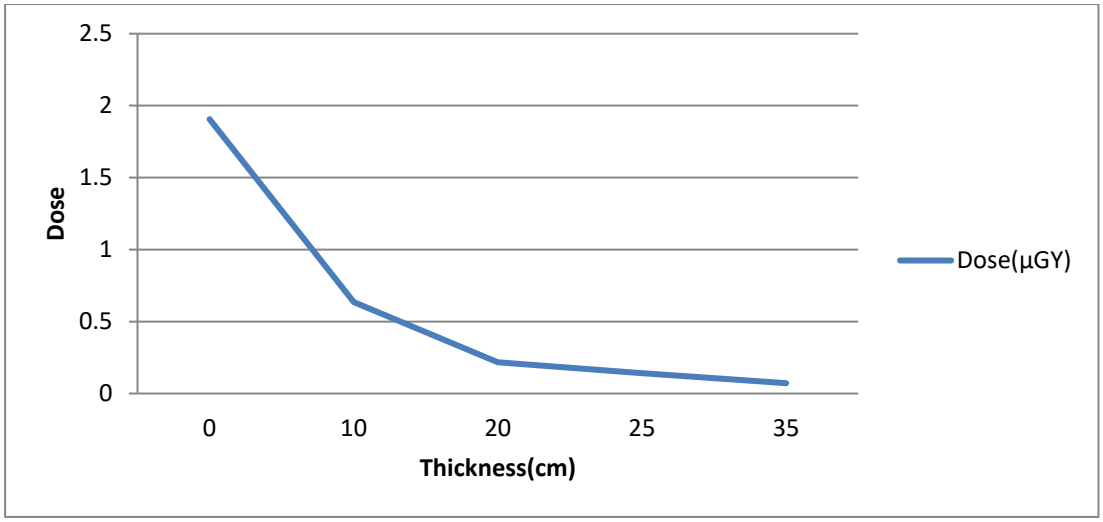

Figure 4.28: Attenuation of Co-60 gamma rays as they pass through cement samples.

Table 4.15: Attenuation coefficient and half value layer for cement cubic's using Cs-137 gamma rays with initial dose 225.65 µGy.

Thickness (cm)	**Dose (µGy)**	**Linear attenuation coefficient µ (cm^{-1})**	**Mass attenuation coefficient μ_m (cm^2/g)**	**Half value layer (cm)**
10	49.99	0.150	0.070	4.598
20	12.10	0.146	0.068	4.737
25	7.04	0.138	0.064	4.996
35	2.81	0.125	0.058	5.530

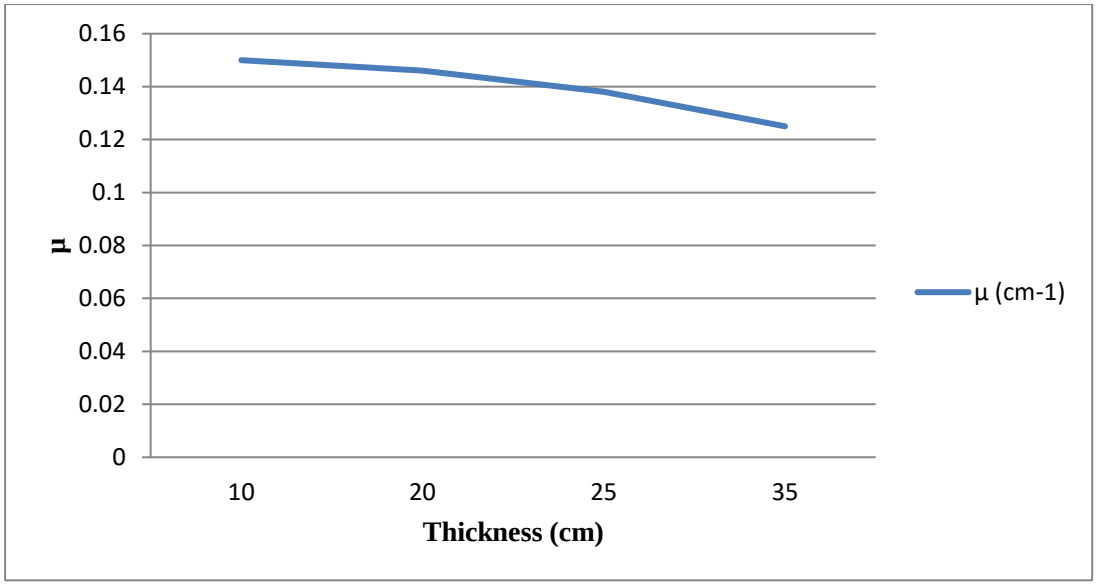

Figure 4.29: Linear attenuation coefficient of Cs-137 source through cement samples as a function of the thickness.

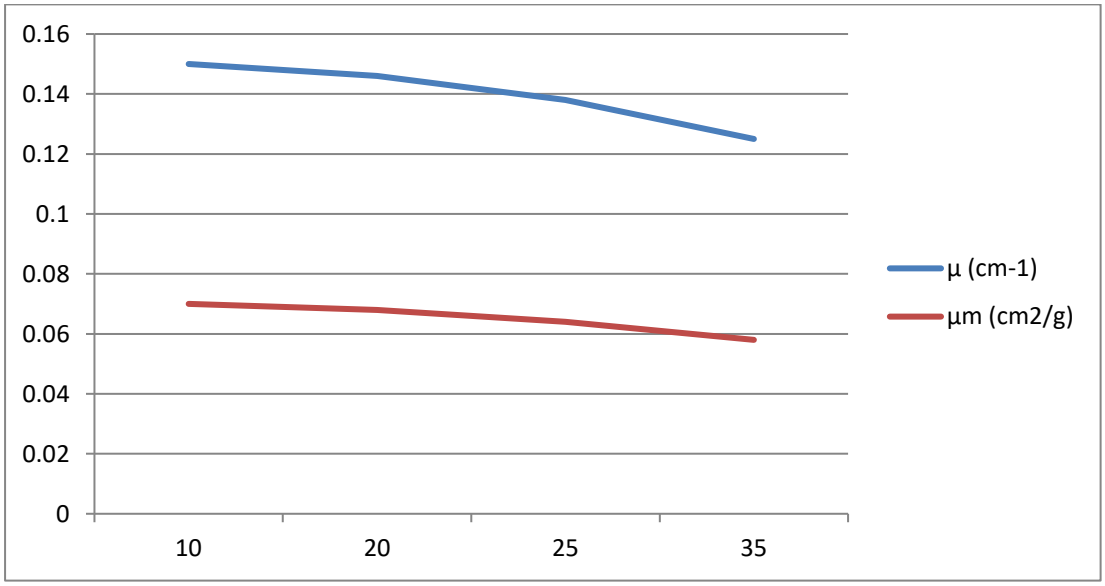

Figure 4.30: Comparison of linear and mass attenuation coefficient of Cs-137 gamma rays through cement samples thickness.

Table 4.16: Attenuation coefficient and half value layer for cement cubic's using Co-60 gamma rays with initial dose1.906 µGy.

Thickness (cm)	Dose (µGy)	Linear attenuation coefficient µ (cm^{-1})	Mass attenuation coefficient μ_m (cm^2/g)	Half value layer (cm)
10	0.636	0.109	0.051	6.314
20	0.218	0.108	0.050	6.392
25	0.141	0.104	0.048	6.653
35	0.072	0.093	0.043	7.403

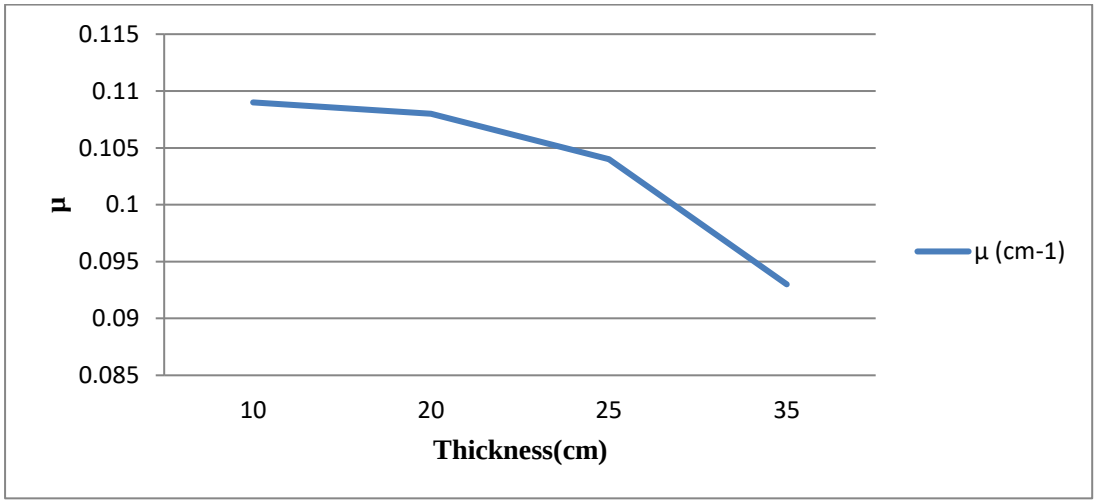

Figure 4.31: Linear attenuation coefficient of Co-60 source through cement samples as a function of the thickness.

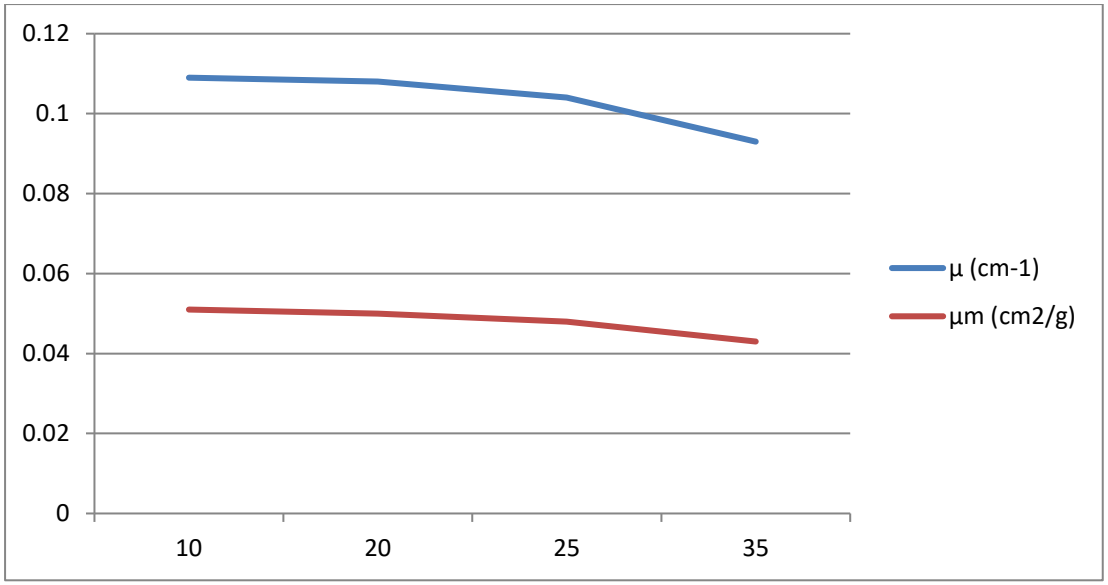

Figure 4.32: Comparison of linear and mass attenuation coefficient of Co-60 gamma rays through cement samples thickness.

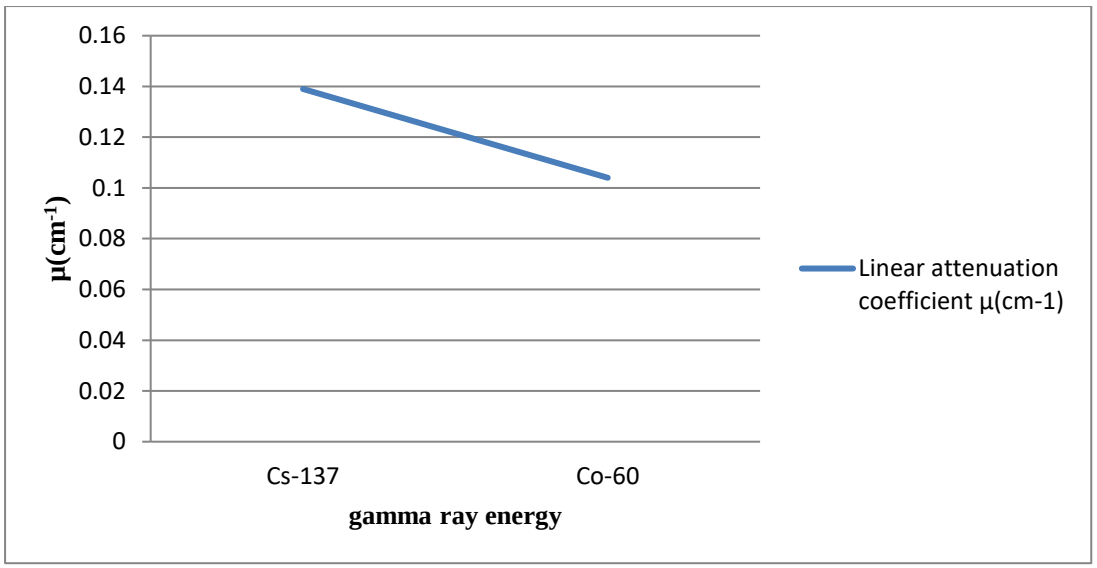

Figure 4.33: Linear attenuation coefficient of cement samples through different gamma rays energies.

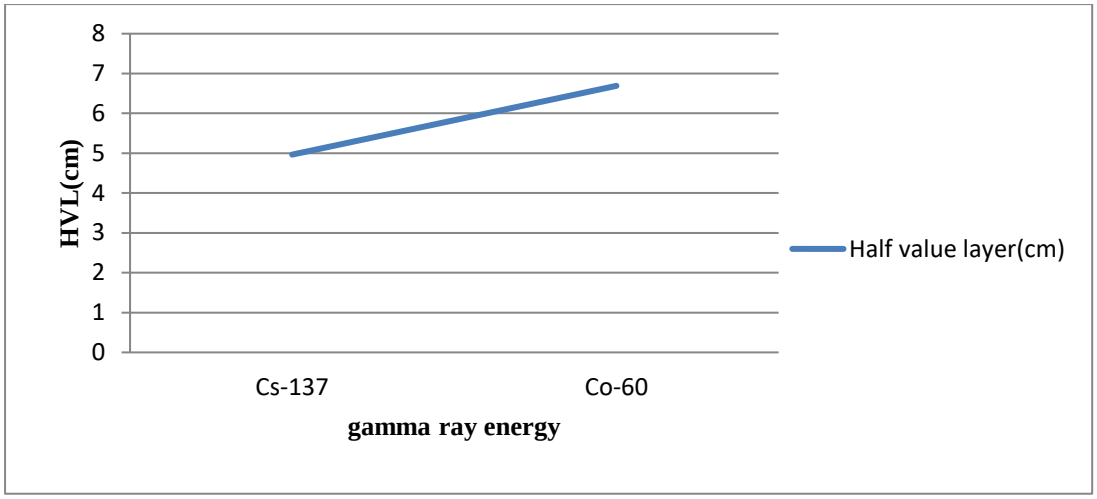

Figure 4.34: Half value layer of cement samples through different gamma rays energies.

Table 4.17: The value of doses through different clay cubic's thickness by using Cs-137 source. The measuring time, temperature and pressure were 30s, 30c^0 and 964.7hpa, respectively.

Material	Thickness (cm)	Frequency	Mean (Dose(µGy))	Std. Deviation
Clay	0	10	225.65	0.0527
	10	10	77.05	0.0120
	20	10	27.26	0.0116
	25	10	18.24	0.0099
	35	10	7.86	0.0080

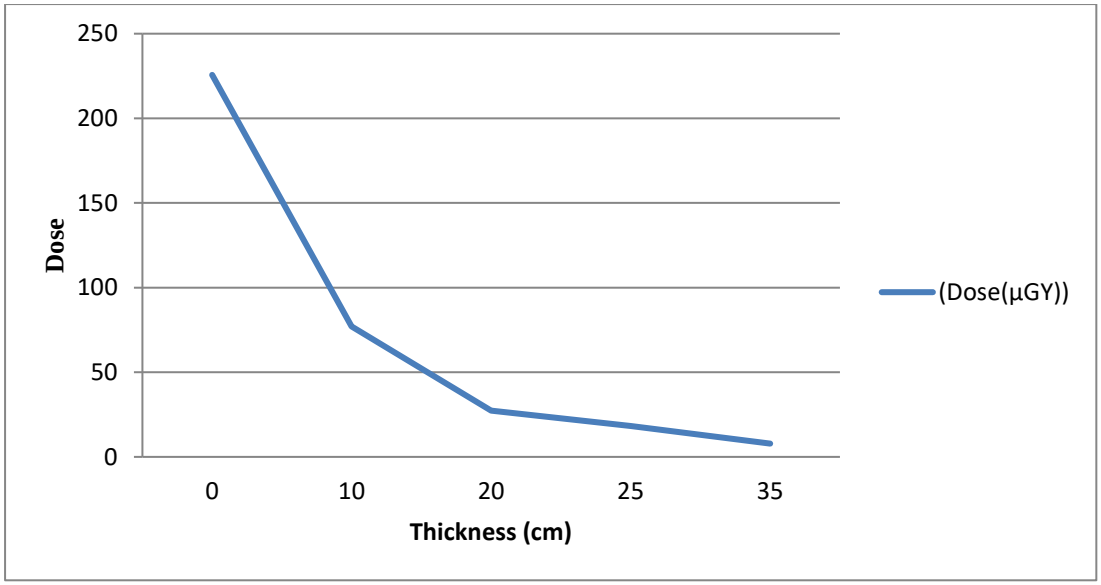

Figure 4.35: Attenuation of Cs-137 gamma rays as they pass through clay samples.

Table 4.18: The value of doses through different clay cubic's thickness by using Co-60 source. The measuring time, temperature and pressure were 30s, 34.5c^0 and 964.8hpa, respectively.

Material	Thickness (cm)	Frequency	Mean (Dose(µGy))	Std. Deviation
Clay	0	10	1.906	0.007
	10	10	0.856	0.003
	20	10	0.396	0.003
	25	10	0.301	0.002
	35	10	0.177	0.001

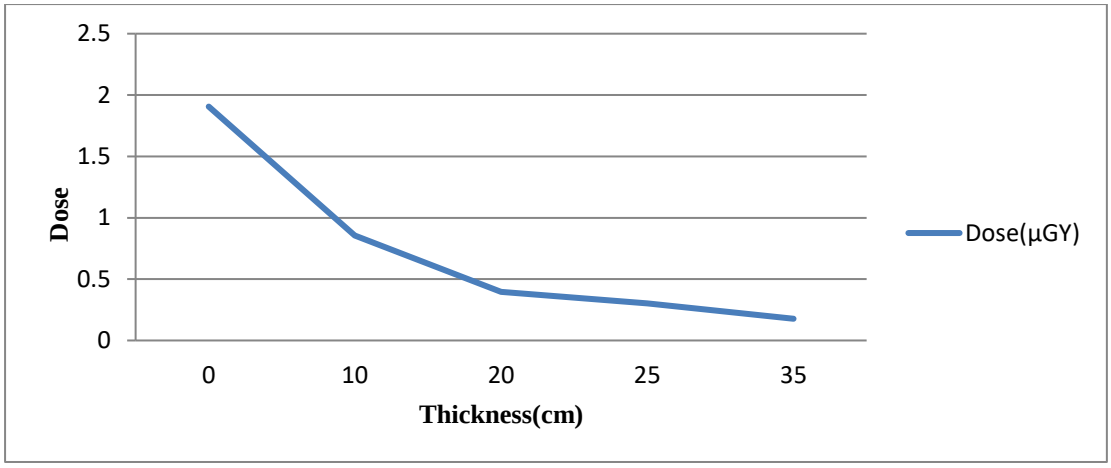

Figure 4.36: Attenuation of Co-60 gamma rays as they pass through clay samples.

Table 4.19: Attenuation coefficient and half value layer for clay cubic's using Cs-137 gamma rays with initial dose 225.65 µGy.

Thickness (cm)	**Dose (µGy)**	**Linear attenuation coefficient µ (cm^{-1})**	**Mass attenuation coefficient μ_m (cm^2/g)**	**Half value layer (cm)**
10	77.05	0.107	0.080	6.449
20	27.26	0.105	0.079	6.557
25	18.24	0.100	0.075	6.887
35	7.86	0.095	0.071	7.224

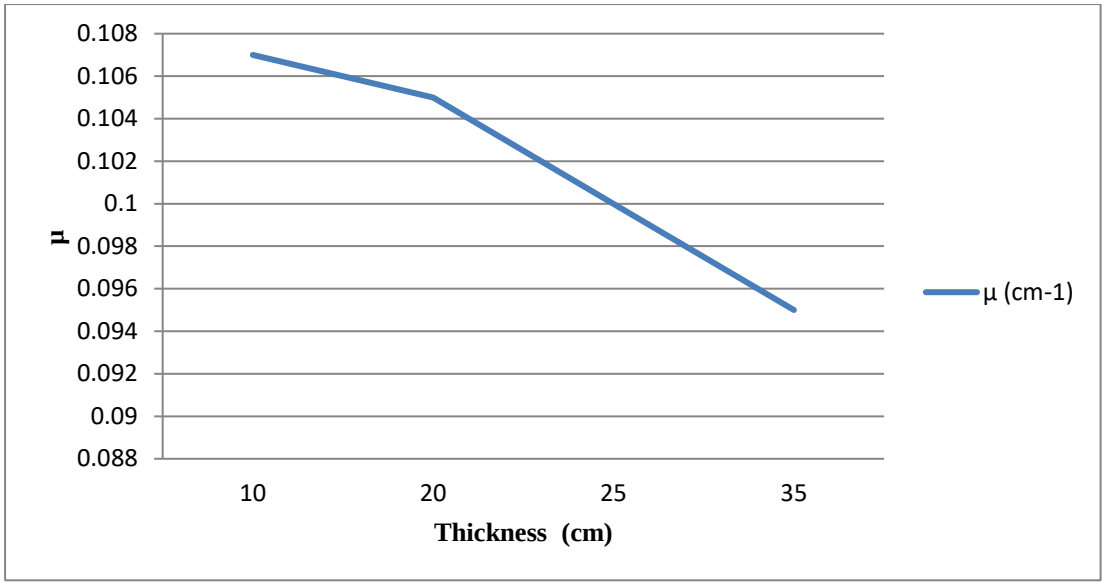

Figure 4.37: Linear attenuation coefficient of Cs-137 source through clay samples as a function of the thickness.

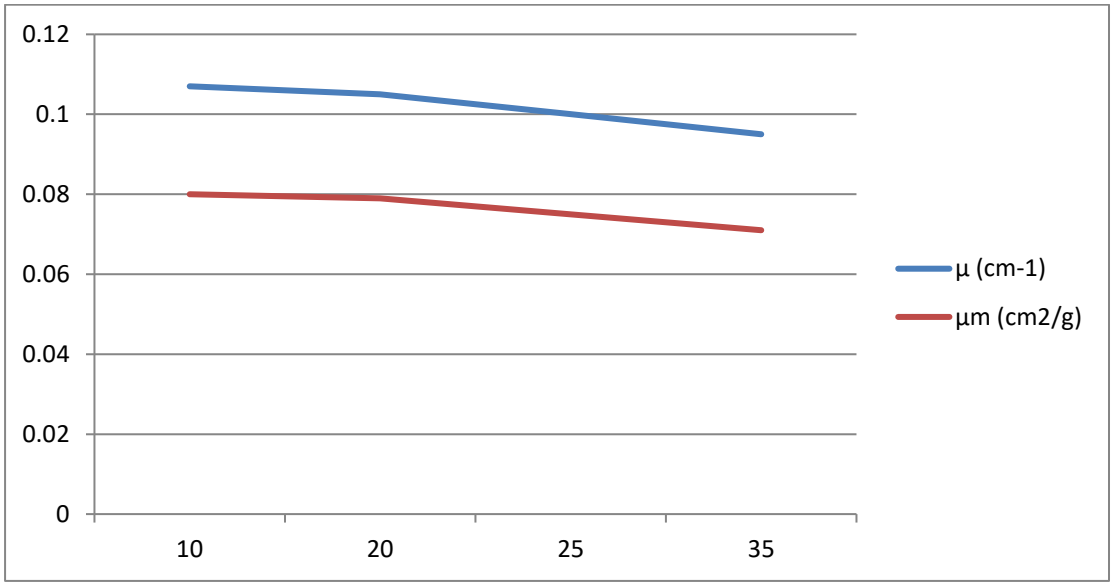

Figure 4.38: Comparison of linear and mass attenuation coefficient of Cs-137 gamma rays through clay samples thickness.

Table 4.20: Attenuation coefficient and half value layer for clay cubic's using Co-60 gamma rays with initial dose1.906 µGy

Thickness (cm)	Dose (µGy)	Linear attenuation coefficient µ (cm^{-1})	Mass attenuation coefficient μ_m (cm^2/g)	Half value layer (cm)
10	0.856	0.080	0.062	8.657
20	0.396	0.078	0.058	8.820
25	0.301	0.073	0.055	9.386
35	0.177	0.067	0.050	10.205

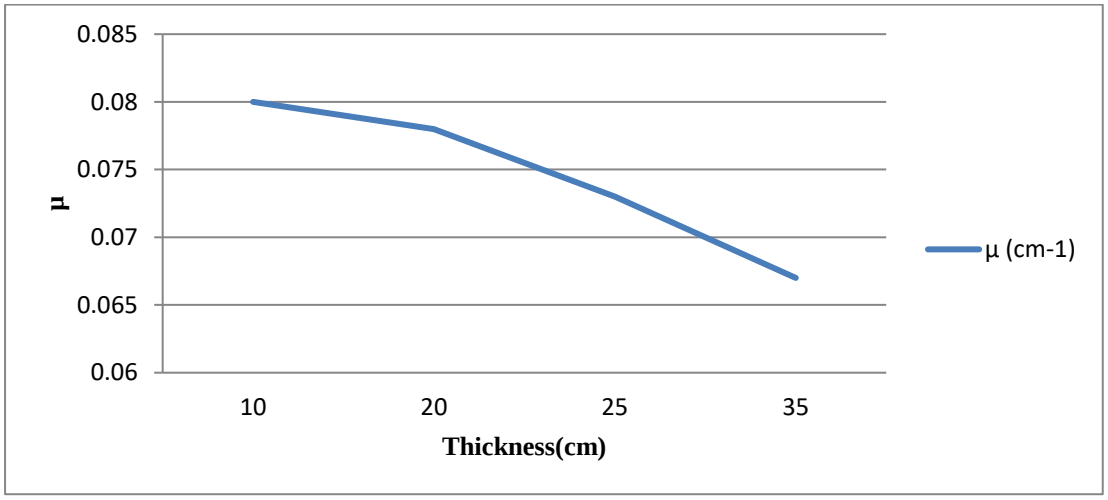

Figure 4.39: Linear attenuation coefficient of Co-60 source through clay samples as a function of the thickness.

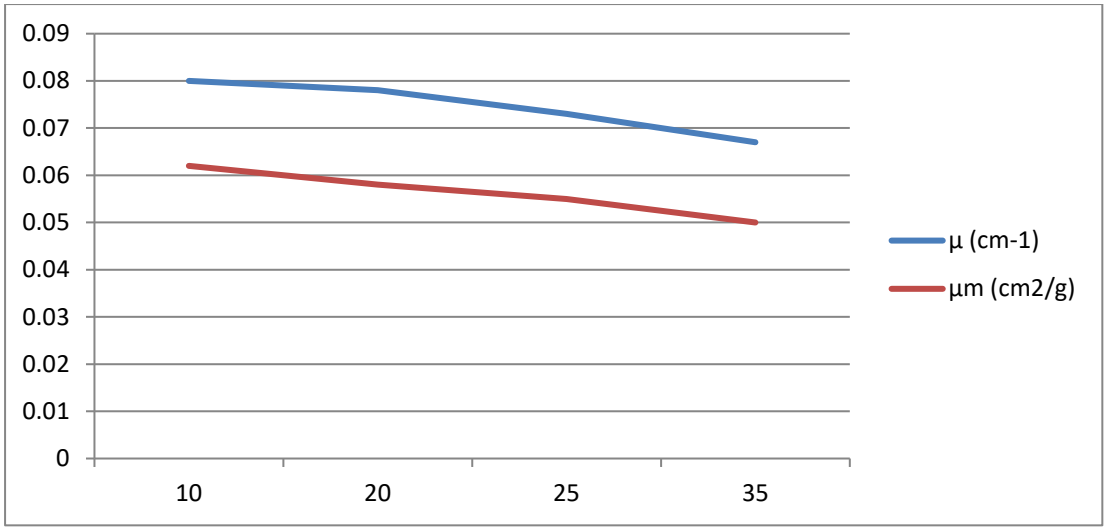

Figure 4.40: Comparison of linear and mass attenuation coefficient of Co-60 gamma rays through clay samples thickness.

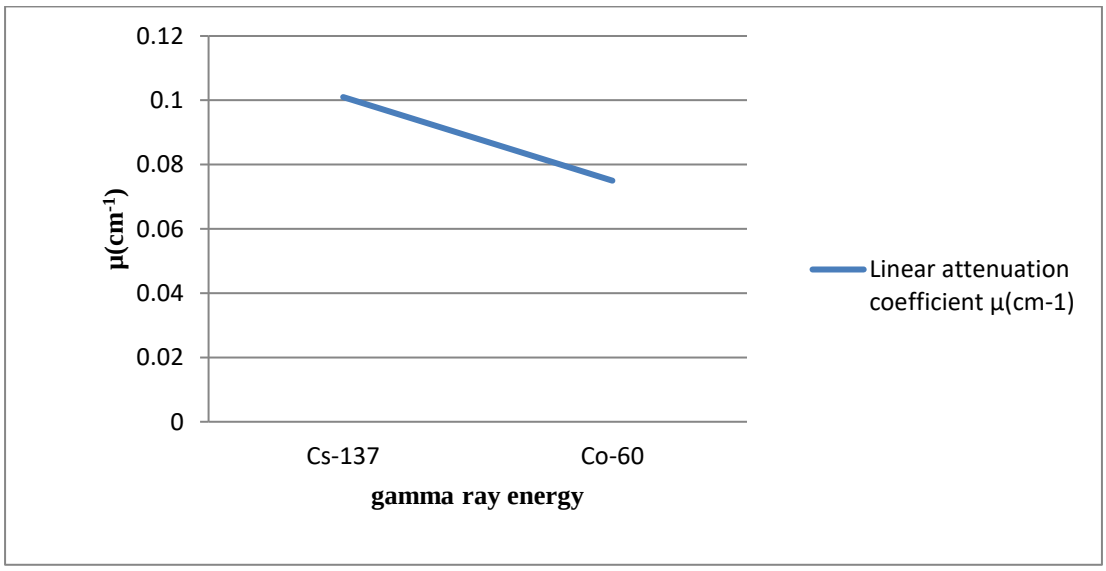

Figure 4.41: Linear attenuation coefficient of clay samples through different gamma rays energies.

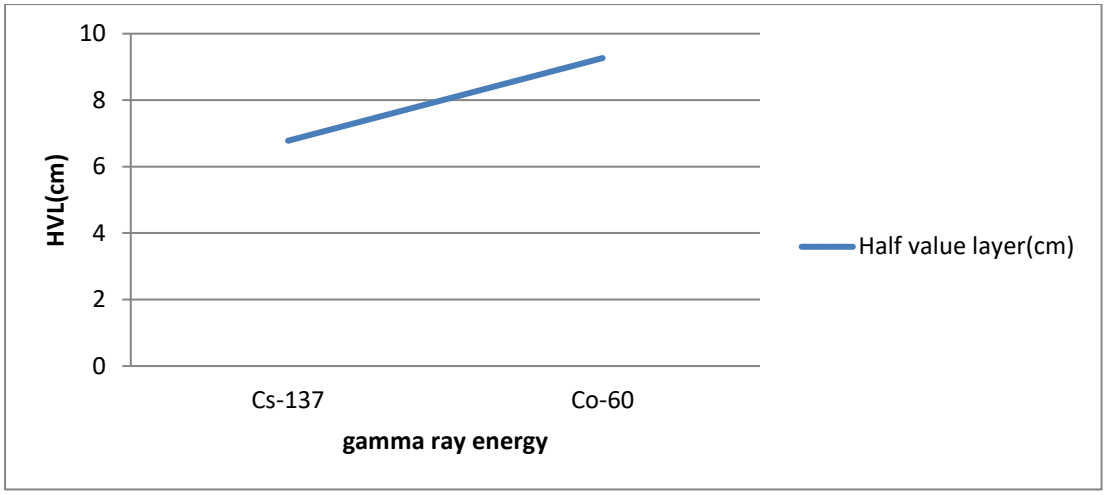

Figure 4.42: Half value layer of clay samples through different gamma rays energies.

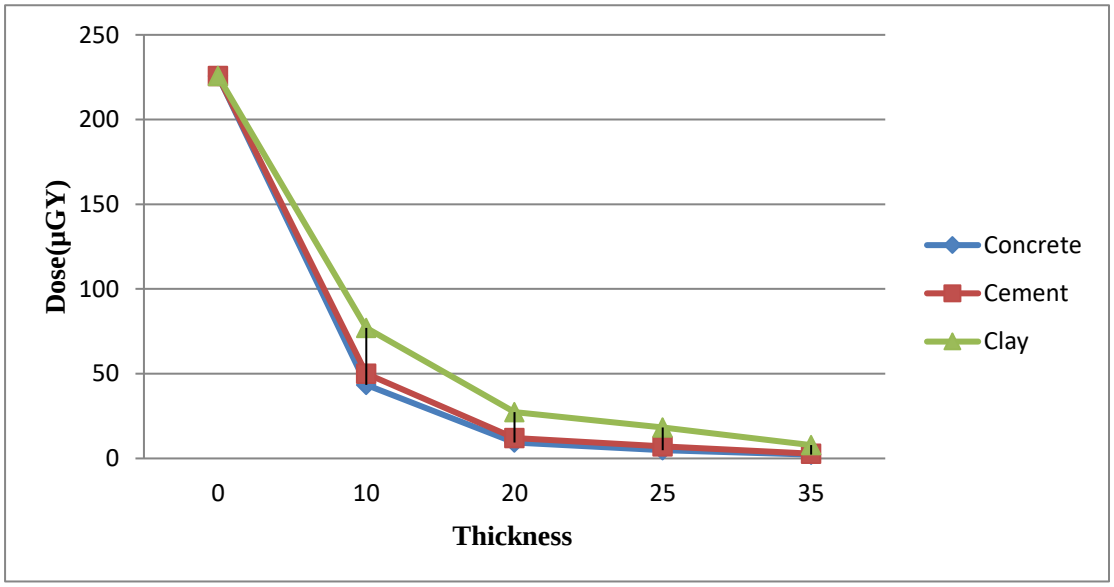

Figure 4.43: Attenuation of Cs-137 gamma rays as a function of thickness through different shield materials**.**

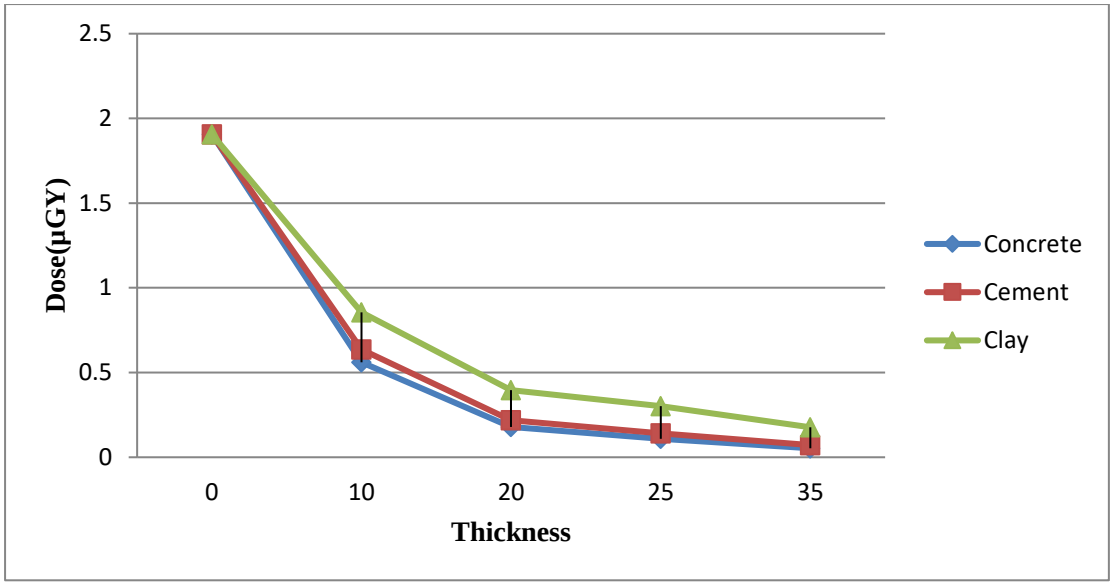

Figure 4.44: Attenuation of Co-60 gamma rays as a function of thickness through different shield materials.

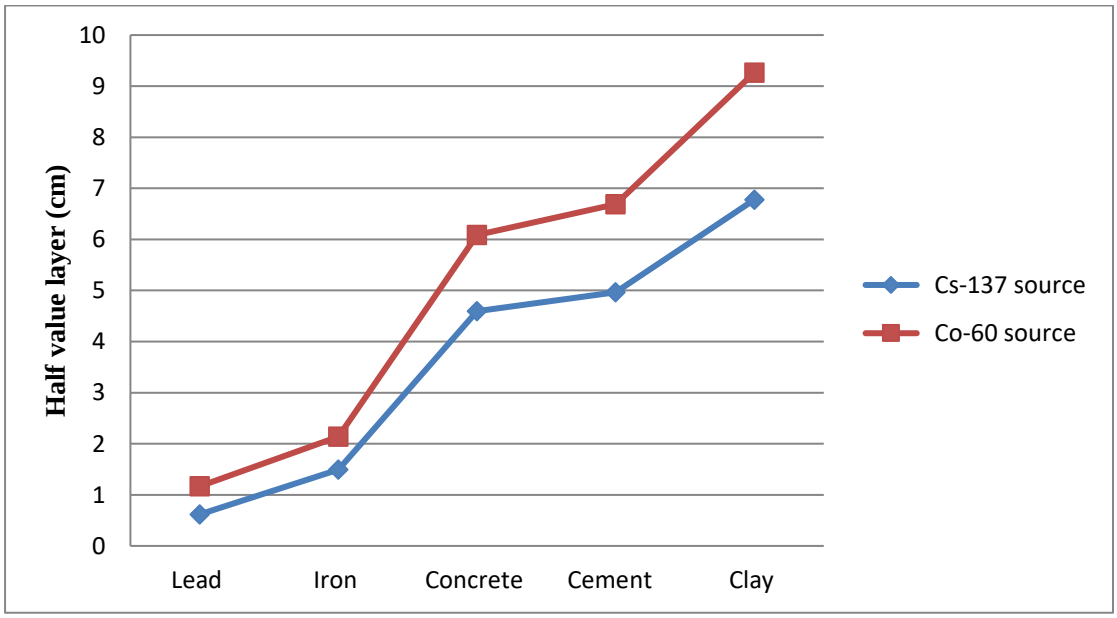

Figure 4.45: Comparison of half value layer of different materials shield using different gamma ray sources.

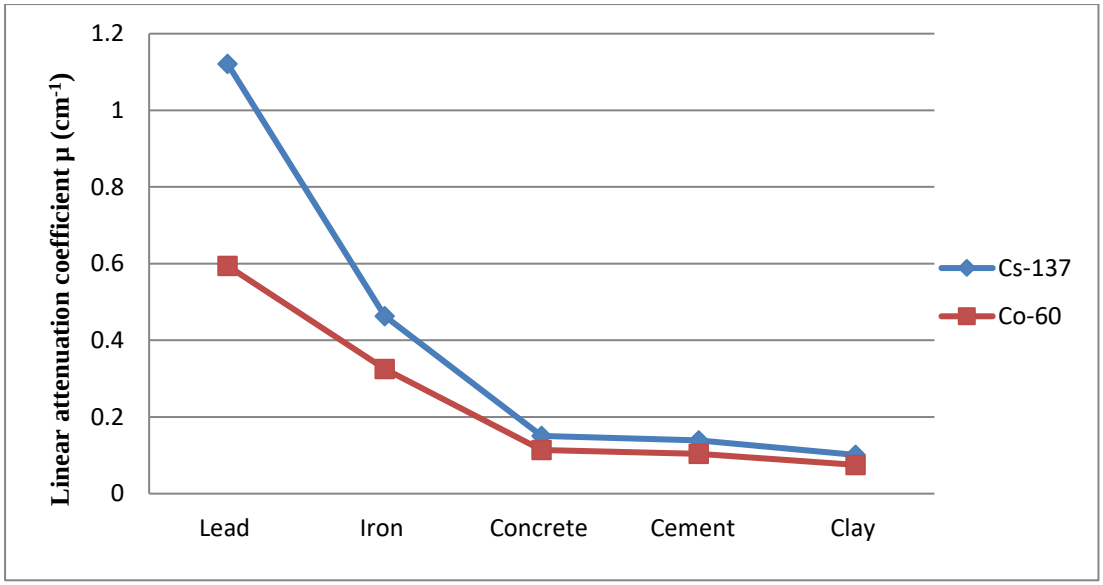

Figure 4.46: Comparison of linear attenuation coefficient of the materials shield as a function of photon energy**.**

Table 4.21: The value of doses through different (lead + iron) slabs thickness by using Cs-137 source. The measuring time, temperature and pressure were 30s, 24.5c^0 and 970.7hpa, respectively.

Material	Thickness (cm)	Frequency	Mean (Dose(μGy))	Std. Deviation
Lead + Iron	0.000	10	237.74	0.0516
	0.154+0.202	10	182.72	0.0919
	0.154+0.522	10	157.52	0.0422
	0.154+1.036	10	122.43	0.0483
	0.154+1.35	10	105.61	0.0316
	0.472+0.202	10	127.20	0.0000
	0.472+0.522	10	110.09	0.0316
	0.472+1.036	10	86.36	0.0280
	0.472+1.35	10	74.86	0.0208
	0.812+0.202	10	87.74	0.0236
	0.812+0.522	10	76.17	0.0103
	0.812+1.036	10	59.86	0.0197
	0.812+1.350	10	51.84	0.0170

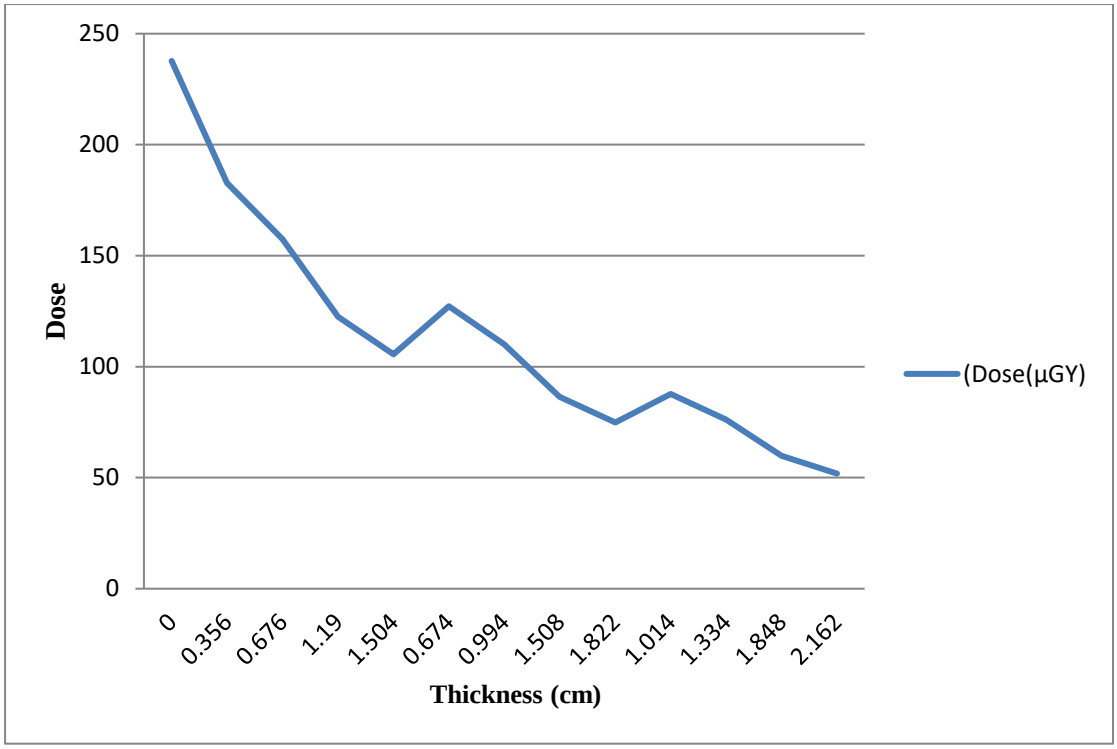

Figure 4.47: Attenuation of Cs-137 gamma rays as they pass through (lead + iron) samples.

Table 4.22: Linear attenuation coefficient and half value layer for (lead + iron) slabs using Cs-137 gamma rays with initial dose 237.74 µGy.

Thickness (cm)	Dose (µGy)	Experimental		Calculated	
		Linear attenuation coefficient µ(cm^{-1})	Half value layer (cm)	Linear attenuation coefficient µ(cm^{-1})	Half value layer (cm)
0.154+0.202	182.72	0.7394	0.937	0.726	0.954
0.154+0.522	157.52	0.608	1.138	0.608	1.138
0.154+1.036	122.43	0.557	1.242	0.558	1.241
0.154+1.350	105.61	0.539	1.284	0.541	1.280
0.472+0.202	127.20	0.927	0.746	0.942	0.735
0.472+0.522	110.09	0.774	0.894	0.793	0.873
0.472+1.036	86.36	0.671	1.032	0.690	1.003
0.472+1.350	74.86	0.634	1.092	0.653	1.060
0.812+0.202	87.74	0.983	0.705	0.987	0.701
0.812+0.522	76.17	0.853	0.812	0.865	0.800
0.812+1.036	59.86	0.746	0.928	0.761	0.909
0.812+1.350	51.84	0.704	0.983	0.720	0.962

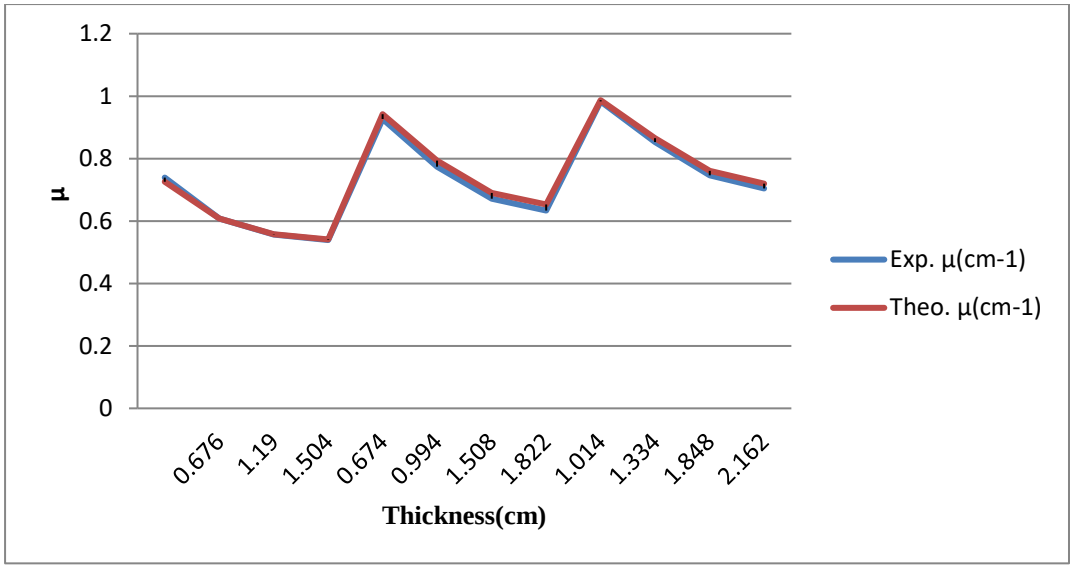

Figure 4.48: Comparison of experimental and calculated linear attenuation coefficient of Cs-137 gamma rays through (lead + iron) slabs samples thickness.

Table 4.23: The value of doses through different (lead slabs +concrete cubic's) thickness by using Cs-137 source. The measuring time, temperature and pressure were 30s, 32 c^0 and 986.7hpa, respectively.

Material	Thickness (cm)	Frequency	Mean (Dose(μGy))	Std. Deviation
Lead + Concrete	0.000	10	233.23	0.0675
	0.154+10	10	43.79	0.0158
	0.154+20	10	15.94	0.0053
	0.154+25	10	4.30	0.0015
	0.154+35	10	2.46	0.0027
	0.472+10	10	31.09	0.0185
	0.472+20	10	11.95	0.0067
	0.472+25	10	3.10	0.0019
	0.472+35	10	1.81	0.0046
	0.812+10	10	22.81	0.0105
	0.812+20	10	9.10	0.0113
	0.812+25	10	2.25	0.0023
	0.812+35	10	1.30	0.0013

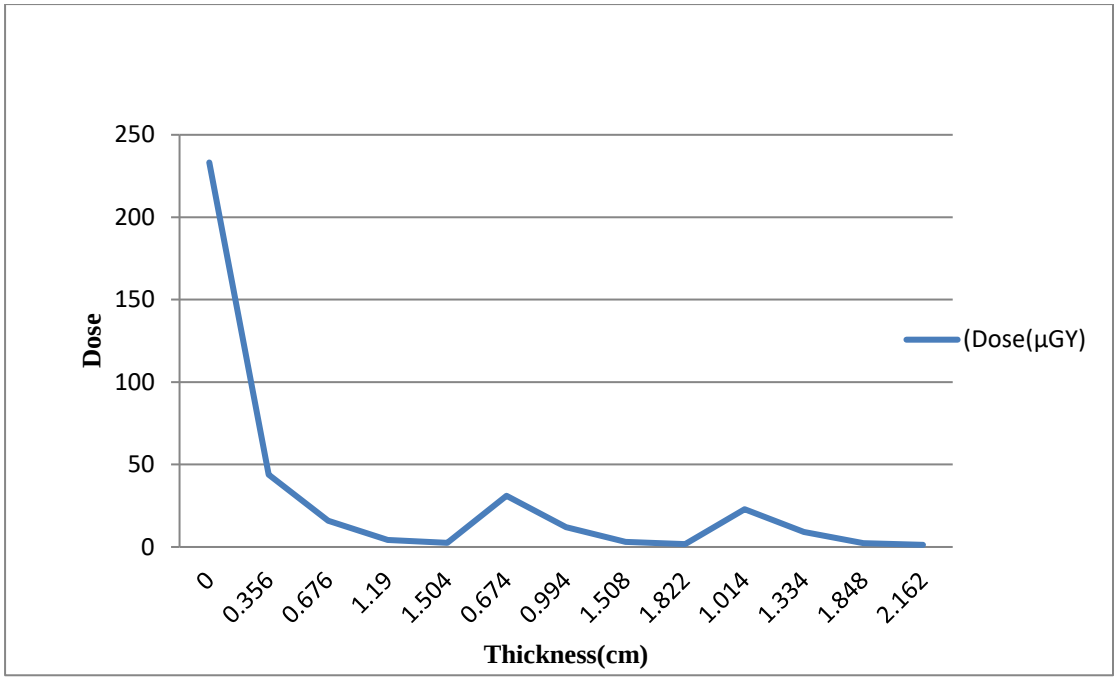

Figure 4.49: Attenuation of Cs-137 gamma rays as they pass through (lead + concrete) samples.

Table 4.24: Linear attenuation coefficient and half value layer for (lead slabs + concrete cubic's) using Cs-137 gamma rays with initial dose 233.23µGy.

Thickness (cm)	Dose (µGy)	Experimental		Calculated	
		Linear attenuation coefficient µ(cm^{-1})	Half value layer(cm)	Linear attenuation coefficient µ(cm^{-1})	Half value layer(cm)
0.154+10	43.79	0.164	4.207	0.178	3.887
0.154+20	15.94	0.133	5.205	0.165	4.194
0.154+25	4.30	0.158	4.365	0.157	4.390
0.154+35	2.46	0.129	5.352	0.135	5.123
0.472+10	31.09	0.192	3.601	0.208	3.318
0.472+20	11.95	0.145	4.774	0.181	3.827
0.472+25	3.10	0.169	4.085	0.170	4.060
0.472+35	1.81	0.137	5.059	0.144	4.789
0.812+10	22.81	0.215	3.222	0.236	2.934
0.812+20	9.10	0.155	4.446	0.195	3.540
0.812+25	2.25	0.179	3.854	0.182	3.795
0.812+35	1.30	0.144	4.782	0.153	4.513

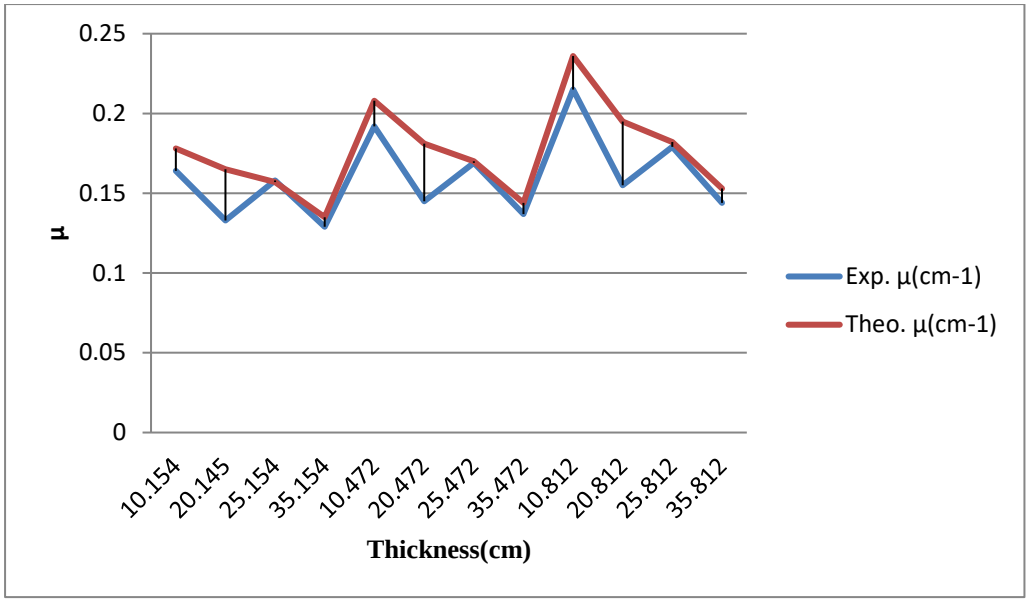

Figure 4.50: Comparison of experimental and calculated linear attenuation coefficient of Cs-137 gamma rays through (lead slabs + concrete cubic's) samples thickness.

Table 4.25: The value of doses through different (lead slabs + cement cubic's) thickness by using Cs-137 source. The measuring time, temperature and pressure were 30s, 30 c^0 and 964.7hpa, respectively.

Material	Thickness (cm)	Frequency	Mean (Dose(μGy))	Std. Deviation
Lead + Cement	0.000	10	233.23	0.0675
	0.154+10	10	47.03	0.0181
	0.154+20	10	16.29	0.0137
	0.154+25	10	6.04	0.0038
	0.154+35	10	3.32	0.0029
	0.472+10	10	33.73	0.0120
	0.472+20	10	12.08	0.0092
	0.472+25	10	4.31	0.0019
	0.472+35	10	2.41	0.0013
	0.812+10	10	24.27	0.0052
	0.812+20	10	9.47	0.0070
	0.812+25	10	3.25	0.0038
	0.812+35	10	1.78	0.0058

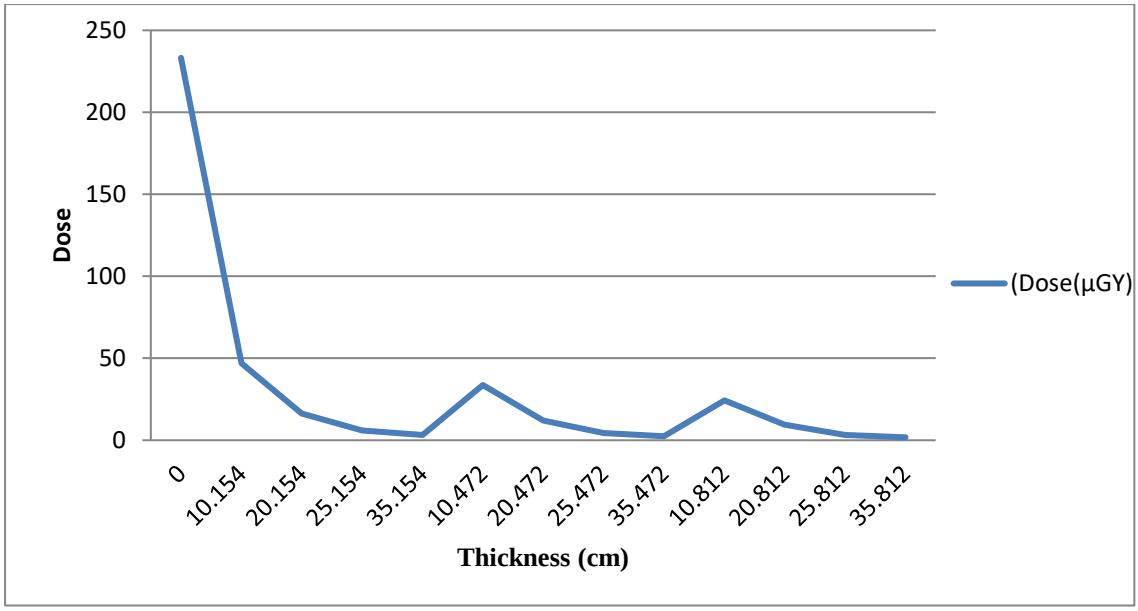

Figure 4.51: Attenuation of Cs-137 gamma rays as they pass through (lead + cement) samples.

Table 4.26: Linear, mass attenuation coefficient and half value layer for (lead slabs + cement cubic's) using Cs-137 gamma rays with initial dose 233.23 µGy.

Thickness (cm)	Dose (µGy)	Experimental		Calculated	
		Linear attenuation coefficient $\mu(cm^{-1})$	Half value layer(cm)	Linear attenuation coefficient $\mu(cm^{-1})$	Half value layer(cm)
0.154+10	47.03	0.157	4.394	0.164	4.213
0.154+20	16.29	0.132	5.247	0.153	4.519
0.154+25	6.04	0.145	4.771	0.143	4.815
0.154+35	3.32	0.121	5.729	0.129	5.359
0.472+10	33.73	0.184	3.753	0.193	3.589
0.472+20	12.08	0.144	4.792	0.169	4.092
0.472+25	4.31	0.156	4.422	0.156	4.416
0.472+35	2.41	0.128	5.376	0.138	4.994
0.812+10	24.27	0.209	3.311	0.223	3.104
0.812+20	9.47	0.153	4.501	0.184	3.762
0.812+25	3.25	0.165	4.185	0.169	4.099
0.812+35	1.78	0.136	5.090	0.147	4.692

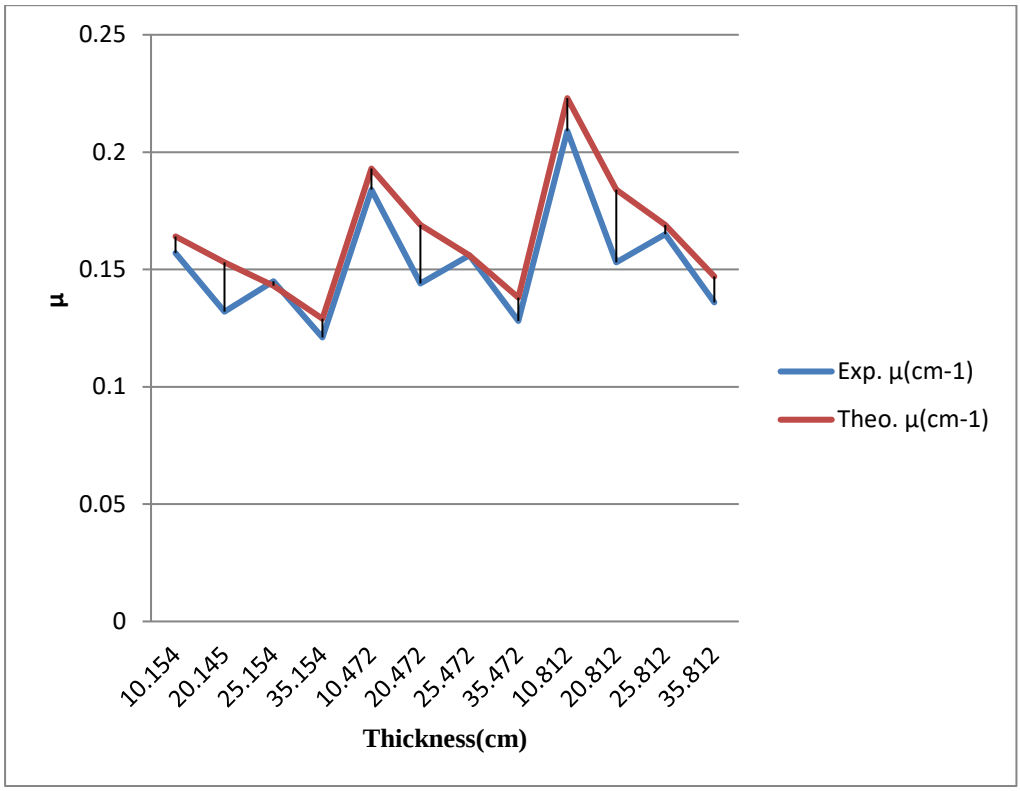

Figure 4.52: Comparison of experimental and calculated linear attenuation coefficient of Cs-137 gamma rays through (lead slabs + Cement Cubic's) samples thickness.

Table 4.27: The value of doses through different (lead slabs + clay cubic's) thickness by using Cs-137 source. The measuring time, temperature and pressure were 30s, 30c^0 and 964.7hpa, respectively.

Material	Thickness (cm)	Frequency	Mean (Dose(µGy))	Std. Deviation
Lead + Clay	0.000	10	233.23	0.0675
	0.154+10	10	94.50	0.0166
	0.154+20	10	58.95	0.0231
	0.154+25	10	20.31	0.0084
	0.154+35	10	13.87	0.0088
	0.472+10	10	67.62	0.0200
	0.472+20	10	42.38	0.0108
	0.472+25	10	14.39	0.0110
	0.472+35	10	9.76	0.0090
	0.812+10	10	47.40	0.0151
	0.812+20	10	28.85	0.0226
	0.812+25	10	9.93	0.0067
	0.812+35	10	6.77	0.0073

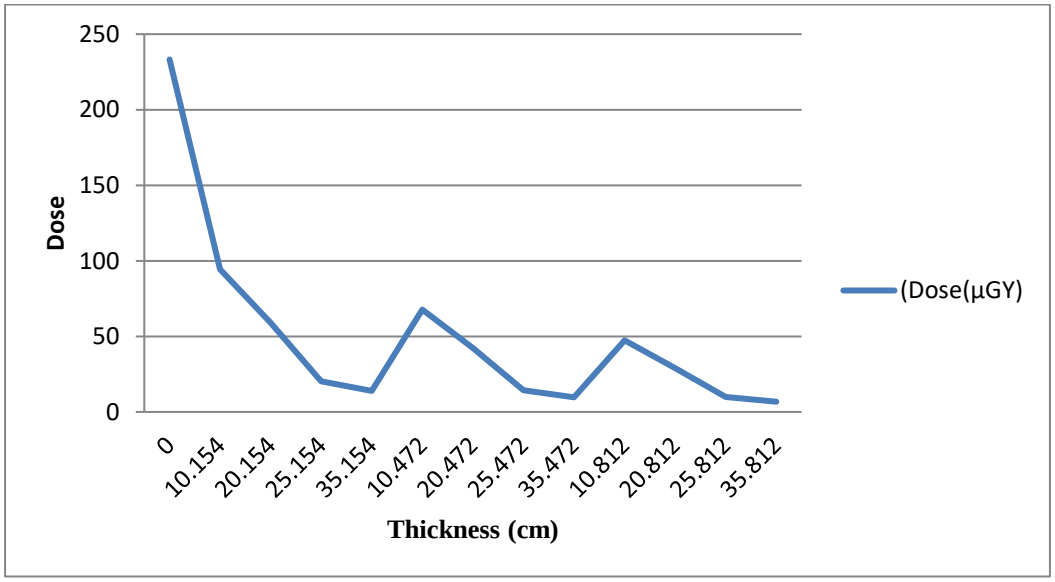

Figure 4.53: Attenuation of Cs-137 gamma rays as they pass through (lead + clay) samples.

Table 4.28: Linear attenuation coefficient and half value layer for (lead slabs + clay cubic's) using Cs-137 gamma rays with initial dose 233.23 µGy.

Thickness (cm)	Dose (µGy)	Experimental		Calculated	
		Linear attenuation coefficient $\mu(cm^{-1})$	Half value layer(cm)	Linear attenuation coefficient $\mu(cm^{-1})$	Half value layer(cm)
0.154+10	75.50	0.111	6.238	0.122	5.674
0.154+20	28.26	0.104	6.617	0.112	6.152
0.154+25	16.31	0.104	6.646	0.106	6.528
0.154+35	6.52	0.100	6.880	0.099	6.970
0.472+10	60.62	0.128	5.386	0.154	4.487
0.472+20	21.38	0.116	5.937	0.129	5.359
0.472+25	14.39	0.109	6.337	0.119	5.793
0.472+35	5.76	0.104	6.641	0.109	6.348
0.812+10	47.40	0.147	4.702	0.183	3.777
0.812+20	18.85	0.120	5.733	0.144	4.786
0.812+25	9.93	0.122	5.667	0.132	5.240
0.812+35	3.77	0.115	6.016	0.118	5.855

Table 4.29: Attenuation coefficient and half value layer for selected shielding materials using Cs-137 gamma rays.

Materials	Linear attenuation coefficient $\mu(cm^{-1})$	Standard error (cm^{-1})	Mass attenuation coefficient $\mu_m\ (cm^2/g)$	Standard error (cm^2/g)	Half value layer (cm)	Standard error (cm)
Lead	1.121	0.028	0.098	0.001	0.617	0.008
Iron	0.463	0.009	0.058	0.001	1.496	0.031
Concrete	0.151	0.007	0.063	0.003	4.593	0.236
Cement	0.139	0.006	0.065	0.003	4.965	0.206
Clay	0.101	0.003	0.076	0.002	6.779	0.175

Table 4.30: Attenuation coefficient and half value layer for selected shielding materials using Co-60 gamma rays.

Materials	Linear attenuation coefficient μ(cm^{-1})	Standard error (cm^{-1})	Mass attenuation coefficient μ_m (cm^2/g)	Standard error (cm^2/g)	Half value layer (cm)	Standard error (cm)
Lead	0.594	0.015	0.051	0.001	1.167	0.034
Iron	0.325	0.023	0.041	0.002	2.137	0.161
Concrete	0.114	0.009	0.046	0.004	6.084	0.484
Cement	0.104	0.007	0.048	0.004	6.691	0.497
Clay	0.075	0.006	0.056	0.005	9.267	0.699

Table 4.31: Linear attenuation coefficient and half value layer for selected shielding materials using Cs-137 gamma rays.

Materials	Experimental				Calculated			
	Linear attenuation coefficient μ(cm^{-1})	Standard error (cm^{-1})	Half value layer (cm)	Standard error (cm^{-1})	Linear attenuation coefficient μ (cm^{-1})	Standard error (cm^{-1})	Half value layer (cm)	Standard error (cm^{-1})
Lead + Iron	0.727	0.040	0.982	0.053	0.737	0.040	0.971	0.053
Lead + Concrete	0.160	0.007	4.412	0.189	0.175	0.008	4.031	0.178
Lead + Cement	0.150	0.007	4.630	0.198	0.164	0.007	4.305	0.182
Lead + Clay	0.115	0.013	6.066	0.628	0.127	0.023	5.580	0.910

Table 4.32: Densities and compositions by mass of selected building materials.

Samples	Densities (g/cm^3)	Cement (kg)	Sand (kg)	Gravel (kg)	Water (kg)
Concrete	2.374	375	805	1115	185
Cement	2.139	8	24	-	4
Clay	1.335	-	-	-	-

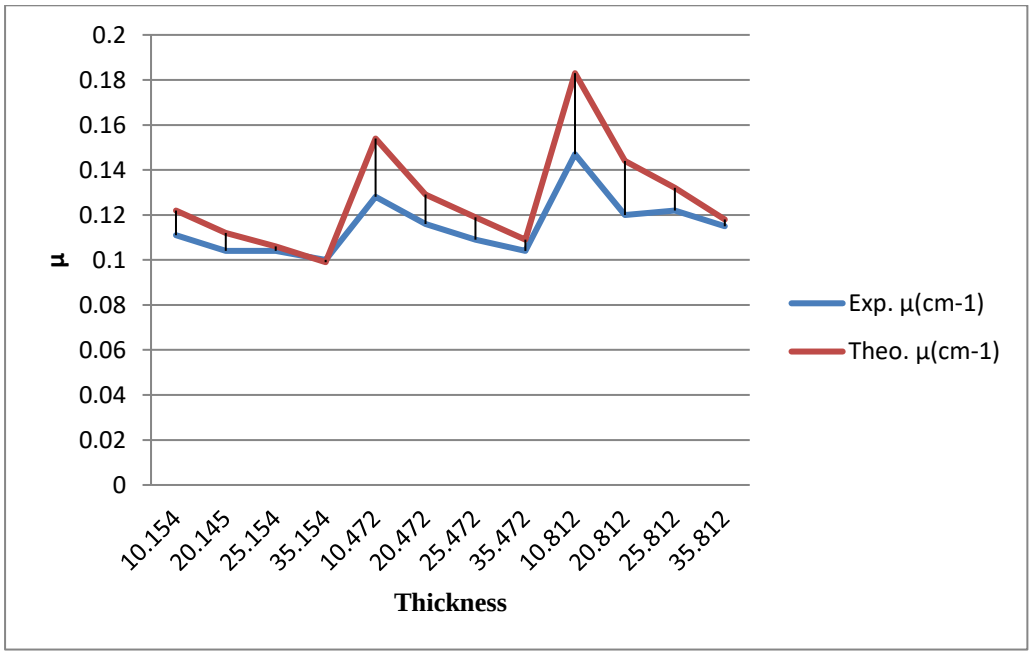

Figure 4.54: Comparison of experimental and calculated linear attenuation coefficient of Cs-137 gamma rays through (lead slabs + clay cubic's) samples thickness.

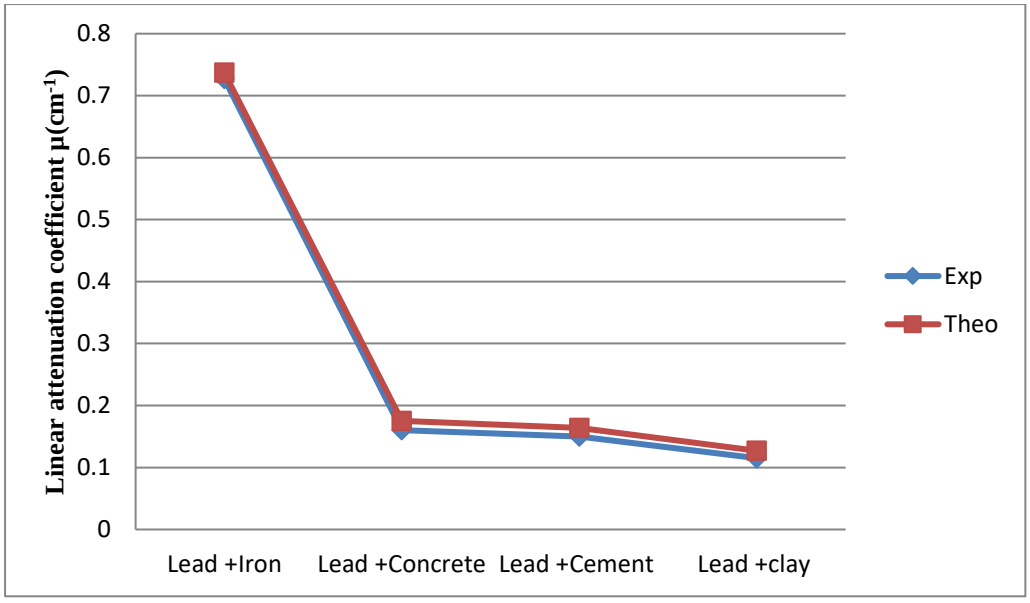

Figure 4.55: Comparison of experimental and calculated linear attenuation coefficient of different shield materials using Cs-137 gamma ray.

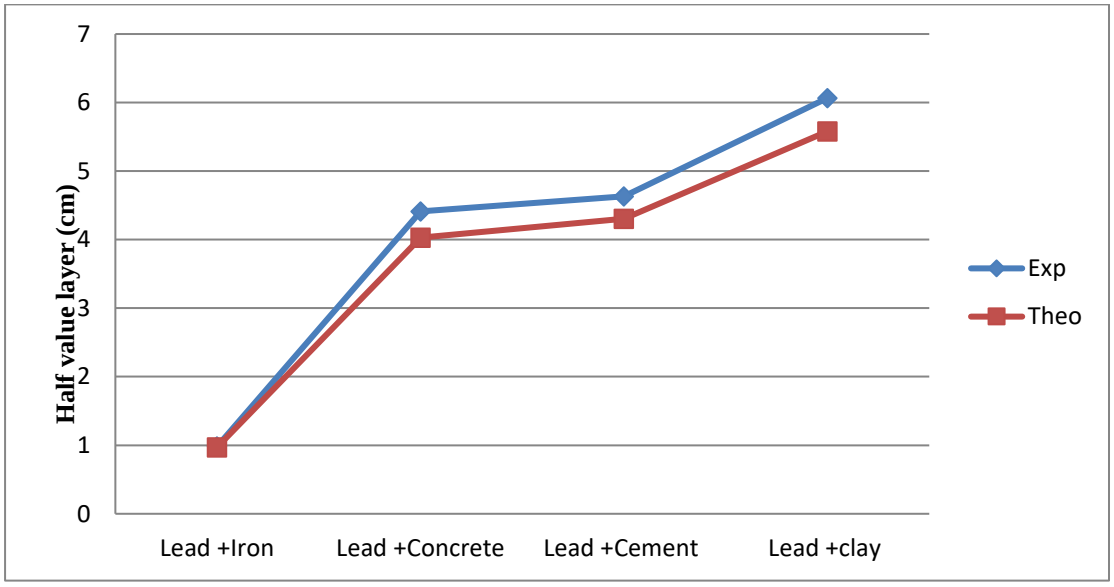

Figure 4.56: Comparison of experimental and calculated half value layer of different shield materials using Cs-137 gamma ray.

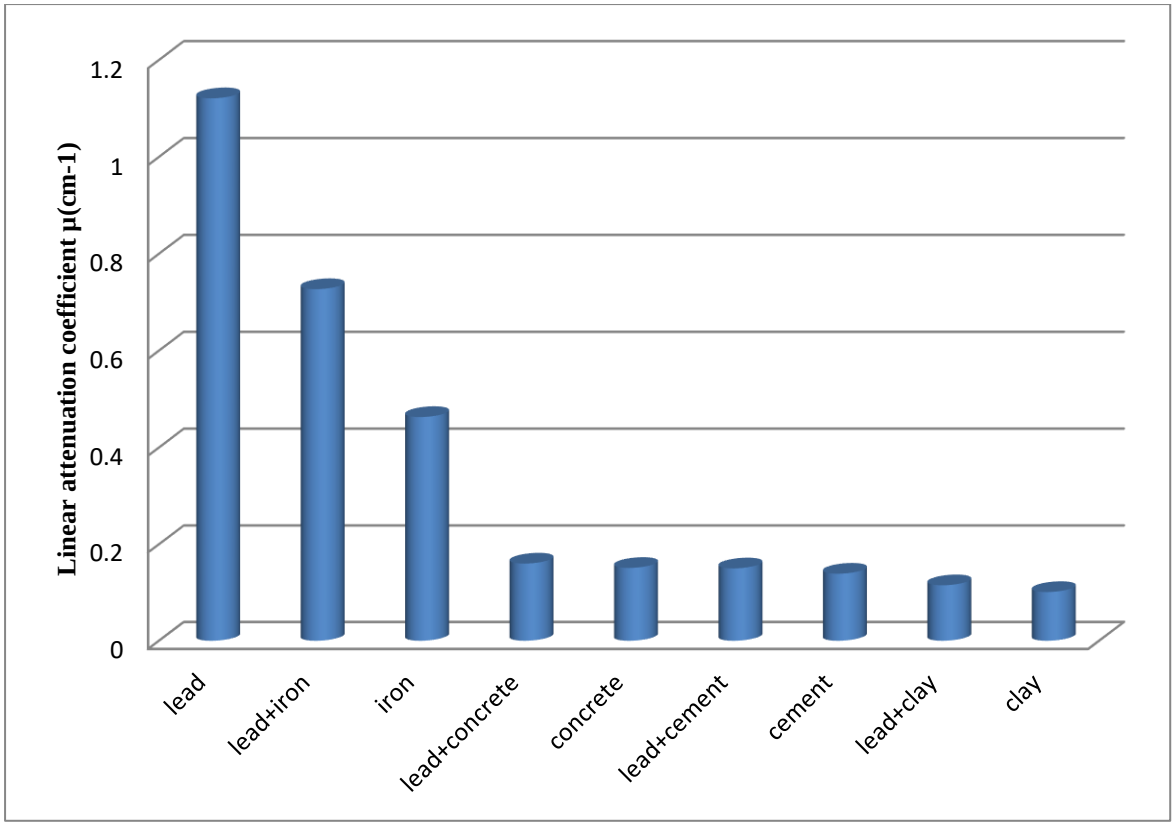

Figure 4.57: Comparison of linear attenuation coefficient of selected shielding materials using Cs-137 gamma ray.

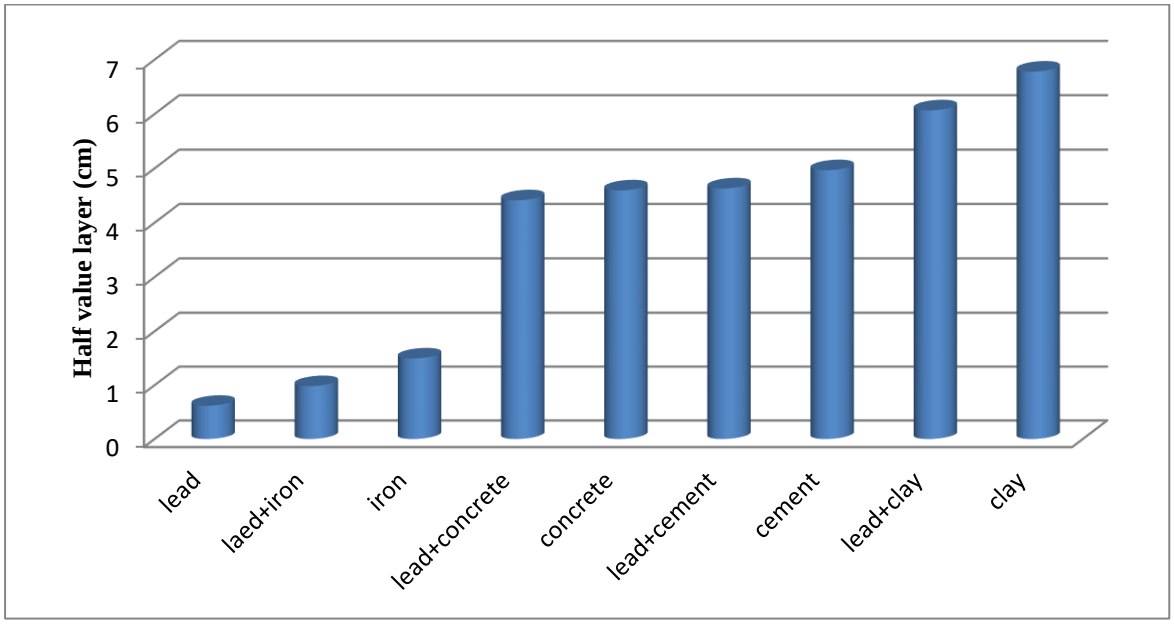

Figure 4.58: Comparison of half value layer of selected shielding materials using Cs-137 gamma ray.

Chapter Five

Discussion, Conclusion and Recommendation

5.1 Discussion

In this study the measurements were performed on the selected samples materials used in shielding gamma radiation, then the decrease of 662, 1173 and 1332 KeV gamma rays with the increase of the thickness of selected materials have been obtained, for each energy the measurements for all types of samples were carried out ten times and the average values listed in Tables **4.1**, **4.2**, **4.5**, **4.6**, **4.9**, **4.10**, **4.13**, **4.14**, **4.17**, **4.18**, **4.21**, **4.23**, **4.25**, and **4.27**.

Also the attenuation coefficients and half value layer for the all studied building materials have been obtained for 662, 1173 and 1332 KeV gamma rays and the results have been listed in Tables **4.3**, **4.4**, **4.7**, **4.8**, **4.11**, **4.12**, **4.15**, **4.16**, **4.19**,and **4.20**. Then the linear attenuation coefficient and half value layer of a combination of lead with the selected building materials have been obtained experimentally and calculated using standard equation, and the results have been listed in tables **4.22**, **4.24**, **4.26**, and **4.28**.

Figures **4.1**, **4.2**, **4.9**, **4.10**, **4.19**, **4.20**, **4.27**, **4.35**, **4.36**, **4.47**, **4.49**, **4.51** and **4.53** show graphical patterns that describe how the photon was attenuated in the selected materials with increasing the thickness, through different energies of gamma ray emitted by Cs-137 and Co-60. It has been observed that all graphs has a similar behavior, in that all curves show that the dose was attenuated with increasing the thickness.

Figures **4.17** and **4.18** show comparison of attenuation as a function of thickness through lead and iron samples using different gamma ray sources. The result showed the higher attenuation of lead than iron.

Figures **4.43** and **4.44** show comparison of attenuation as a function of thickness through concrete, cement and clay samples using different gamma ray sources. The result showed that concrete has higher attenuation than cement, whereas the clay has the lowest attenuation.

According to these results, it could be seen that the lead has a higher attenuation for gamma ray, then iron, concrete, cement, and clay.

Figures **4.3**, **4.11**, **4.13**, **4.21**, **4.23**, **4.29**, **4.31**, **4.37** and **4.39** show linear attenuation coefficient of selected samples as a function of the thickness, through different energies of gamma ray emitted by Cs-137 and Co-60.

Figures **4.4**, **4.6**, **4.12**, **4.14**, **4.22**, **4.24**, **4.30**, **4.32**, **4.38** and **4.40** show comparison of linear and mass attenuation coefficient of selected samples as a function of the thickness, , through different energies of gamma ray emitted by Cs-137 and Co-60.

Figures **4.7**, **4.15**, **4.25**, **4.33**, and **4.41** show linear attenuation coefficient of selected samples through different gamma rays energies.

Figures **4.8**, **4.16**, **4.26**, **4.34** and **4.42** show half value layer of selected samples through different gamma rays energies.

Figure **4.45** show comparison of half value layer of different materials shield (lead, iron, concrete, cement and clay) using different gamma ray sources. The result showed that the half value layer increase with increase the gamma ray energy.

Figure **4.46** shows comparison of linear attenuation coefficient of the materials shield (lead, iron, concrete, cement and clay) as a function of photon energy. The result showed that the linear attenuation coefficient decrease with increase the gamma ray energy.

Figures **4.48**, **4.50**, **4.52**, **4.54** and **4.55** show comparison of experimental and calculated values of linear attenuation coefficient of Cs-137 gamma rays through a composite of ((lead + iron), (lead+ concrete), (lead +cement) and (lead+ clay)) slabs samples of various thickness. The result showed agreement between experimental and calculated readings.

Figure **4.56** shows comparison of experimental and calculated values of half value layer of different shield materials ((lead + iron), (lead+ concrete), (lead +cement) and (lead+ clay)) using Cs-137 gamma ray. The result also showed the agreement between experimental and calculated readings.

Figure **4.57** shows comparison of linear attenuation coefficient of selected shielding materials using Cs-137 gamma ray.

The effectiveness of gamma ray shielding is described in terms of the linear attenuation coefficient μ of the selected materials (lead, iron, concrete, cement, and clay) and the combination (lead with the iron, concrete, cement, and with the clay) as shown in Figure **4.57**. The higher the value of μ, the better the radiation material in terms of absorption requirements, so the increase in density of materials increases μ value.

The results showed that lead is still the standard shield for gamma ray, it has a higher μ value followed by, the iron, concrete, cement, whereas the clay has a lowest μ value, most likely due to its density independence.

On the other hand, the combination of lead and iron have a higher μ value than iron, the combination of lead with concrete have a higher μ value than concrete, the combination of lead with cement have a higher μ value than cement, and also the combination of lead with clay have a higher μ value than clay as showed in figure **4.57**.So it was seen that, the lead improve the performance of (iron, concrete, cement and clay) as the gamma ray shielding become more effective when using a combination of lead with these building materials.

Figure **4.58** shows comparison of half value layer of selected shielding materials using Cs-137 gamma ray.

Also effectiveness of gamma ray shielding is described in terms half value layer (HVL) of the selected materials (lead, iron, concrete, cement, and clay) and the combination (lead with the iron, concrete, cement, and with the clay) as shown in Figure **4.58**. The lower value of HVL, the better the radiation shield material in terms of thickness requirements, so the increase in density of materials decreases HVL value.

The results showed that the lead still standard for gamma ray shielding, it has a lower HVL value, followed by the iron, concrete, cement, whereas the clay has a higher HVL value, may be due to density independence.

The combination of lead and iron have a lower HVL value than iron, the combination of lead with concrete have a lower HVL value than concrete, the combination of lead with cement have a lower HVL value than cement, and also the combination of lead with clay have a lower HVL value than clay as showed in figure **4.58**. So it was seen that, the lead improve the performance of (iron, concrete, cement and clay) as a gamma ray shielding when it is combined with each of them.

5.2 Conclusion

Gamma ray shielding properties of some building materials have been evaluated and discussed in terms of attenuation coefficients and half value layer at different gamma ray energies. The investigated materials are commonly used as a building materials in Sudan, the lead is still dominant as gamma shielding material, whereas a combination of lead with the some building materials showed an improvement in the efficiency of these selected materials as the gamma ray shielding. This conclusion was made upon the obtained results which showed that linear attenuation coefficients decrease with the increasing photon energy, and half value layer increase with increasing gamma ray energy for these materials. From the present study, it was found that the investigated building materials can be used as a gamma ray shielding materials.

5.3 Recommendations

The results of this work are limited by the number and type of materials investigated. While studies have shown that high density materials are more effective to attenuate gamma ray than low density materials, more investigation of combination of density materials with low density are required to reach a cost effective composite of different types of materials to be suitable for gamma ray shielding.

References

A.B.Tugru, B.B.a., 2014. Comparison of Lead and WC_Co Materials against Gamma Irradiation. Proceedings of the 3rd International Congress, 125, pp.24-28.

Abdo, A.E.-S., 2002. Calculation of the cross-sections for fast neutrons and gamma-rays in concrete shields. Annals of Nuclear Energy , 29, pp.1977-88.

Ahmed, S.N., 2007. Physics and Engineering of Radiation Detection. London: Elsevier.

Ahmed, S.N., 2007. Physics and Engineering of Radiation Detection. USA: Elsevier.

Alan Martin, S.A.H., 1980. An Introduction to Radiation Protection. US: Springer.

AL-Dhuhaibat, M.J.R., 2015. Study of the shielding properties for some composite materials manufactured from polymer epoxy supported by cement, aluminum, iron and lead against gamma rays of the cobalt radioactive source (Co-60). International Journal of Application or Innovation in Engineering & Management (IJAIEM), 4(6), pp.2319 - 4847.

Antoni, R.a.L.B., 2017. Applied Physics of External Radiation Exposure. springer.

Attix, F.H., 1986. Introduction to radiological physics and radiation dosimetry.. John Wiley & Sons.

Ayodeji, O.A.a.A., 2016. Measurement of Shielding Effectiveness of Building Blocks against 662 KeV Photons. Journal of Physical Science, 27(2), pp.55-65.

B. R. Martin, G.S., 2008. Particle Physics. UK: JohnWiley & Sons Ltd.

Bodansky, D., 2004. NUCLEAR ENERGY. SECOND EDITION ed. New York: Springer.

Burns, D.T..&.B.L., 2009. Free-air ionization chambers. Metrologia, 46(2).

California, U.o., 2000. Radiation Safety Fundamentals Workbook. Fourth Edition ed. San Francisco: Environmental Health & Safety.

Cardarelli, J., 2011. Ionizing and Nonionizing Radiation. 6th ed. Occupational and Environmental Health: Recognizing and Preventing Disease and Injury.

Cerrito, L., 2017. Introduction to the Physics of Radiation and Detection Devices. USA: Springer International Publishing.

Charanjeet Singh, T.S.A.K.G.S.M., 2004. Energy and chemical composition dependence of mass attenuation coefficients of building materials. Annals of Nuclear Energy , 31, pp.1199-205.

El-Sayed A. Waly, M.A.B., 2015. Comparative study of different concrete composition as gamma-ray shielding materials. Elsevier, 85, pp.306-10.

El-Sayed A. Waly, M.A.F..M.A.B., 2016. Gamma-ray mass attenuation coefficient and half value layer factor of some oxide glass shielding materials. Annals of Nuclear Energy, 96, pp.26-30.

F.I. El-Hosin, N.A.E.-F., 2000. Shielding of gamma radiation by hydrated Portland cement±lead pastes. Radiation Measurements, 2000, pp.93-99.

Fred A. Mettler, J..M.D..M.P.H..a.G.L.V.M.D., 2002. Major Radiation Exposure — What to Expect and How to Respond. The New England Journal of Medicine, 346(20), pp.1554-61.

Fundamentals, D., 1993. Nuclear physics and reactor theory . Washington : U.S. Department of Energy.

Gupta, T.K., 2013. Radiation, Ionization, and Detection in Nuclear Medicine. New York: Springer-Verlag Berlin Heidelberg.

H. M. Soylu, F.Y.L.O.A.E., 2015. Gamma radiation shielding efficiency of a new lead-free composite material. Journal of Radioanalytical and Nuclear Chemistry, 305(22), pp.529-34.

Hamby, E.D.D.a.D.M., 2014. Experimental shielding evaluation of the radiation protection provided by the structurally significant components of residential structures. Society for Radiological Protection, 34, pp.201-21.

Harjinder Singh Mann, G.S.B.K.S.M.a.G.S.M., 2016. Experimental Investigation of Clay Fly Ash Bricks for Gamma-Ray Shielding. N u c l e a r E n g i n e e r i n g and Te c h n o l o gy , 48, pp.1230-36.

Hefne JAMEEL, A.-D.O.A.-h.O.B.A.A.-A.T., 2010. Gamma Ray Shielding from Saudi White Sand. Energy and Power Engineering, pp.6-9.

Herman Cember, T.E.J., 2009. Introduction to Health Physics. McGraw-Hill Medical.

HUSSEIN, E.M.A., 2003. Handbook on Radiation Probing, Gauging, Imaging and Analysis. New York: Kluwer Academic Publishers.

HUSSEIN, E.M.A., 2004. Handbook on Radiation Probing, Gauging, Imaging and Analysis. New York: Kluwer Academic Publishers.

I. Akkurt, H.C., 2011. Radiation attenuation of boron doped clay for 662, 1173 and 1332 keV gamma rays. Iranian Journal of Radiation Research, 9(1), pp.37-40.

I. Akkurt, C.B.A.A.S.K.B.M.a.K.G., 2012. Determination of Some Heavyweight Aggregate Half Value Layer Thickness Used for Radiation Shielding. Proceedings of the International Congress on Advances in Applied Physics and Materials Science, Antalya, 121.

I. Akkurta, C.B.A.A.S.K.B.M. & Günoglua, c.a.K., 2012. Determination of Some Heavyweight Aggregate Half Value Layer Thickness Used for Radiation Shielding. Proceedings of the International Congress on Advances in Applied Physics and Materials Science, 121.

I.C.P. Salinas, C.C.C.R.T.L., 2006. Effective density and mass attenuation coefficient for building material in Brazil. Applied Radiation and Isotopes , 64, pp.13-18.

K Srinivasan, E.J.J.S., 2017. Evaluation of radiation shielding properties of the polyvinyl alcohol/iron oxide polymer composite. Journal of Medical Physics, 42(4), pp.273-78.

Kaundal, R.S., 2016. Comparative Study of Radiation Shielding Parameters for Bismuth Borate Glasses. Materials Research, 19(4), pp.776-80.

Kh. REZAEE EBRAHIM SARAEE, S.P.B..O.T., 2015. Application of solid waste containing lead for gamma ray shielding material. Cumhuriyet Science Journal, 36(3), pp.1300-949.

Knoll, G.F., 2000. Radiation Detection and Measurement. Wiley.

Kulwinder SinghMann, B..G..A., 2013. Investigationsofsomebuildingmaterialsfor g-rays shieldingeffectiveness. RadiationPhysicsandChemistry, 87, pp.16-25.

M.H. Kharita, M.T..M.A.S.Y., 2008. Development of special radiation shielding concretes using natural local materials and evaluation of their shielding characteristics. Progress in Nuclear Energy, 50, pp.33-36.

M.N. Alam, M.M.H.M.M.I.C.M.K.S.G.R.R., 2001. Attenuation coe• cients of soils and some building materials of Bangladesh in the energy range 276 - 1332 keV. Applied Radiation and Isotopes , 54, pp.973-76.

Majid Jalalia, *.A.M., 2008. Gamma ray attenuation coefficient measurement for neutron-absorbent materials. Radiation Physics and Chemistry, 77, pp.523-27.

Marilyn E. Noz, G.Q.M.J., 2007. Radiation Protection in the Health Sciences. Second Edition ed. Singapore: World Scientific Publishing Co. Pte. Ltd.

Medhat, M.E., 2009. Gamma-ray attenuation coefficients of some building materials available in Egypt. Annals of Nuclear Energy, 36, pp.849–52.

Mehmet Erdem, O..M..F.o.¨.u., 2010. A novel shielding material prepared from solid waste containing lead for gamma ray. Elsevier, 79, pp.917-22.

Mohammad I. Awadallah, M.M.A.I., 2007. Experimental investigation of g-ray attenuation in Jordanian building materials using HPGe-spectrometer. Journal of Environmental Radioactivity, 94, pp.129-36.

N. Chanthima, P.P.J.K.P.L., 2012. Simulated radiation attenuation properties of cement containing with BaSO4 and PbO. Procedia Engineering , 32, pp.976-81.

National Council on Radiation Protection, N., 2006. Structural Shielding Design and Evaluation for Megavoltage X- and Gamma-Ray Radiotherapy Facilities. National Council on Radiation Protection and Measurements.

Nations, F.a.A.O.o.t.U., 1996. Radiation protection and the safety of radiation sources. Periodic. Vienna : International Atomic Energy Agency IAEA.

Nil Kucuk, M.C.a.N.A.I., 2013. MASS ATTENUATION COEFFICIENTS, EFFECTIVE ATOMIC NUMBERS AND EFFECTIVE ELECTRON DENSITIES FOR SOME POLYMERS. Radiation Protection Dosimetry, 153, pp.127-34.

Ouda, A.S., 2015. Development of high-performance heavy density concrete using different aggregates for gamma-ray shielding. HBRC Journal, 79, pp.48-55.

Podgorsak, E.B., 2005. Radiation Oncology Physics. Vienna: IAEA.

Powsner, R.A.P.a.E.R., 2006. Nuclear Medicine Physics. USA: Blackwell.

Prince, R., 2012. Radiation Protection at Light Water Reactors. New York: Springer.

Protection, A.C.o.R., 2000. Radiation Safety Officers Handbook. The Canadian Nuclear Safety Commission.

R. L. Grasty, a.J.R.L., 2004. THTHE ANNUAL EFFECTIVE DOSE FROM NATURAL SOURCES OF IONISING RADIATION IN CANADA. Radiation Protection Dosimetry, 108, pp.215-26.

Ravinder Singh, S.S.G.S.K.S.T., 2017. Gamma Radiation Shielding Properties of Steel and Iron Slags. New Journal of Glass and Ceramics, 7, pp.1-11.

Shapiro, J., 2002. Radiation Protection. 4th ed. President and Fellows of Harvard College.

Stabin, M.G., 2007. Radiation Protection and Dosimetry. New York: Springer Science+Business Media, LLC.

Stabin, M.G., 2007. Radiation Protection and Dosimetry. New York: Springer.

Suat Akbulut, A.S.H.E.S.Ç., 2015. A research on the radiation shielding effects of clay, silica fume and cement samples. Radiation Physics and Chemistry, 117, pp.88-92.

Tarim, O.G.a.U.A., 2016. Determination of Radiation Shielding Properties of Some Polymer and Plastic Materials against Gamma-Rays. ACTA PHYSICA POLONICA A, 130.

Thoraeus, R., 1965. ATTENUATION OF GAMMA RADIATION FROM 6oCo, 13'Cs, """I, AND 226RaI N VARIOUS MATERIALS USED IN RADIOTHERAPY. A C T A R A D I O L O G I C A, 3, pp.81-86.

Tsoulfanidis, N., 1995. Measurement and Detection of Radiation. Washington: Taylor & Francis.

Tsoulfanidis, S.L.a.N., 2011. Measurement and Detection of Radiation. 3rd ed. Taylor and Francis Group, LLC.

Tsoulfanidis, S.L.a.N., 2015. Measurement and Detection of Radiation. 4th ed. Taylor & Francis Group, LLC.

Turgay Korkut, H.K.A.K.G.B., 2011. A new radiation shielding material: Amethyst ore. Annals of Nuclear Energy , 38, pp.56-59.

Turner, J.E., 2007. Atoms Radiation and Radiation Protection. USA: Wiley-VCH Verlag GmbH & Co. KGaA.

Vishwanath P. Singh, N.M.B., 2014. Gamma ray and neutron shielding properties of some alloy materials. Annals of Nuclear Energy 64 (2014) 301–310, 64, pp.301-10.

Y. Elmahroug, B.T.C.S., 2015. Determination of total mass attenuation coefficients, effective atomic numbers and electron densities for different shielding materials. Annals of Nuclear Energy , 75, pp.268-74.

Appendix

Table 1: Clay Cubic's information.

No. of Clay Bricks	Dimensions (cm)			Volume (cm^3)	Mass (g)
	Length	Width	Height		
1	10	10	10	1000	1305.1
2	10	10	10	1000	1324.9
3	15	15	15	3375	4650.7

Table 2: Concrete Cubic's information.

No. of Concrete Bricks	Dimensions (cm)			Volume (cm^3)	Mass (g)
	Length	Width	Height		
1	10	10	10	1000	2300.5
2	10	10	10	1000	2304.9
3	15	15	15	3375	8503.5

Table 3: Cement Cubic's information.

No. of Cement Bricks	Dimensions (cm)			Volume (cm^3)	Mass (g)
	Length	Width	Height		
1	10	10	10	1000	2098.1
2	10	10	10	1000	2103.8
3	15	15	15	3375	7484.6

Table 4: lead slab's thickness.

No. of Lead slab	Lead thickness (cm)					Mean (cm)
1	0.14	0.15	0.15	0.17	0.16	0.154
2	0.32	0.31	0.32	0.31	0.33	0.318
3	0.35	0.34	0.32	0.34	0.35	0.340
4	0.16	0.14	0.16	0.17	0.14	0.154

Table 5: lead slab's thickness.

No. of Lead slab	Thickness (cm)
1	0.154
1&2	0.472
1&2&3	0.812
1&2&3&4	0.966

Table 6: Iron slab's thickness.

No. of Iron Slab	Iron thickness (cm)					Mean (cm)
1	0.21	0.20	0.21	0.21	0.18	0.202
2	0.31	0.32	0.32	0.33	0.32	0.32
3	0.51	0.51	0.52	0.52	0.51	0.514
4	0.32	0.31	0.32	0.31	0.31	0.314

Table 7: Iron slab's thickness.

No. of Iron slab	Thickness (cm)
1	0.202
1&2	0.522
1&2&3	1.036
1&2&3&4	1.350

[i] the amount of energy required to remove an electron from an isolated atom or molecule